COST «Cosmic Wispers» Training School
Lecce, September 14th, 2023

Antonios Gardikiotis
INFN – LNL

OUTLINE

- Axion helioscope : CAST
- Dielectric haloscope: MADMAX
- Cavity haloscope: QUAX

CAST 2002-2022

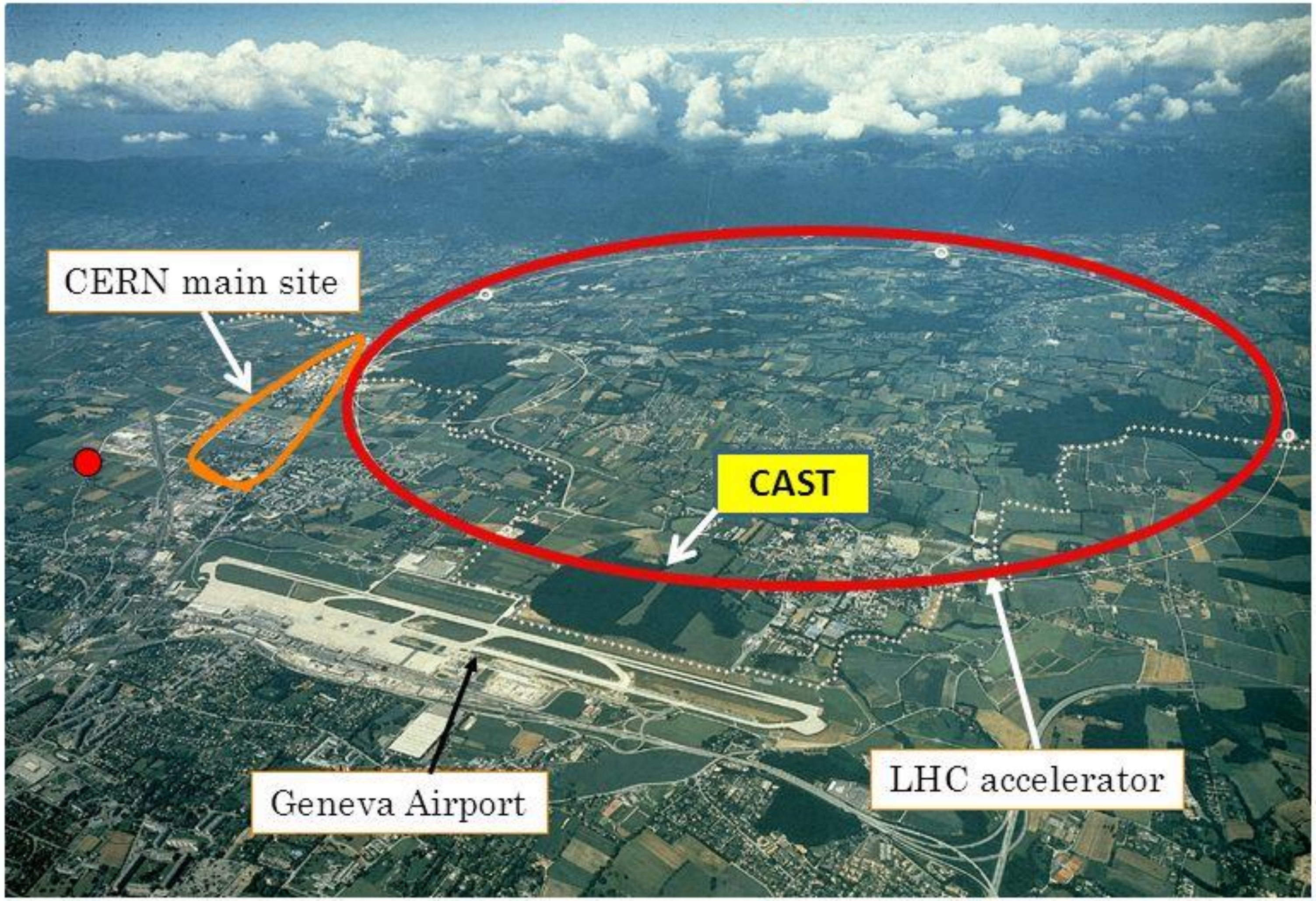

CAST (Cern Axion Solar Telescope) – 2002 -2022

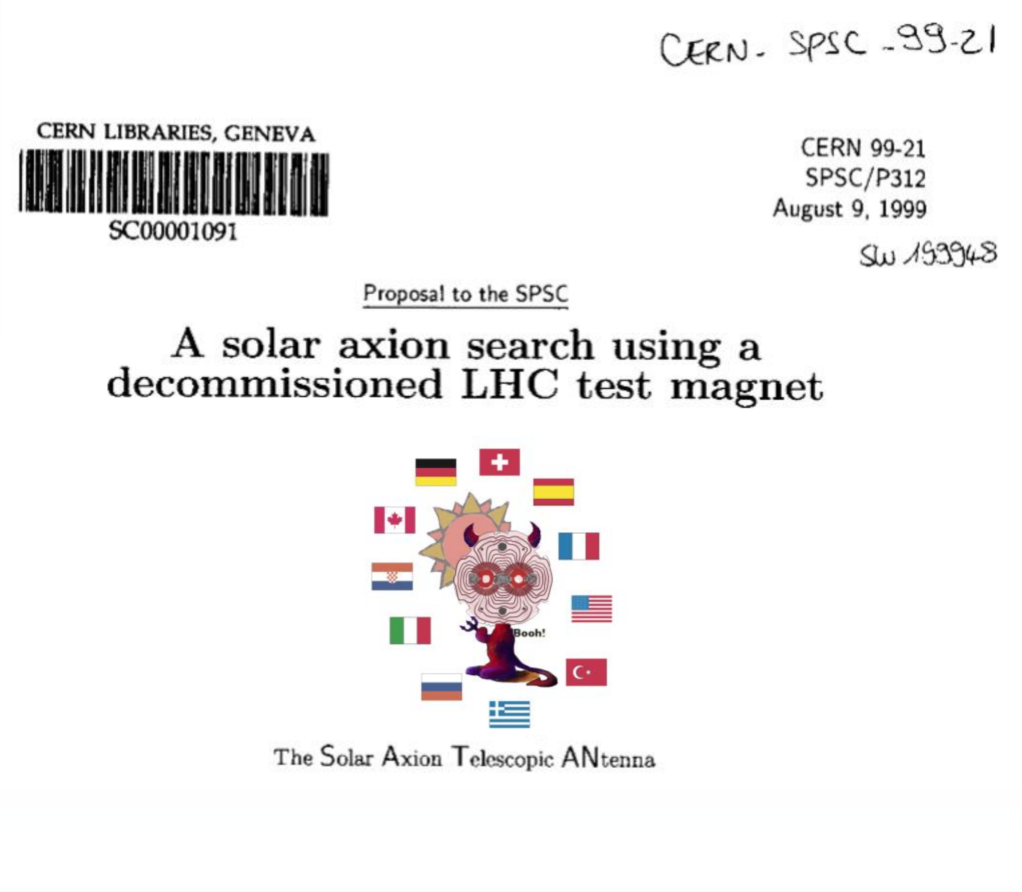

CERN- SPSC -99-21

CERN 99-21
SPSC/P312
August 9, 1999

Sw 199948

Proposal to the SPSC

A solar axion search using a decommissioned LHC test magnet

Booh!

The Solar Axion Telescopic ANtenna

Axion *Helioscope* Experiment

Axion source :

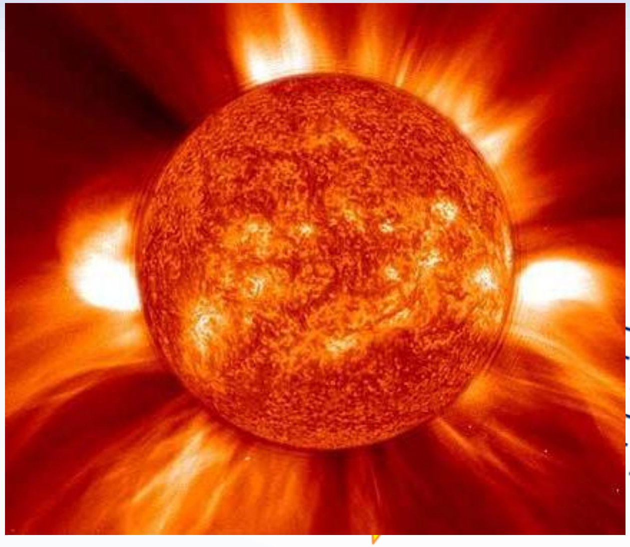

Standard Solar Model

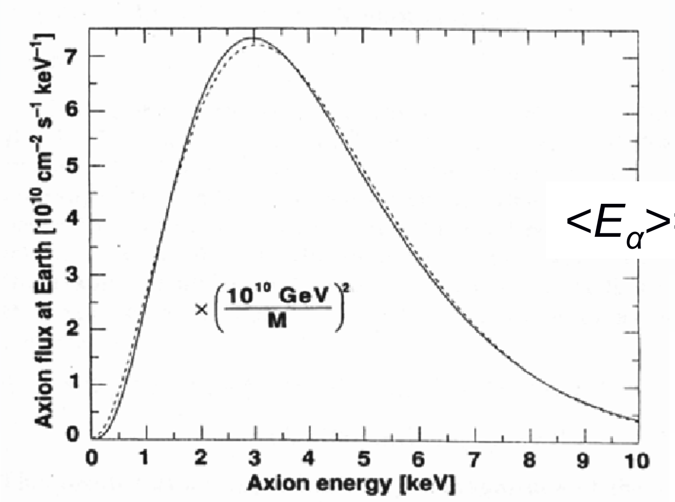

$\langle E_\alpha \rangle$= 4.2 keV

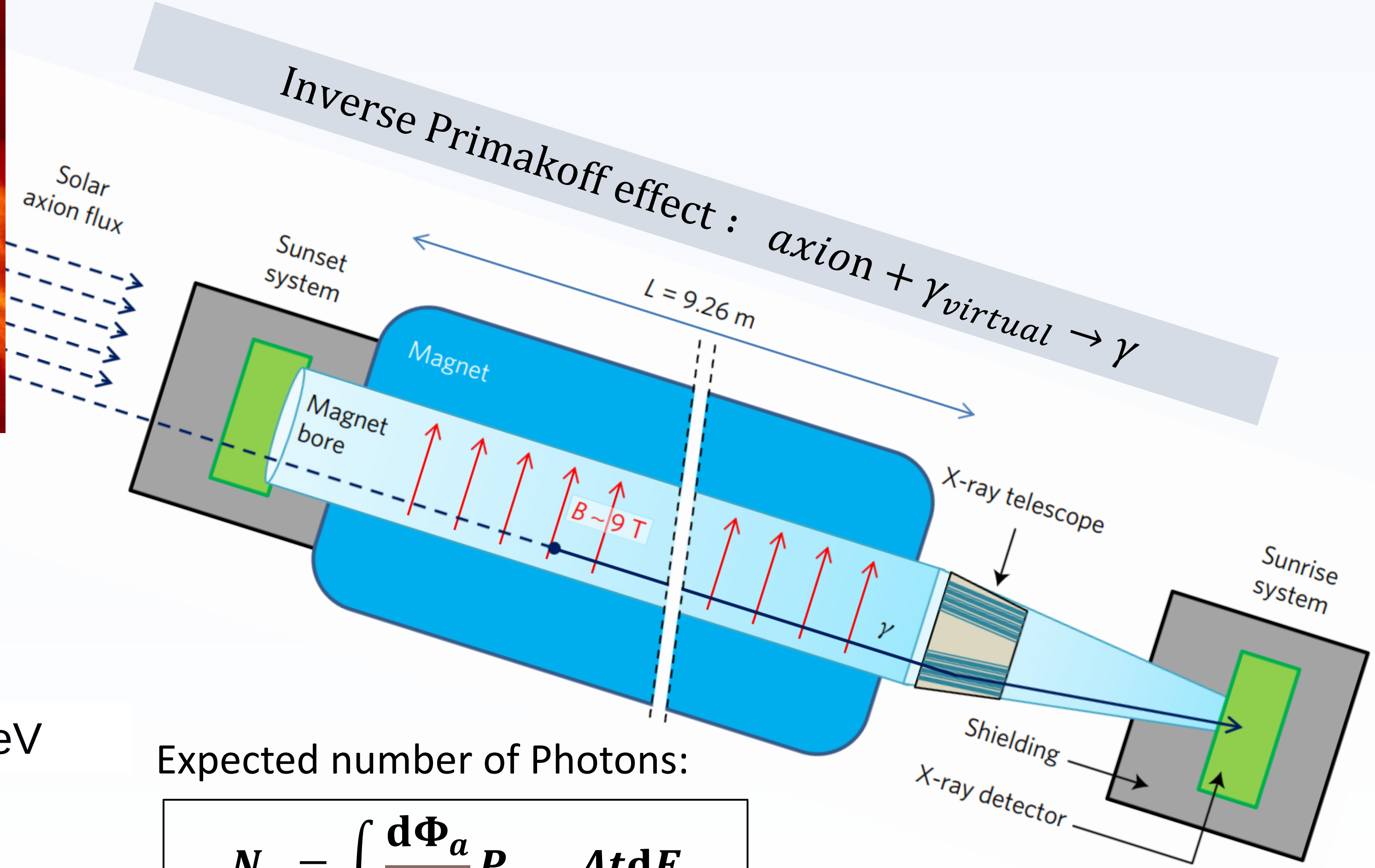

Expected number of Photons:

$$N_\gamma = \int \frac{d\Phi_a}{dE} P_{\alpha\to\gamma} A t dE$$

$$\frac{d\Phi_\alpha}{dE} = g_{10}^2 6.0 \times 10^{10} cm^{-2} s^{-1} keV^{-1} E^{2.481} e^{-E/1.205}$$

G. G. Raffelt. Physical Review D 1986. Volume 33

CAST Axion Helioscope

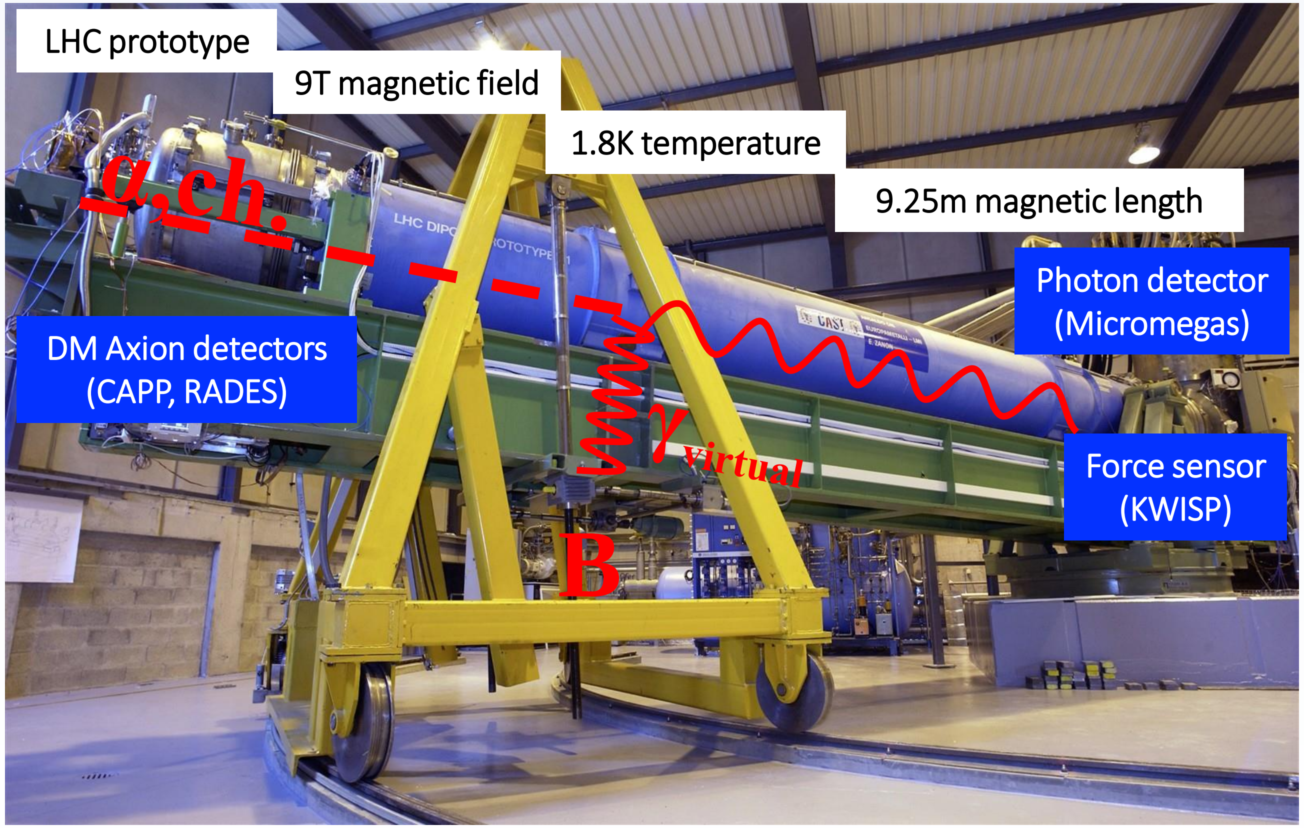

Rotating platform

- (Vertical: ±8o, Horizontal: ±40o)
- 2x90 min solar tracking/day
- Sunrise: X-ray Focusing Device coupled to a CCD + 1 Micromegas
- Sunset: 2 Micromegas

CAST Axion Helioscope

Decommissioned LHC (Large Hadron Collider) superconductive dipole magnet

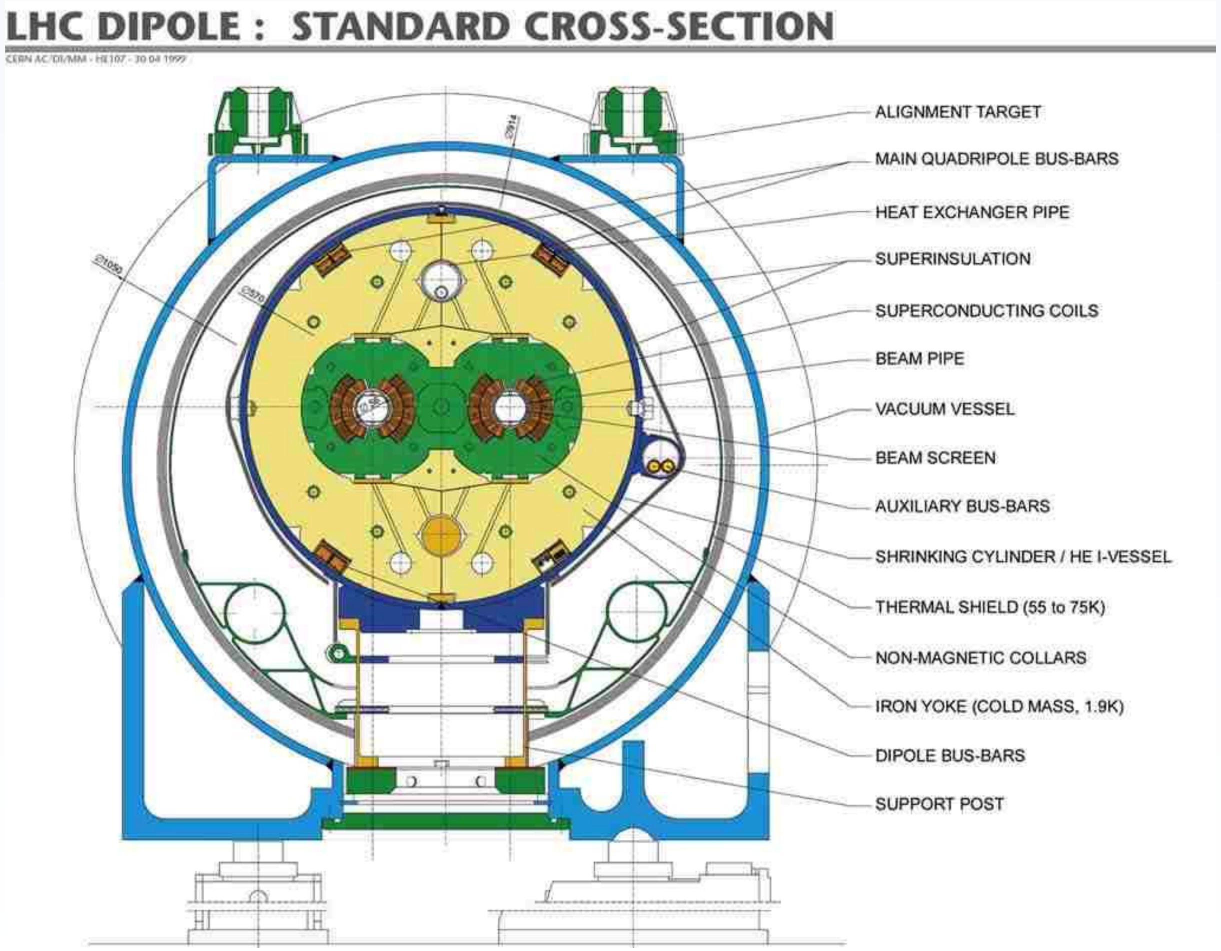

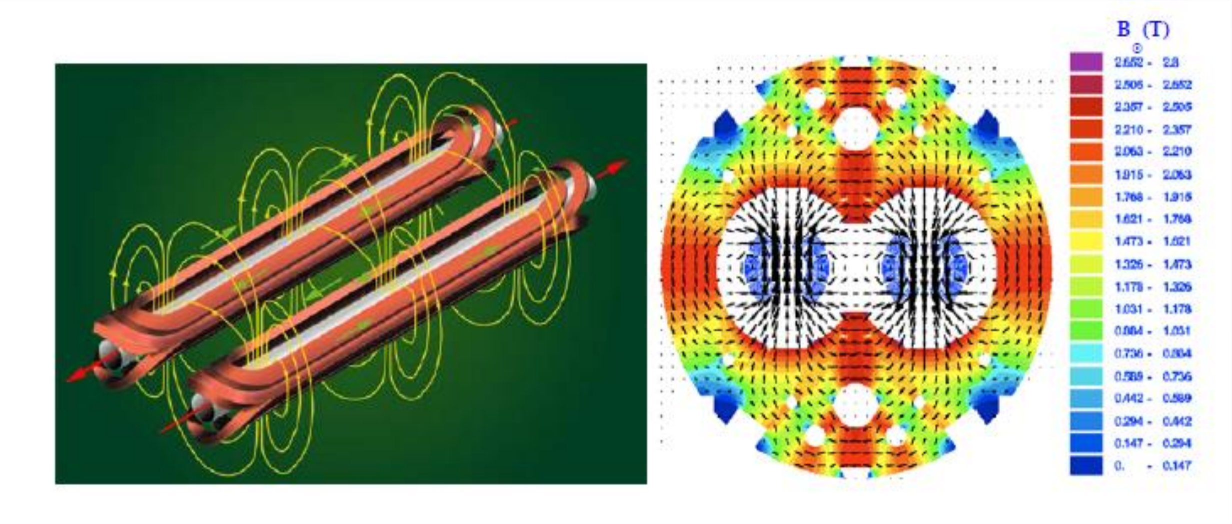

spare LHC magnet
- 45 mm bore diameter
- cross section area A = 14.5 cm^2
- ~10 m long
- B ~ 9 T

CAST Cryogenics

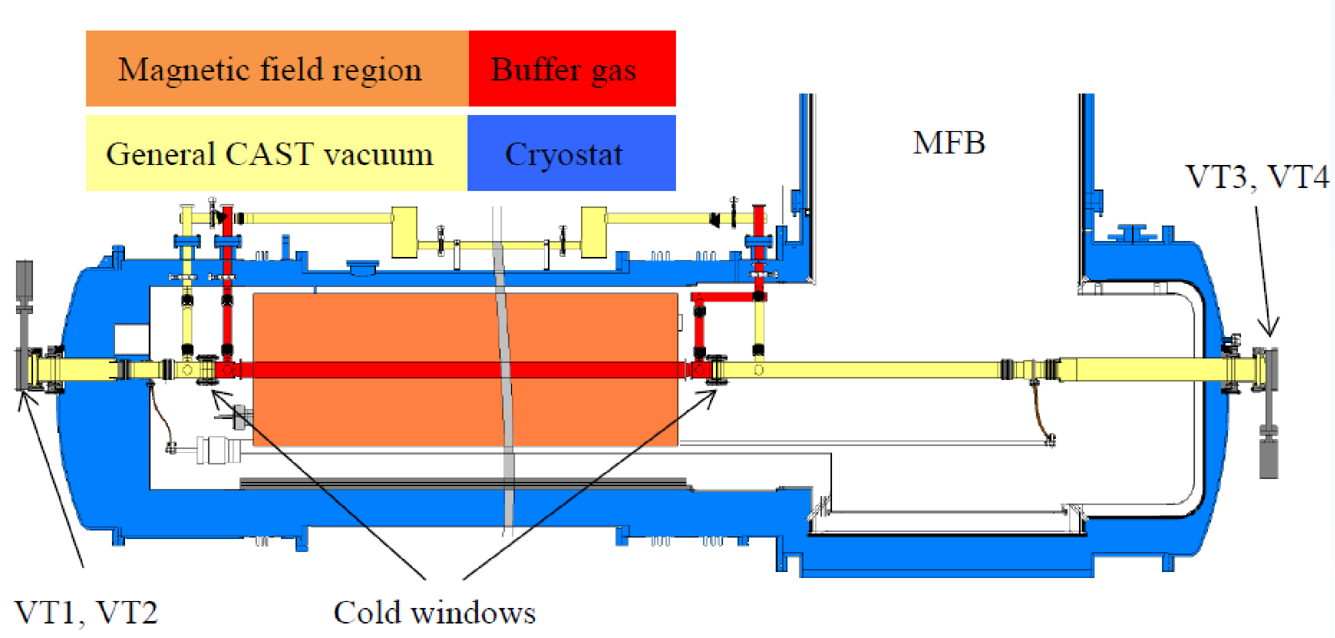

The **interlocks** system (PLC) automatically protects the vacuum setup, the buffer gas, the detectors vacuum side and the cryostat whenever a problem occurs

Quench : a fast discharge of the current is triggered

Solar Tracking

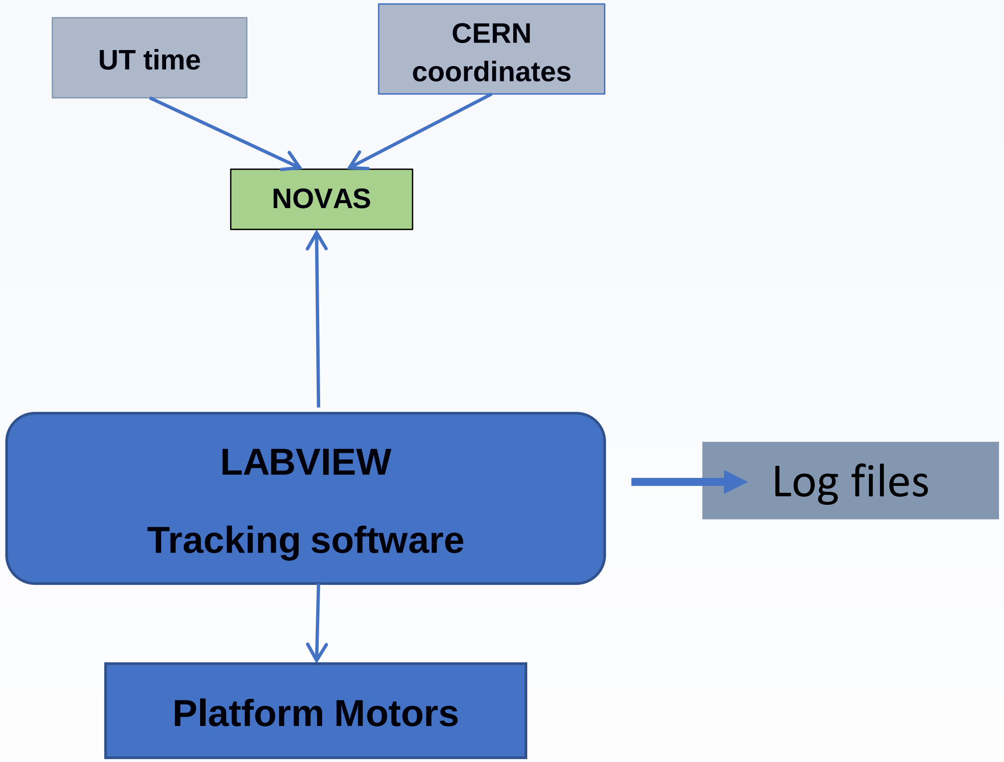

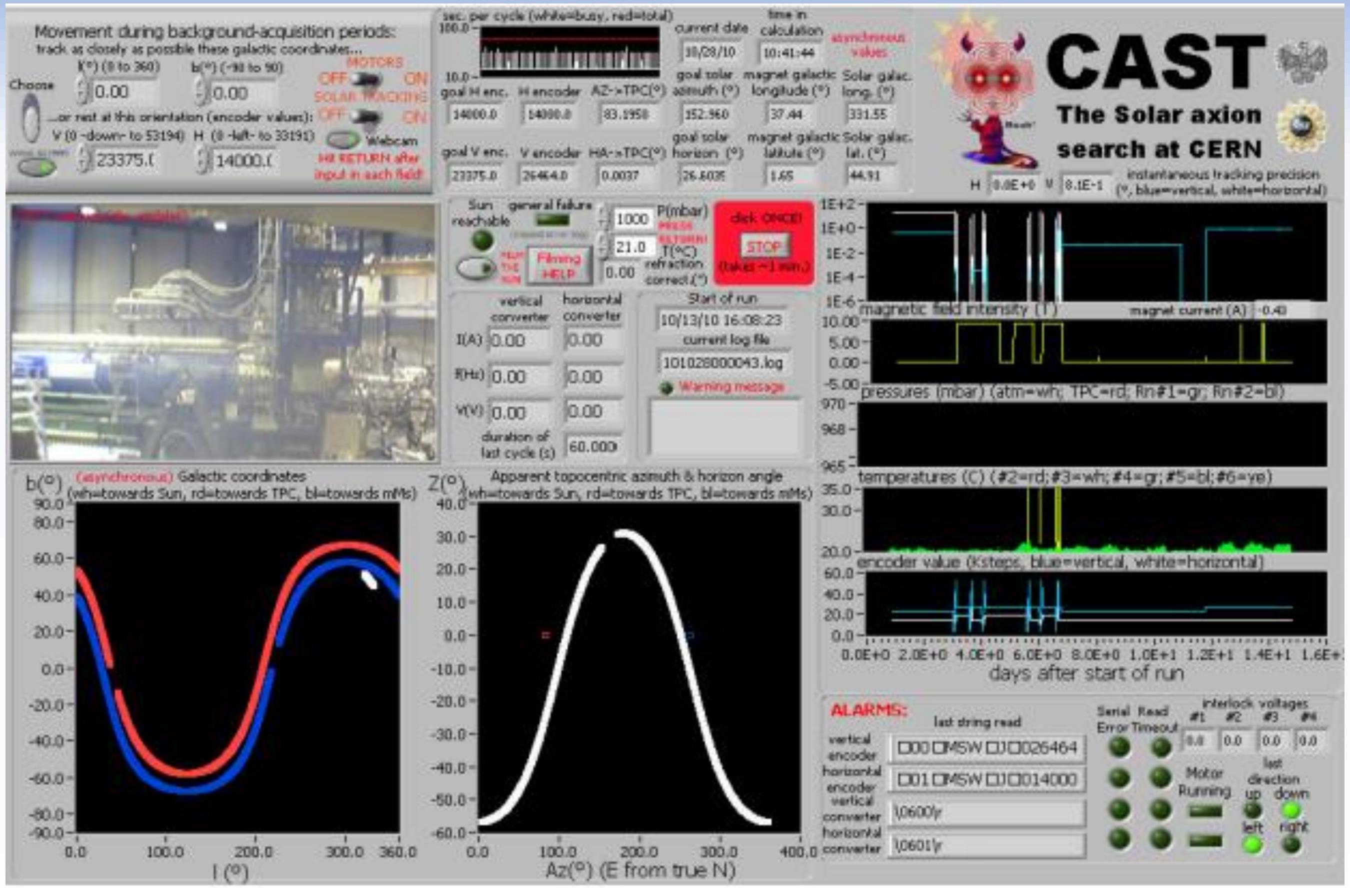

magnet positions to encoder values
1 vertical encoder unit = 30µm of magnet movement

Grid measurements and Sun filming

- independent magnet positions

  in a set of reference coordinates (GRID)
- green circle: required precision of 1 arcmin

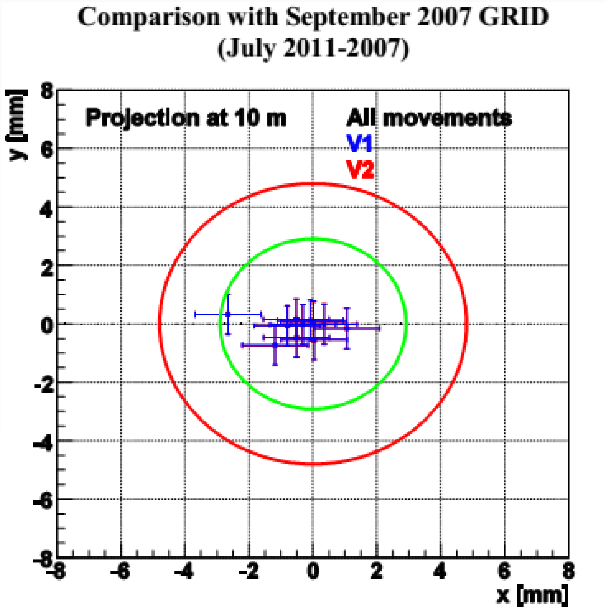

cross-check the tracking system precision: the Sun-filming

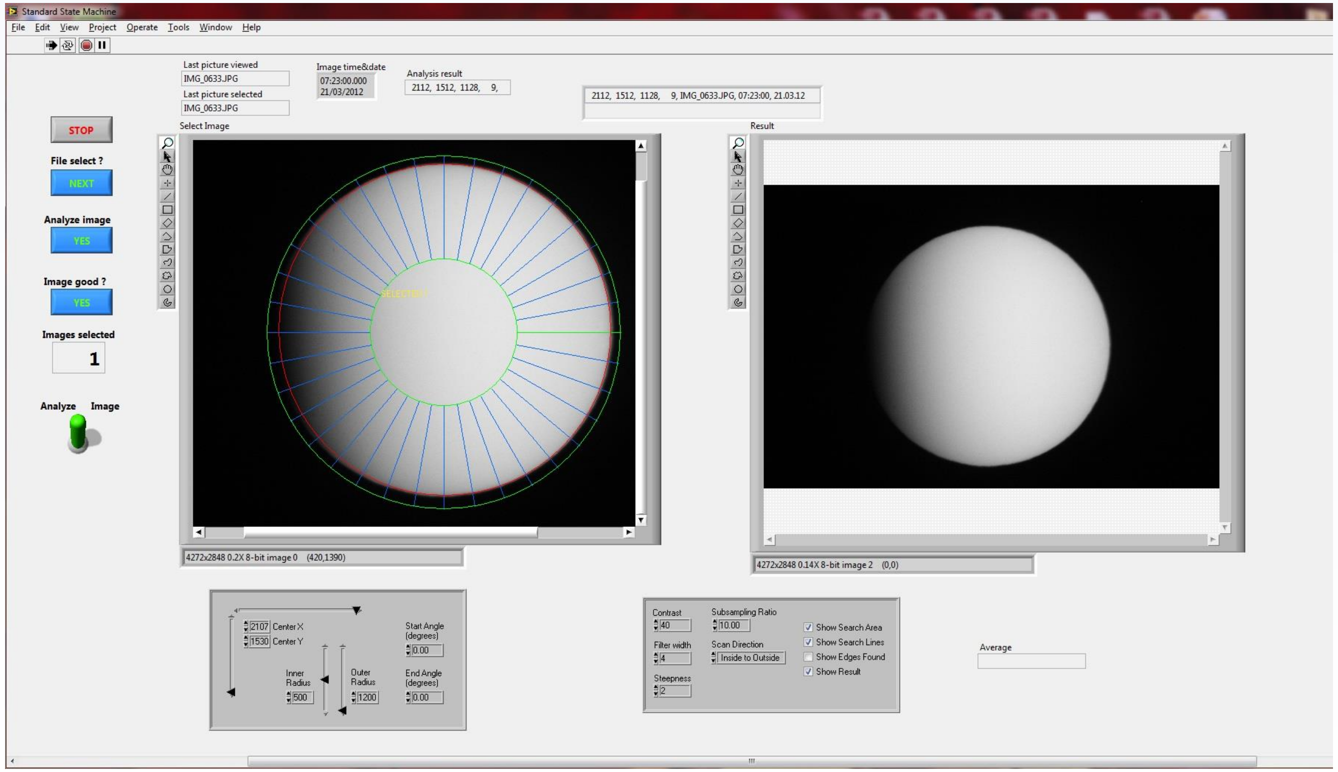

total estimated CAST tracking precision was better than 0.01º

Slow control of the CAST experiment

- Vacuum and cryostat pressure
- Pressures in the cold bores – detectors
- Various temperatures in different parts of the magnet
- Magnet movement parameters
- Magnet valves status (open or closed)
- Safety of the system and alarms

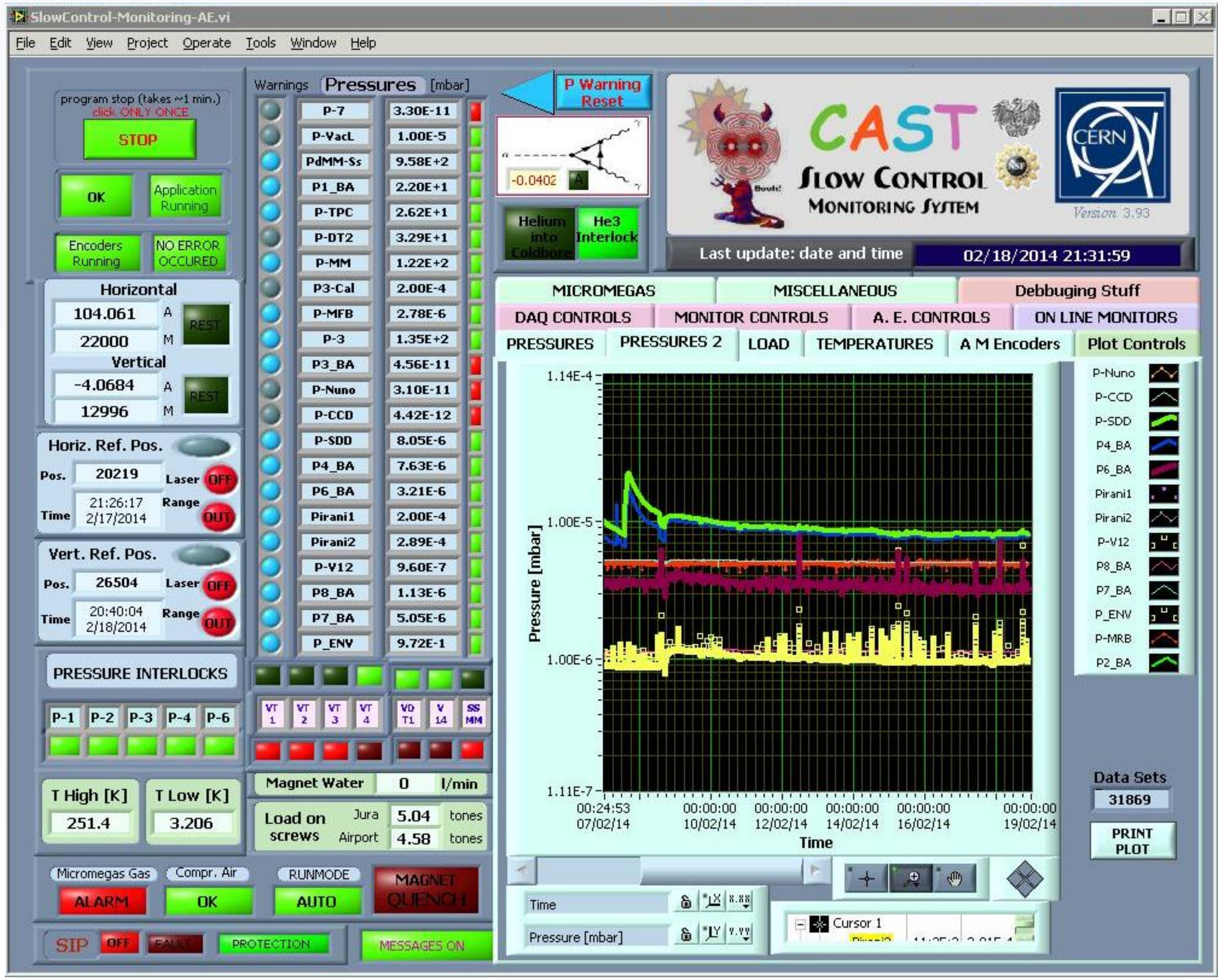

Typical values recorded every minute

Buffer Gas into the CAST coldbores

conversion probability inside a 10 m long pipe of magnetic field at 9T

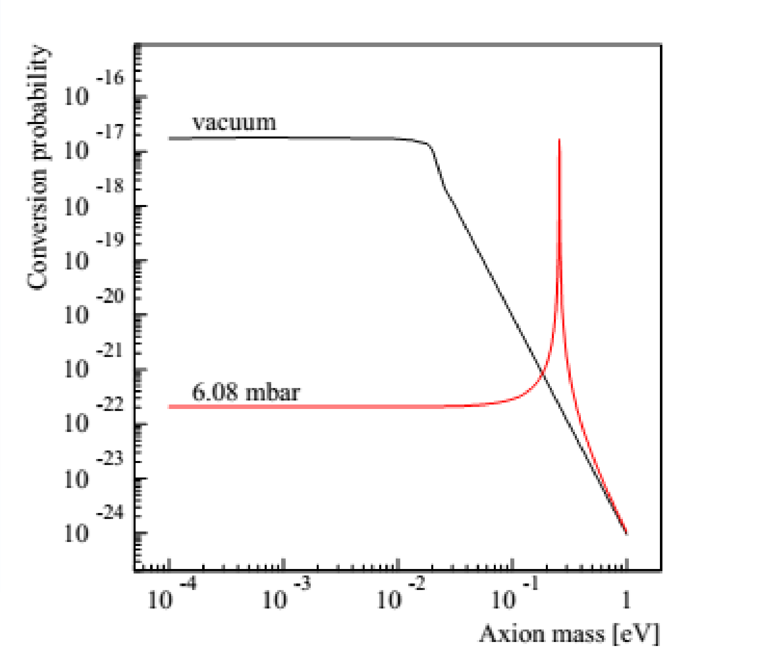

conversion probability for a uniform optical medium

$$P_{\alpha\to\gamma} = \left(\frac{g_{\alpha\gamma}B}{2}\right)^2 \frac{1}{q^2+\Gamma^2/4}\left[1+e^{-\Gamma L}-2e^{-\Gamma L/2}\cos qL\right]$$

L= magnet length, Γ=absorption coefficient

$$q = \left|\frac{m_\gamma^2 - m_\alpha^2}{2E_\alpha}\right|$$

In CAST phase I (vacuum), coherence was lost for m_a > 0.02 eV

By using a buffer gas such as helium, the photon velocity can be decreased to match the incoming axion velocity

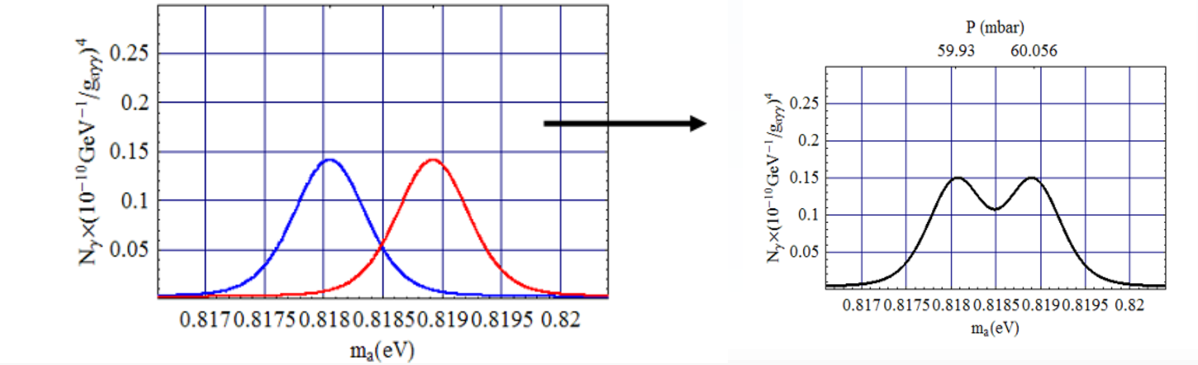

Physical Review Letters 107 (26), 261302

Density profile in the CB

The effective photon mass from Primakoff conversion is related directly to the square root of the gas density

$$\frac{m_\gamma}{c^2} \cong 23.4267\sqrt{\rho\left[\frac{g}{cm^3}\right]}\left[\frac{eV}{c^2}\right]$$

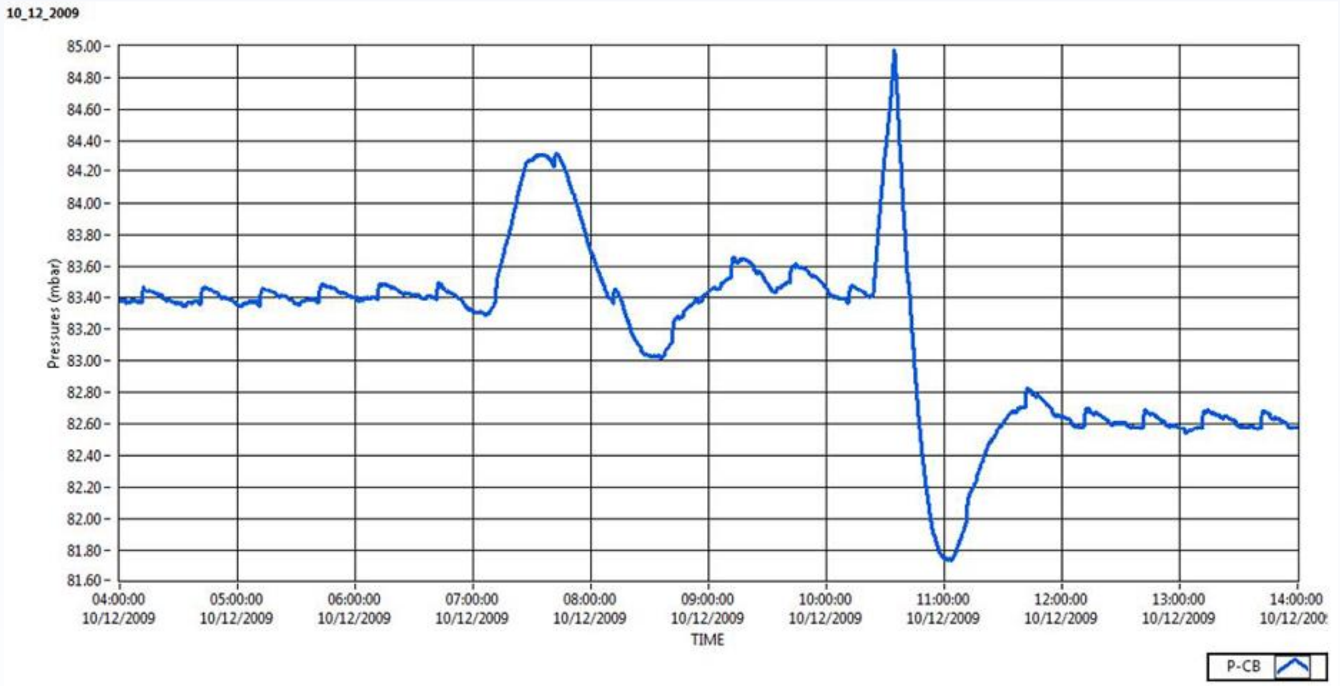

A vertical movement of the magnet of +6 degrees at 37mbars causes a shift in P_{cb} of about +1.05 mbar

The actual **density profile** which is needed to directly calculate the coherence length cannot be measured directly

Computational Fluid Dynamics (CFD) simulations

The ^{3}He gas system

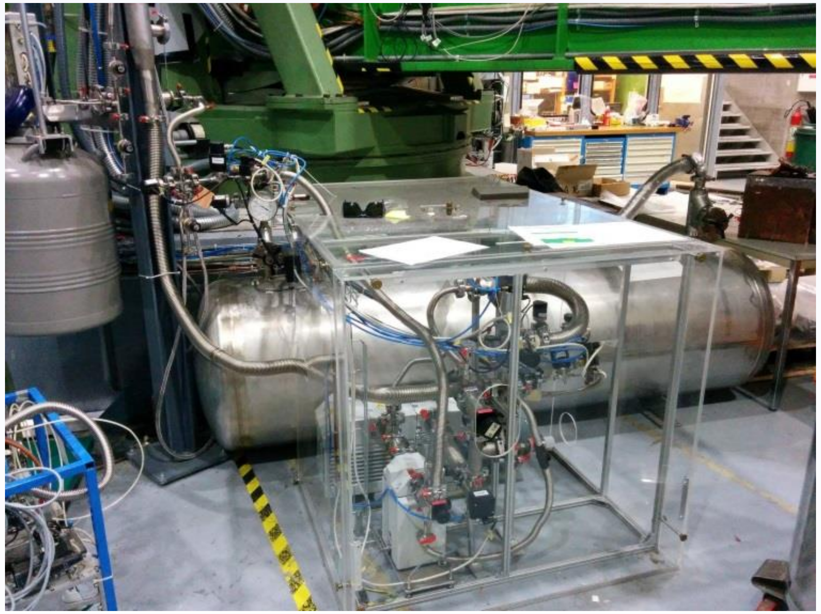

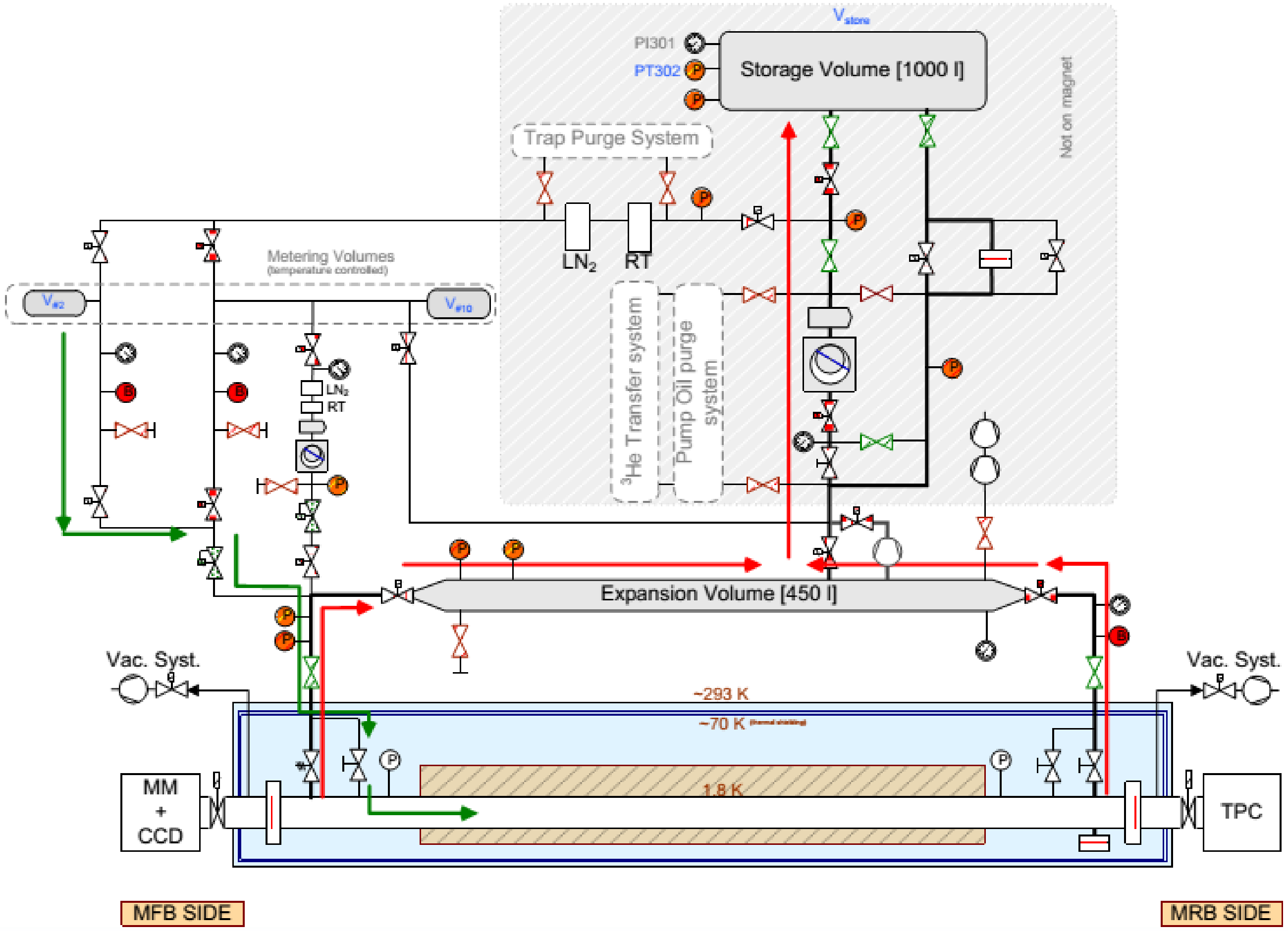

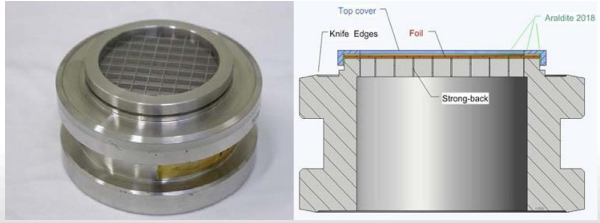

^{3}He gas system had to be accurate, stable and capable to precisely measuring small quantities of gas inserted into the cold bore volume in a reproducible way.

Pressure setting --0.08 mbar

^{3}He CFD simulations for CAST (heat transfer and turbulence)

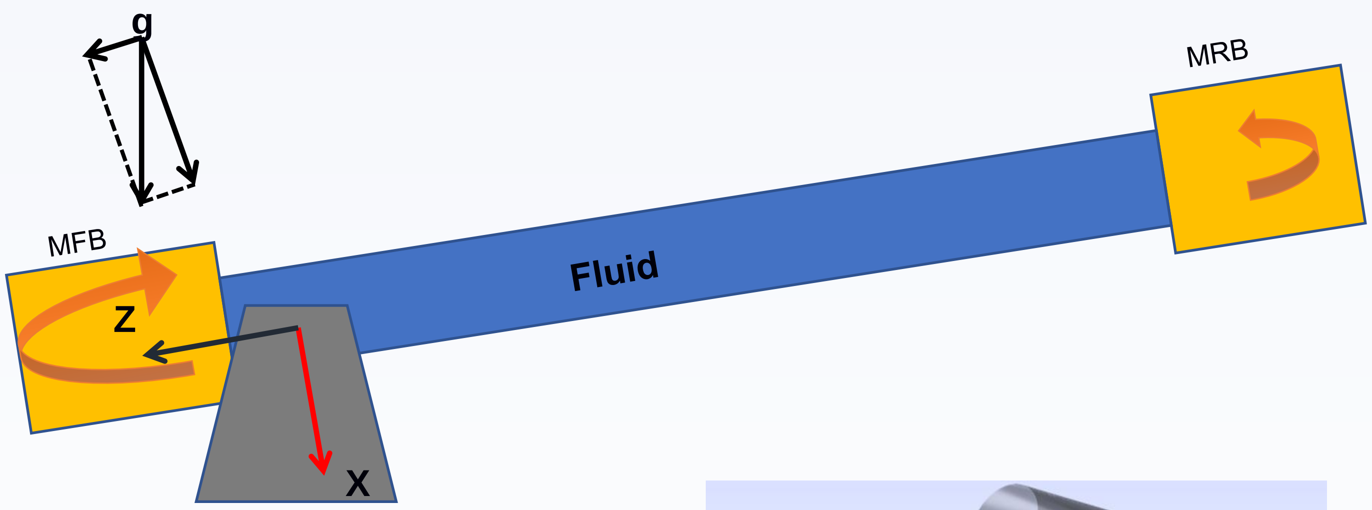

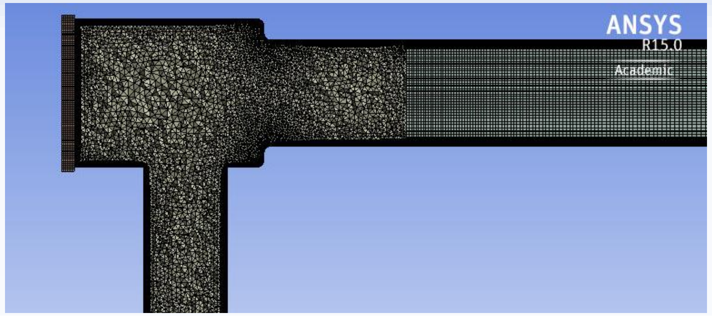

Peng-Robinson equation of state:

$$P = \frac{RT}{V_m - b} - \frac{a(T)}{V_m^2 + 2V_m b - b^2}$$

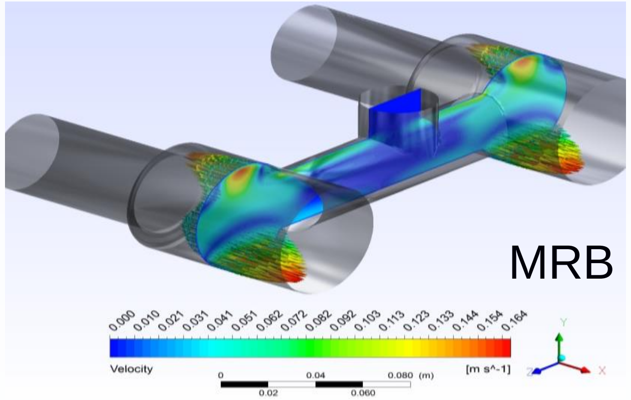

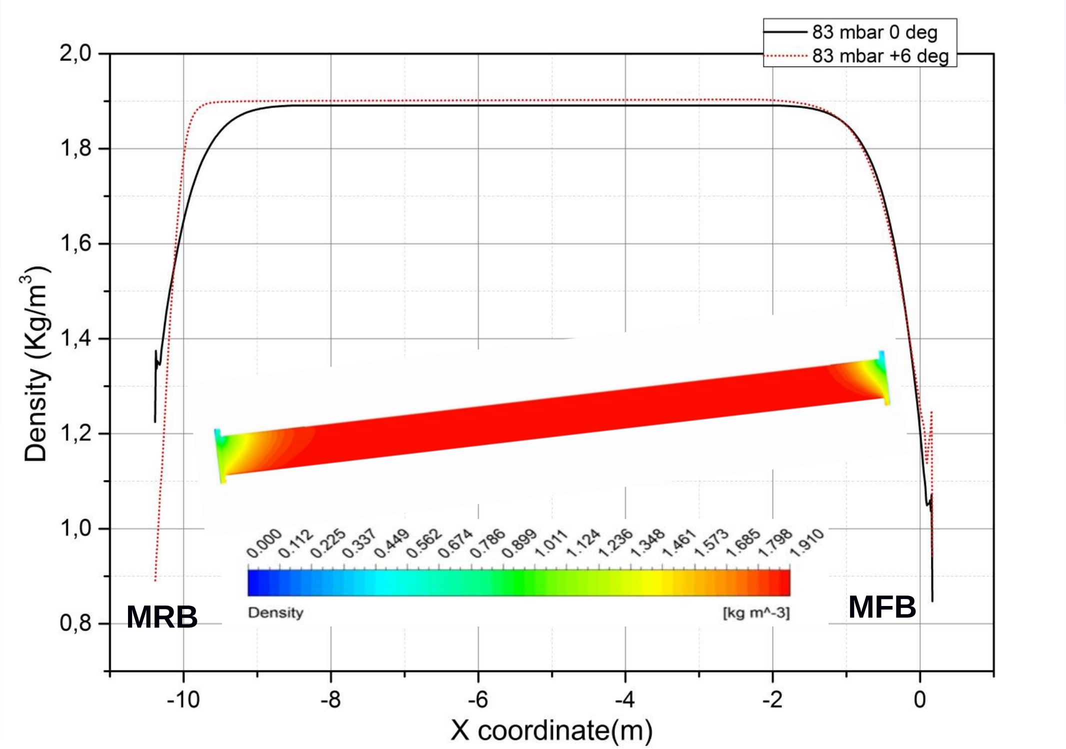

Extensive simulations for a most detailed model of the system under the different configuration

Density distributions along the center longitudinal line of the model

CAST Detectors

axion signal:
Excess of X-ray in tracking over background

$$N_\gamma = \int \frac{\mathrm{d}\Phi_a}{\mathrm{d}E} P_{\alpha\to\gamma} A t \mathrm{d}E$$

- ❑ time projection chamber (TPC)
- ❑ gaseous chamber Micromegas
- ❑ charge coupled device (CCD)

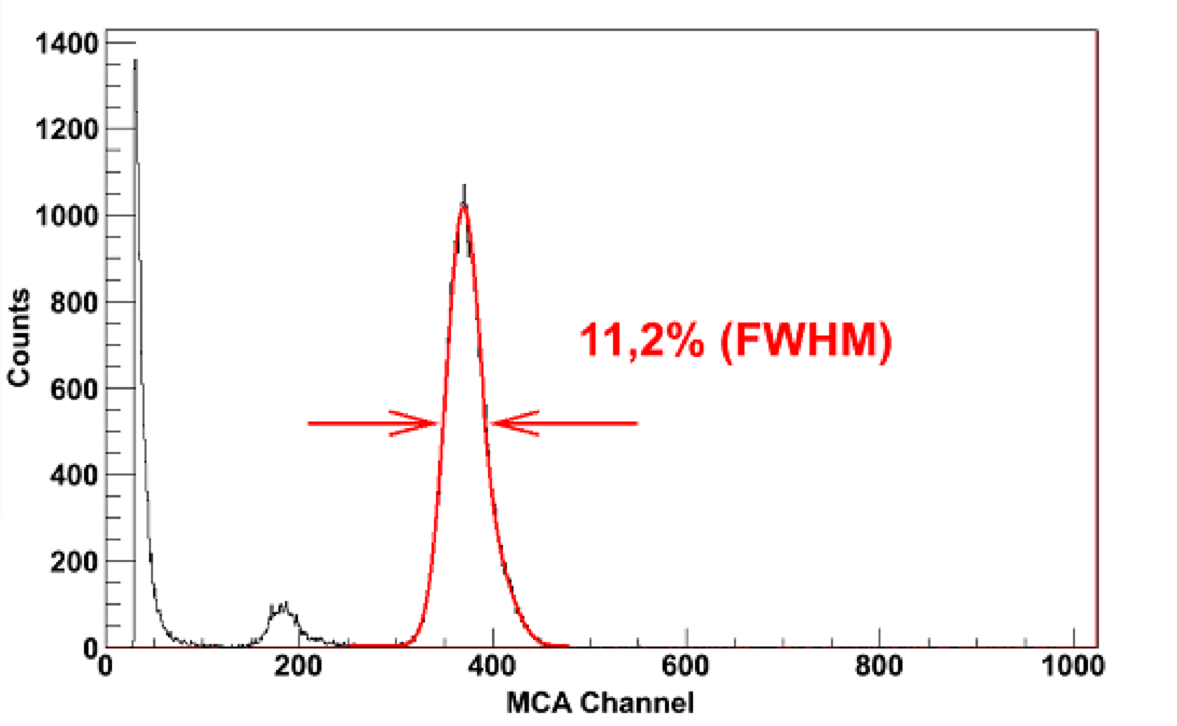

X-ray telescope of the CAST experiment

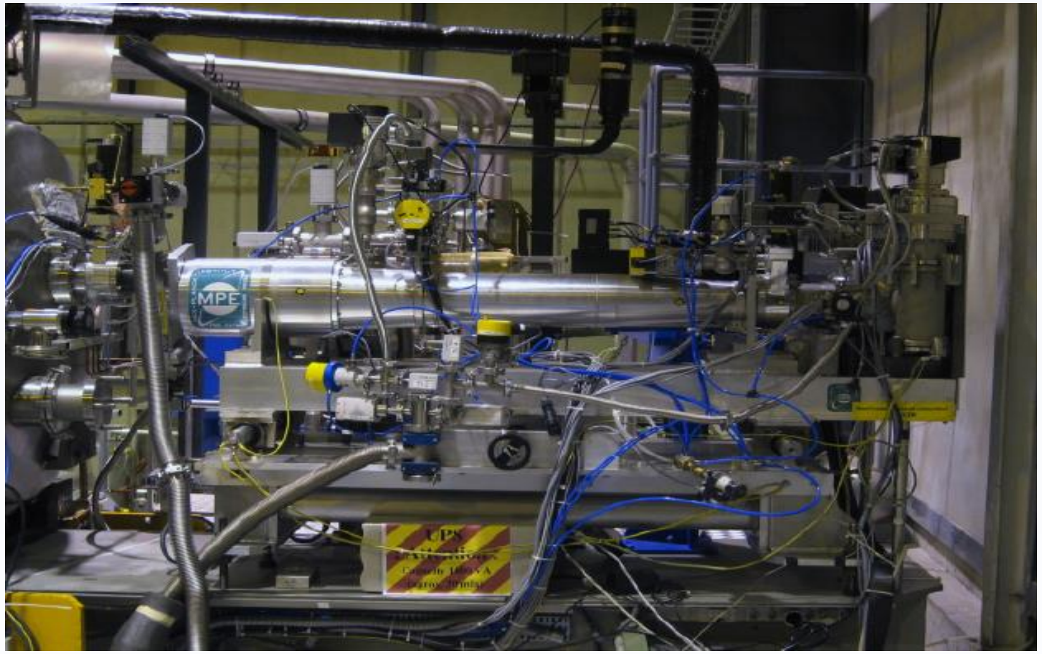

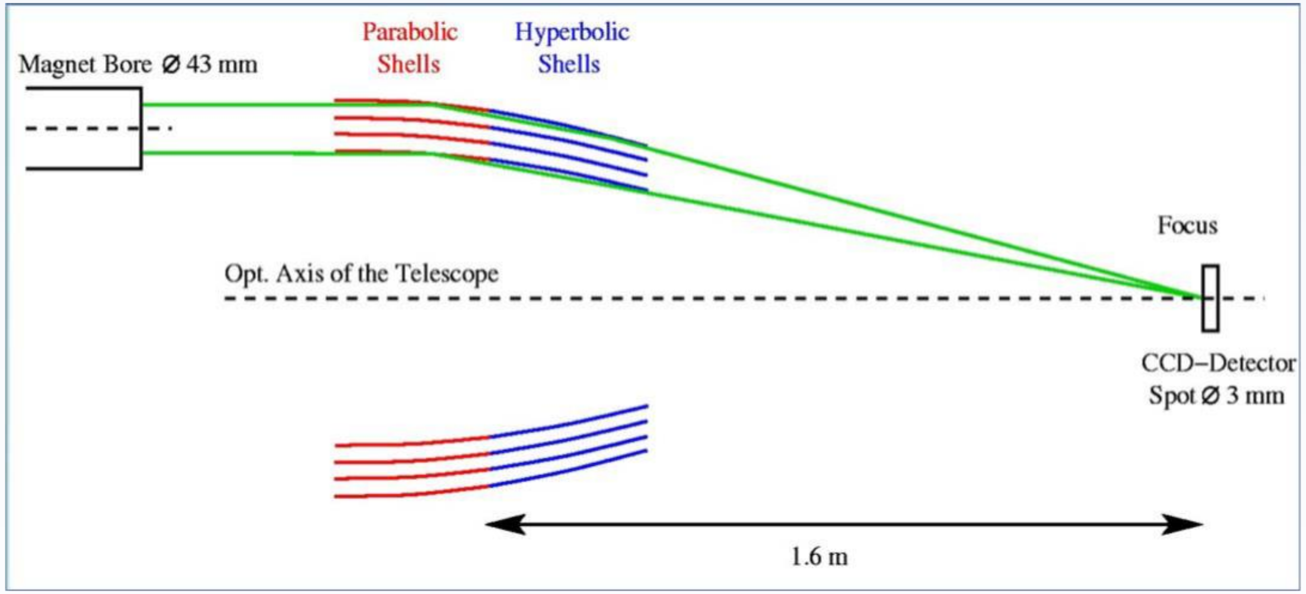

S/B improvement of ~150!

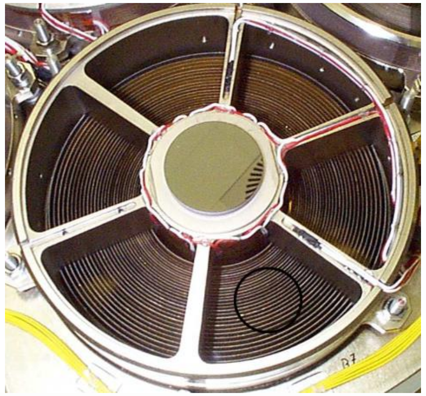

Wolter-I-type telescope (Prototype of ABRIXAS mission)
- 27 nested, gold-coated mirror shells
- Only one sector of telescope illuminated at CAST

pn-CCD (Prototype of XMM-Newton mission)
- Very good spatial and energy resolution
- Simultaneous measurement of signal and background

Charged Coupled Device (CCD) and the X-ray telescope

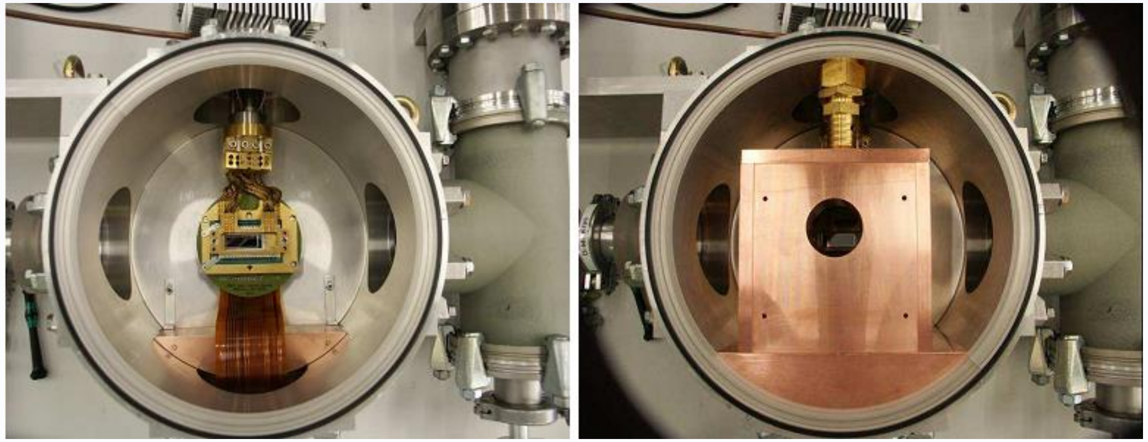

1×3 cm^2 sensitive area
64 × 200 pixels
280 **m**m thick
14 frames/sec

Tracking

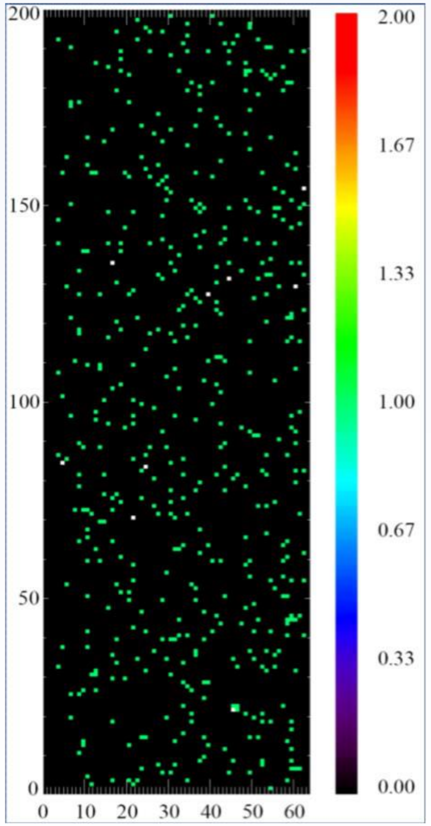

Background

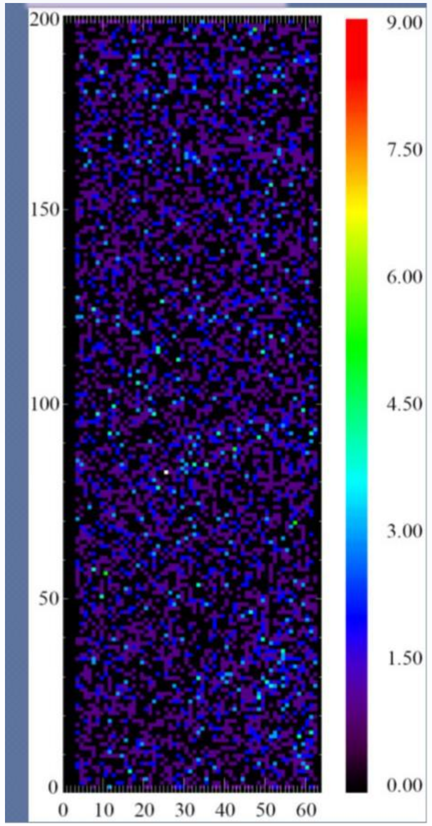

Signal simulation

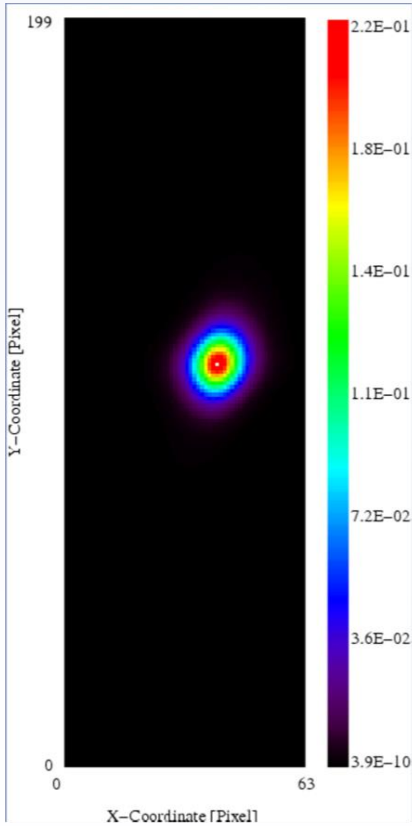

- Lower background (better selection of materials)
- Lower threshold (~200 eV)
- Better E resolution (<160 eV (FWHM) @ 6 keV)
- State of the art technology

Micromegas detectors (MICRO MEsh GAseous Structure)

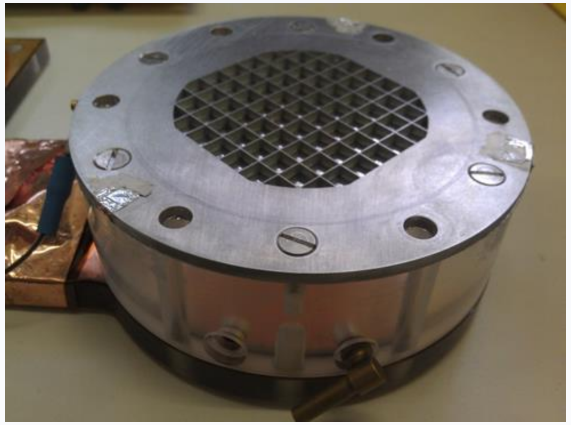

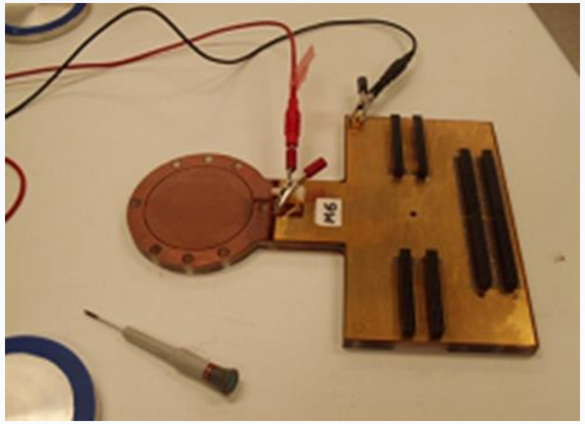

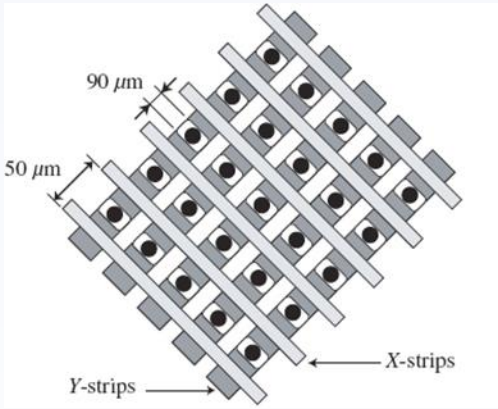

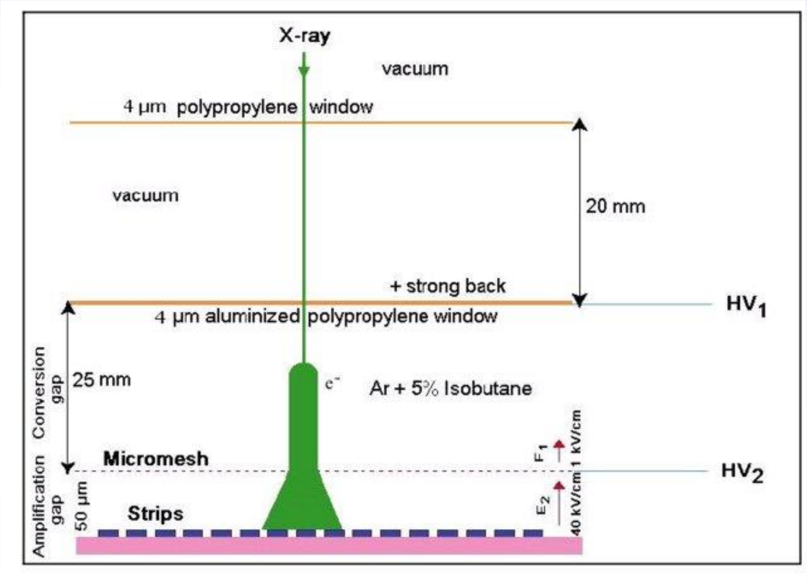

Micromegas area : 33.9 cm^2
Magnet cold-bore area : 14.55 cm^2

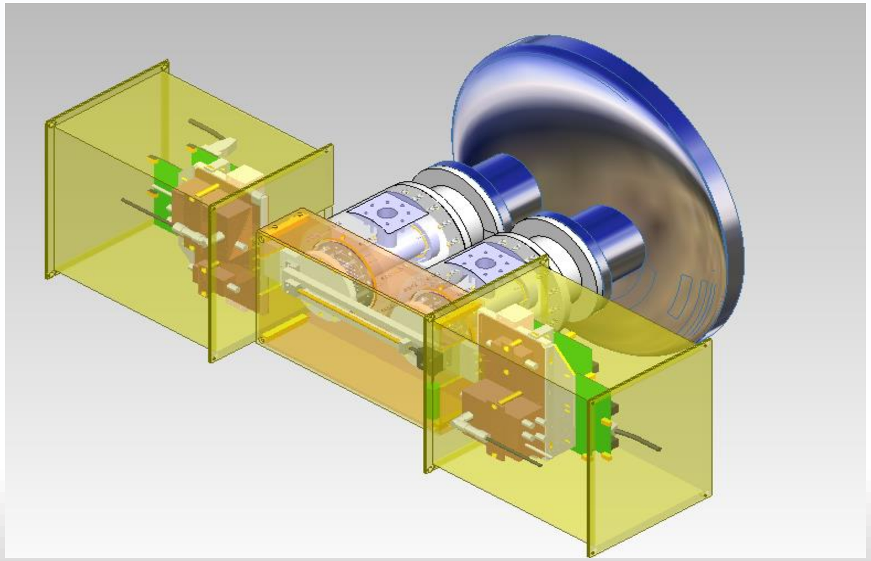

- The track time resolution of a Micromegas detector is ~ 0.60 ns
- Very stable operation during long periods
- The space resolution is less than 100 µm.
- High counting rate capabilities.
- sparking probability is now reduced

Typical rate: <2 c/h

Nobel Prize, for the invention of the MultiWire Proportional Chamber (MWPC) by G. Charpak in 1968

Micromegas detectors -- Sunrise

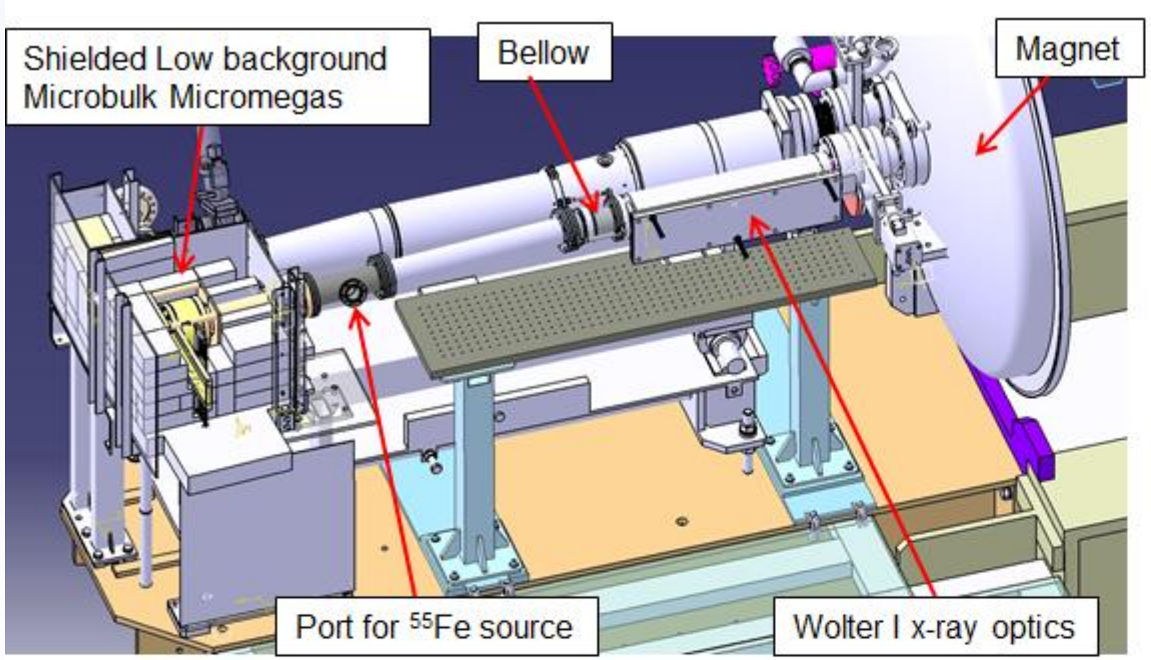

^{55}Fe calibration

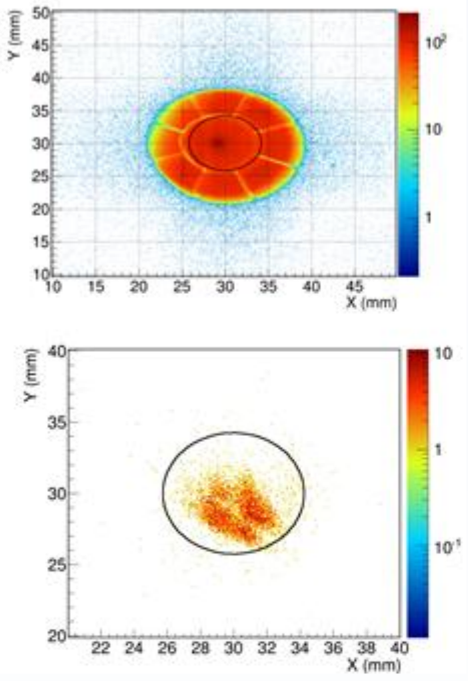

^{55}Fe calibration @13 m

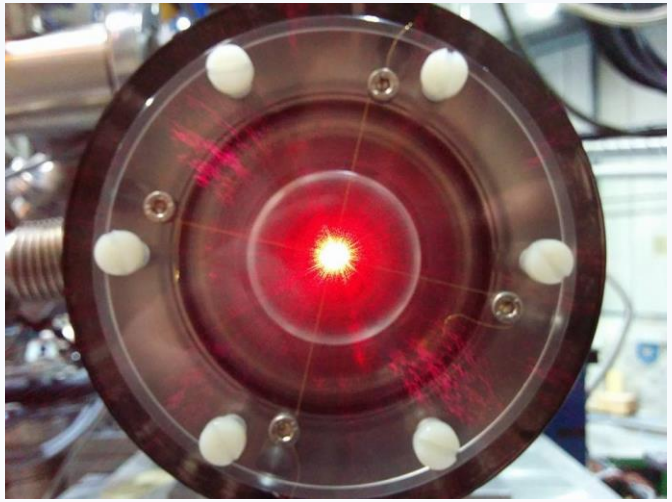

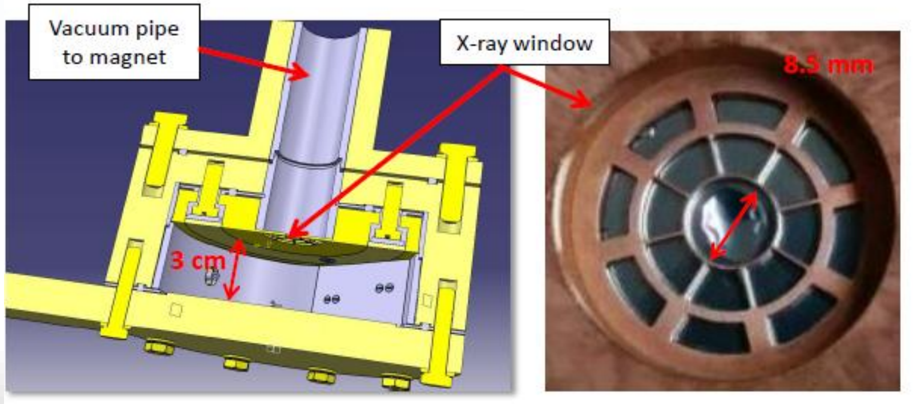

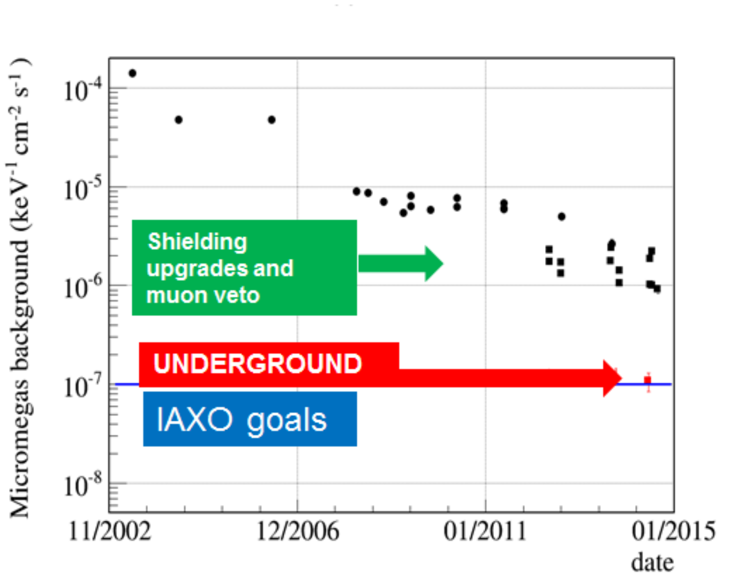

Improving Micromegas: InGrid X-ray Detector

X-ray detector based on the combination of an integrated Micromegas stage with a pixel chip

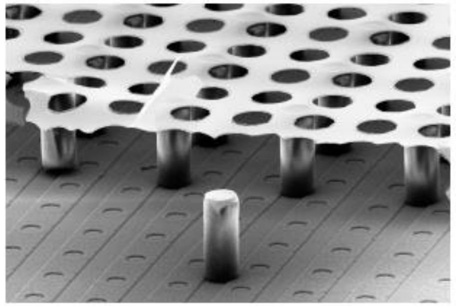

(a)

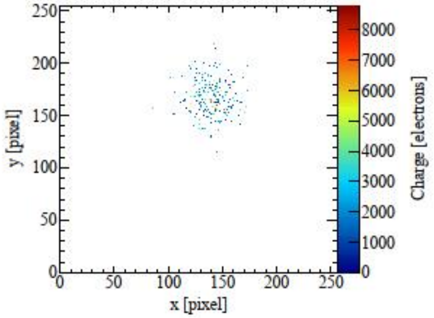

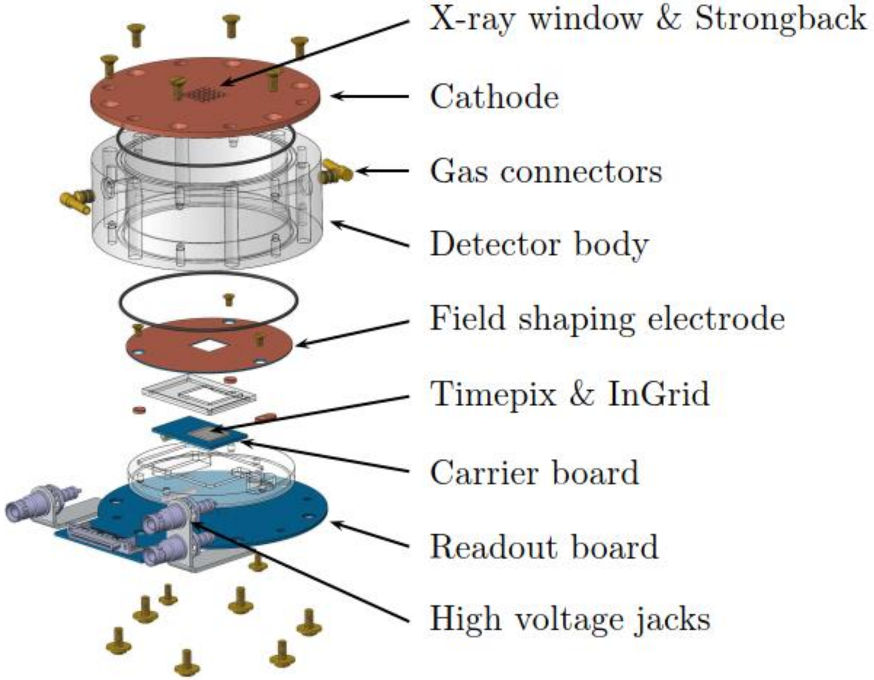

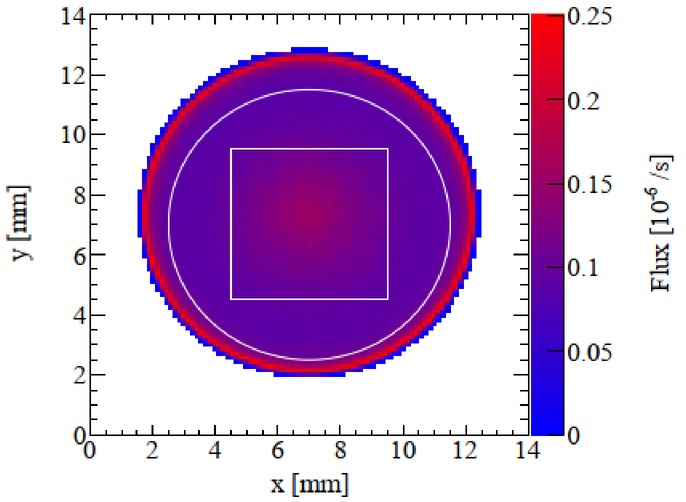

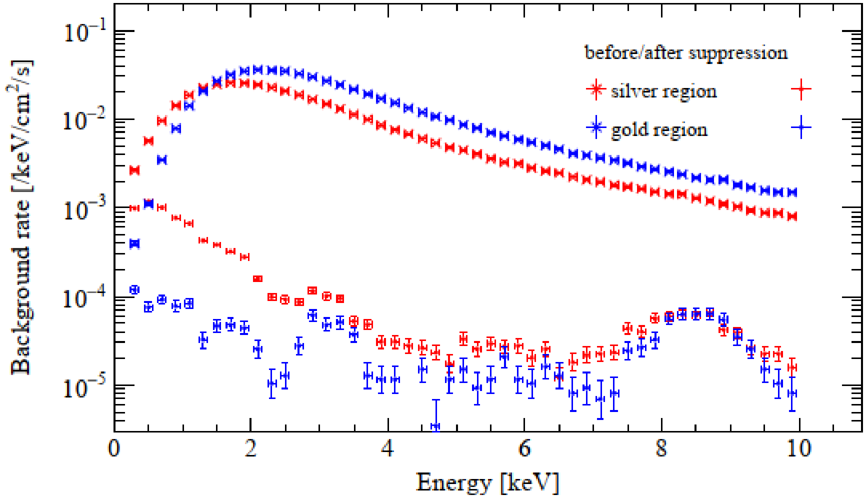

1×2 cm² sensitive area
256 × 256 pixels

CAST → IAXO (International Axion Observatory)

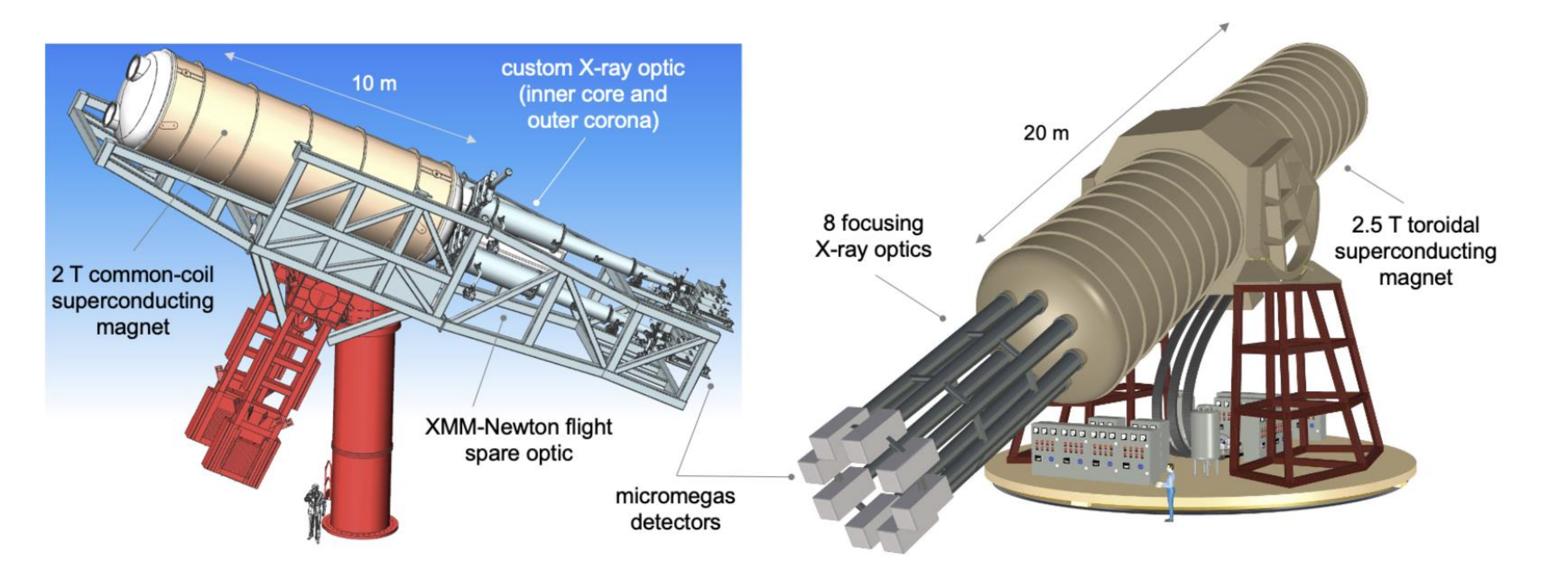

BabyIAXO (left) and IAXO (right)
A next-generation axion helioscope, designed to search for axions from the Sun that are reconverted into X-ray photons via a strong laboratory magnetic field

IAXO: factor of 20 improvement in sensitivity

BabyIAXO : factor of 5 improvement in sensitivity

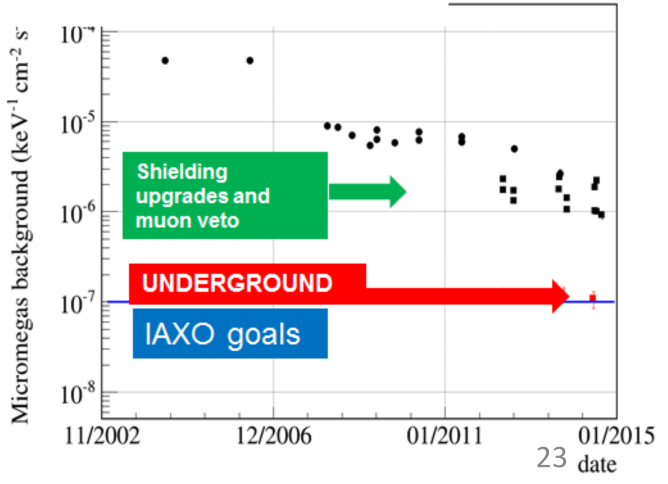

CAST 2019 → axion Haloscope

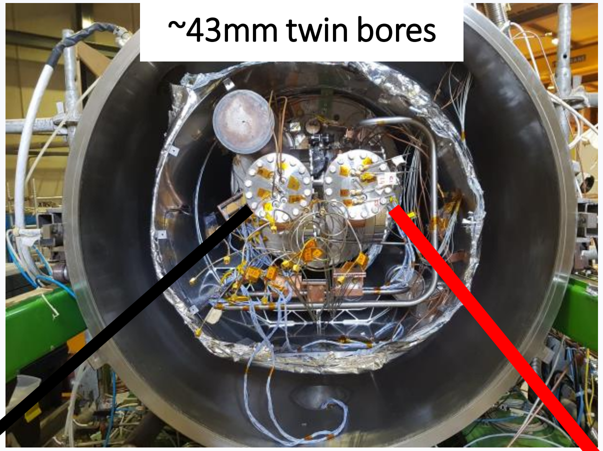

23 x 25 x 390 mm
$V = 224 \cdot 10^{-6}\ m^3$
$Q_L = 20000$
$T_{SYS} = 10\ K$
$C = 0.53$

CAST-RADES

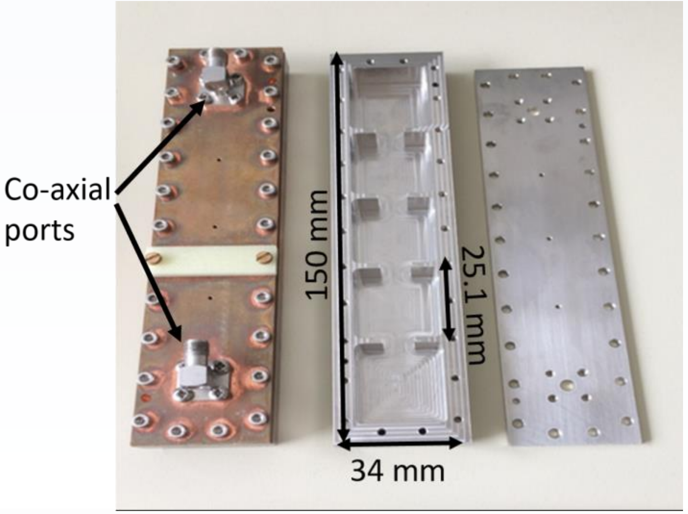

CAST-CAPP

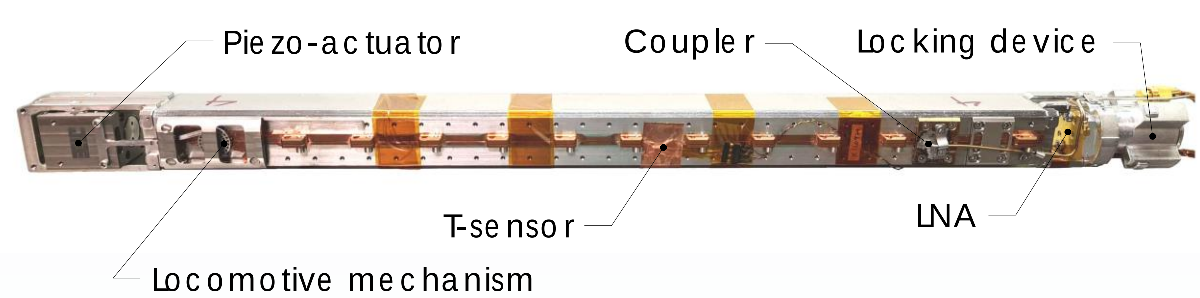

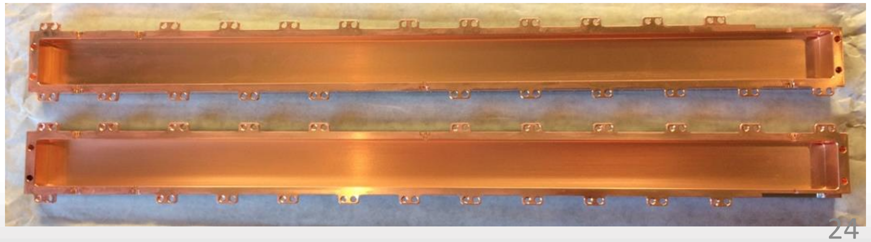

CAST-CAPP haloscope

- ✓ Phase-matching of all four cavities.
- ✓ Fast resonance scanning.
- ✓ Unexplored parameter space.

"phase matching" technique by combining coherently the power outputs of each frequency-matched cavity after individual signal amplification

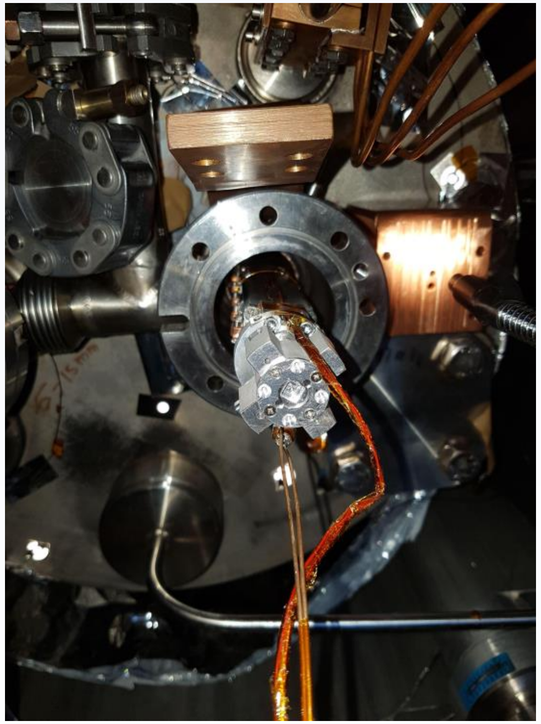

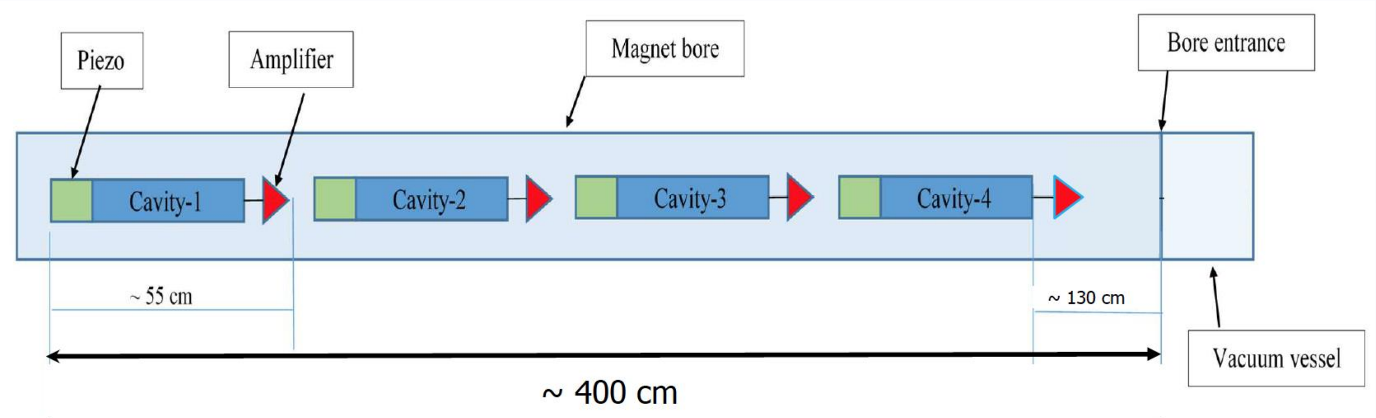

- Electromagnetic mode of interest : TE_{101}
- Frequency range: ~4.8 – 5.4 GHz (660 MHz)
- Axion mass range: ~19.7 – 22.4 μeV
- Resolution: 100 Hz
- Max piezo speed: 10 MHz / min

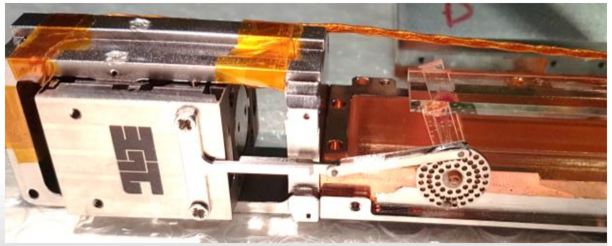

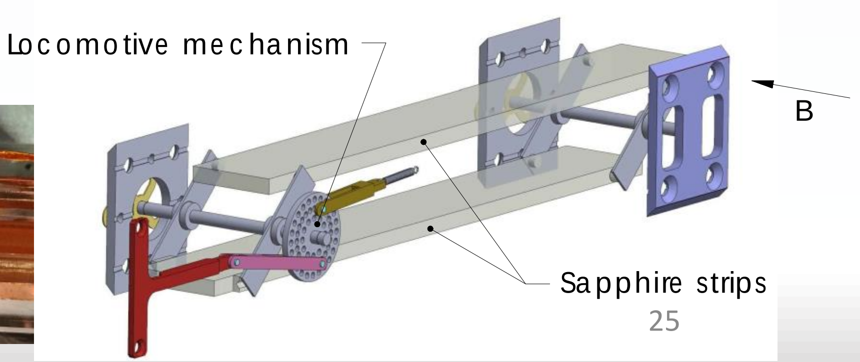

Detection scheme of CAST-CAPP

- CAST-CAPP diagram:
  - CAST cryostat layers (colors)
  - Cavities aligned in magnet bore
  - Cold and warm amplifiers
  - Power combiner
- 2nd receiver channel setup for environmental EMI

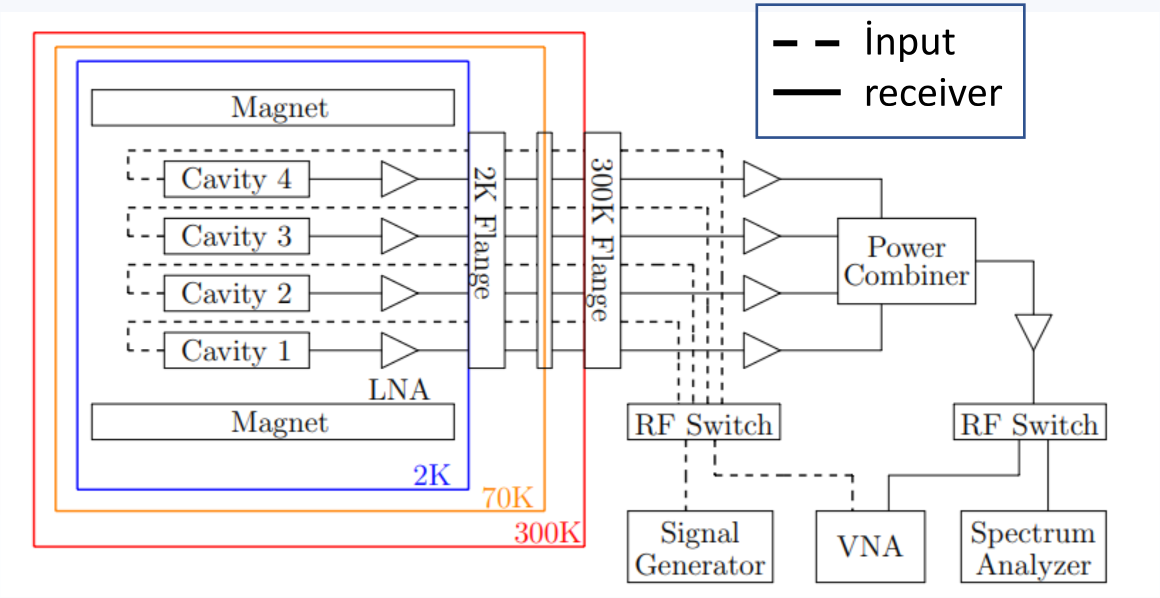

Vector Network Analyzer

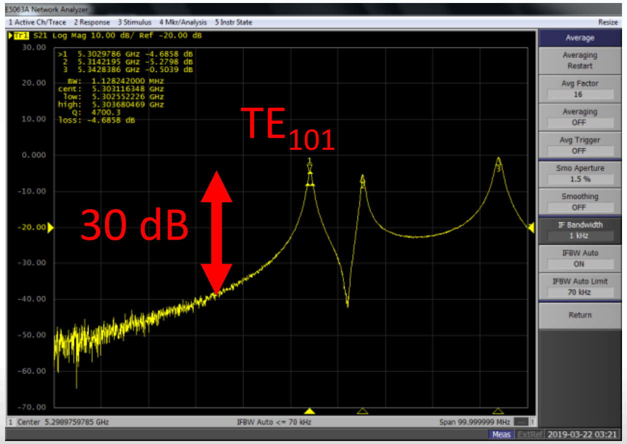

Spectrum Analyzer

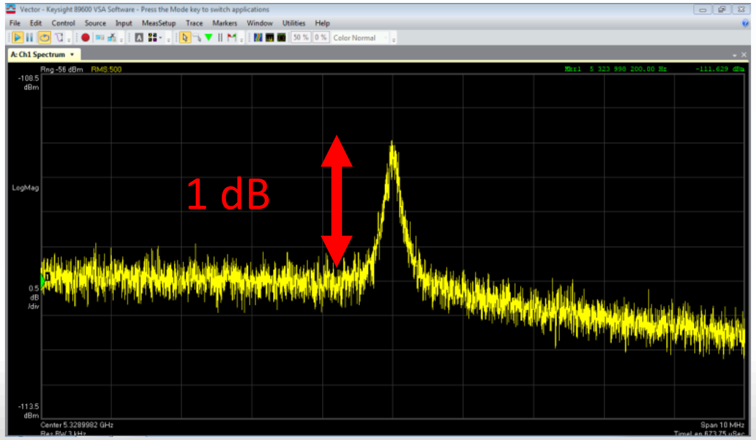

CAST axion limits and major publications

2013–2015 run

2019 to 2021 run

$g_{\alpha\gamma} \leq 3.3 \times 10^{-10}\ GeV^{-1}$ at 95% CL.
0.64–1.17 eV

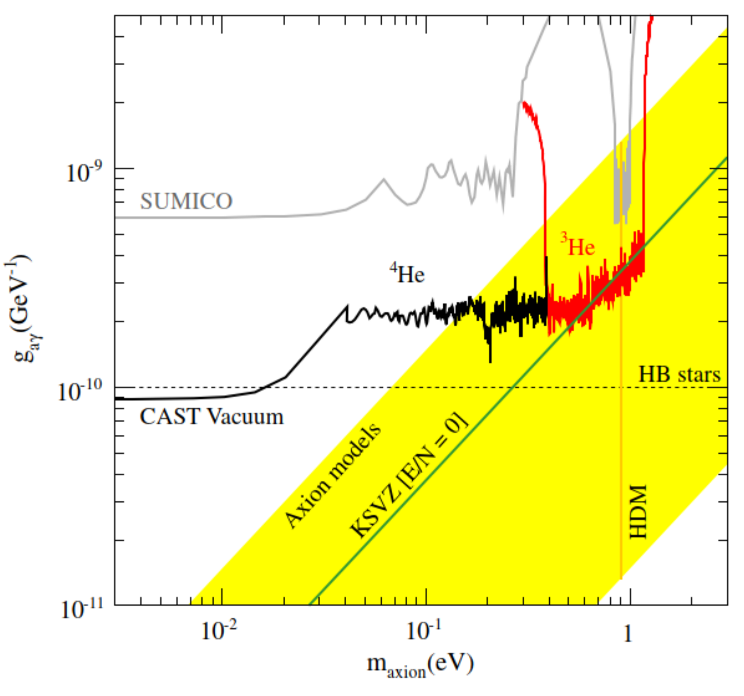

PRL 112, 091302 (2014)

$g_{\alpha\gamma} \leq 0.66 \times 10^{-10}$ GeV at 95% CL.
$m_a \lesssim 0.02$ eV

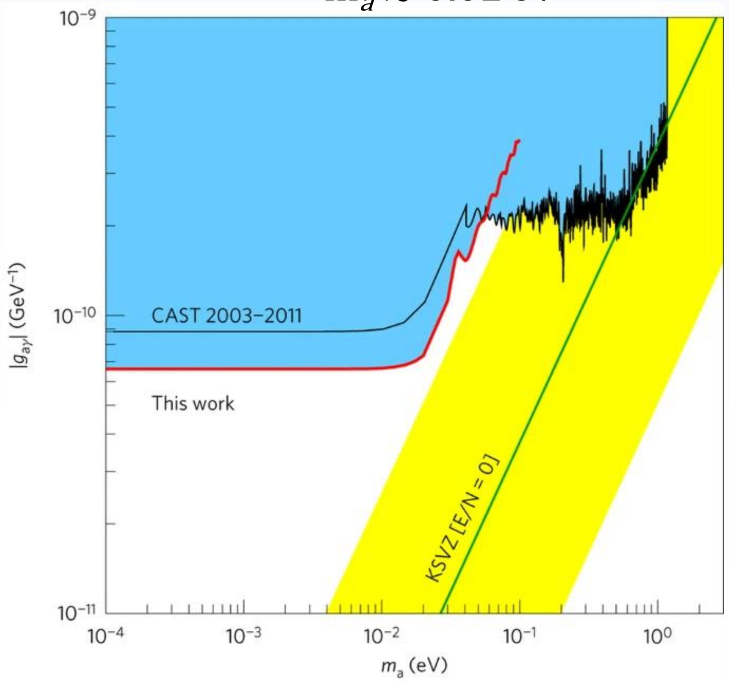

Nature Phys. 13 (2017) 584-590

$g_{\alpha\gamma} \leq 8 \times 10^{-14}\ GeV^{-1}$ at 90% CL.
19.74 μeV and 22.47 μeV

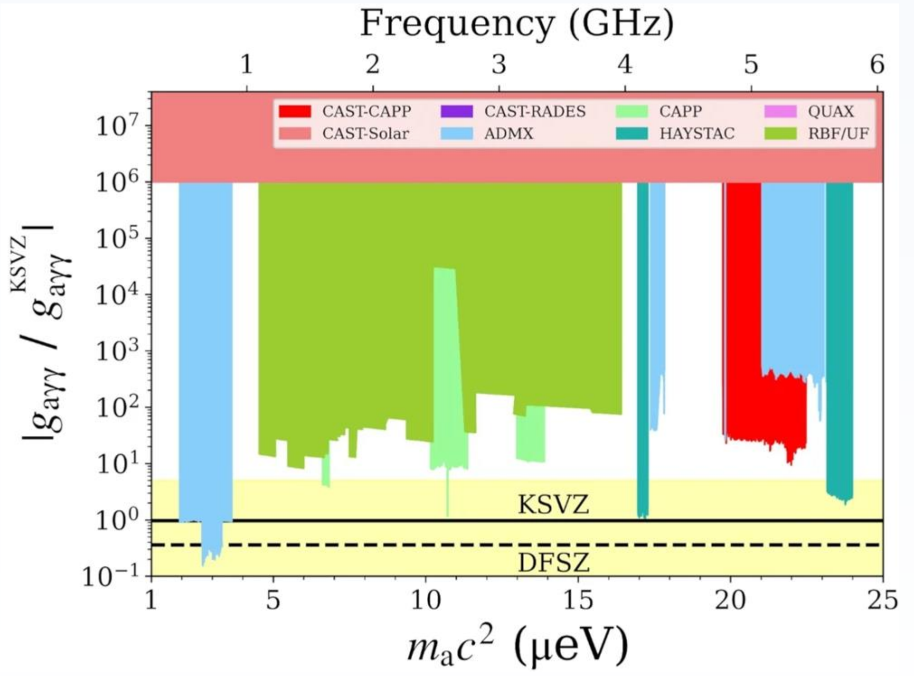

Nat Commun 13, 6180 (2022)

Detection of Solar Chameleons through Radiation Pressure

A force sensor that is called KWISP for “Kinetic WISP detection” (Weakly Interactive slim Particles)

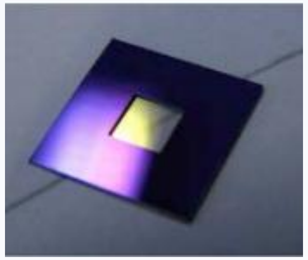

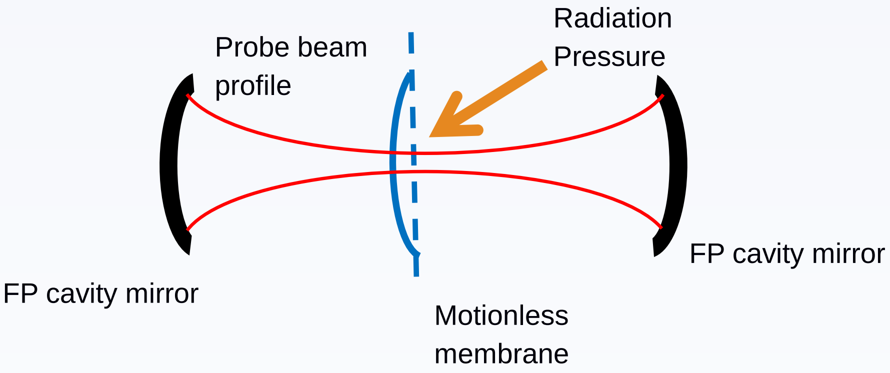

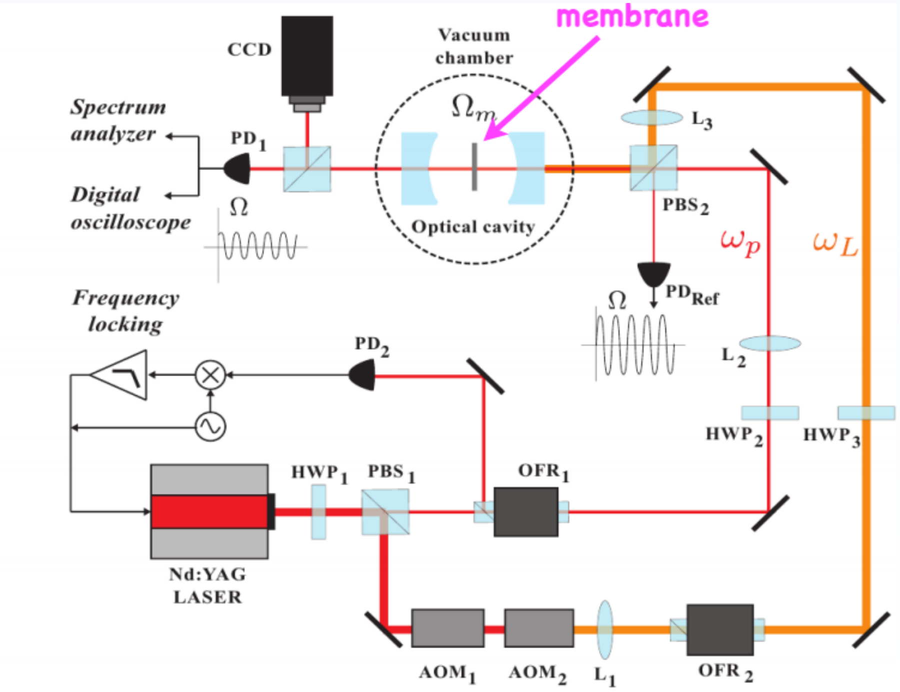

Commercially available

- "large" area, up to 5x5 mm
- Transparent @1064 nm
- Density ~ 3 g/cm3
- Can be coated with metal
- High stress
- High resonant frequency
- High mechanical Q ~ 10

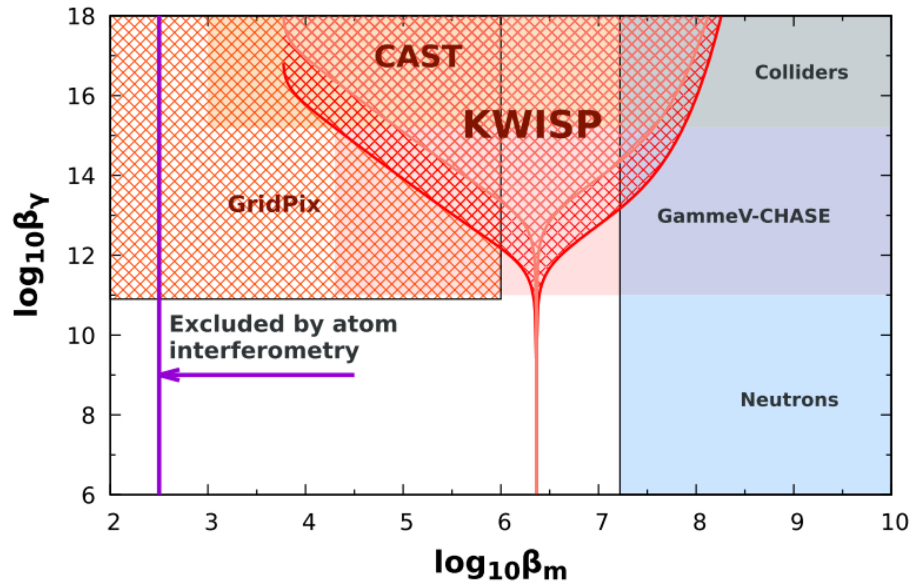

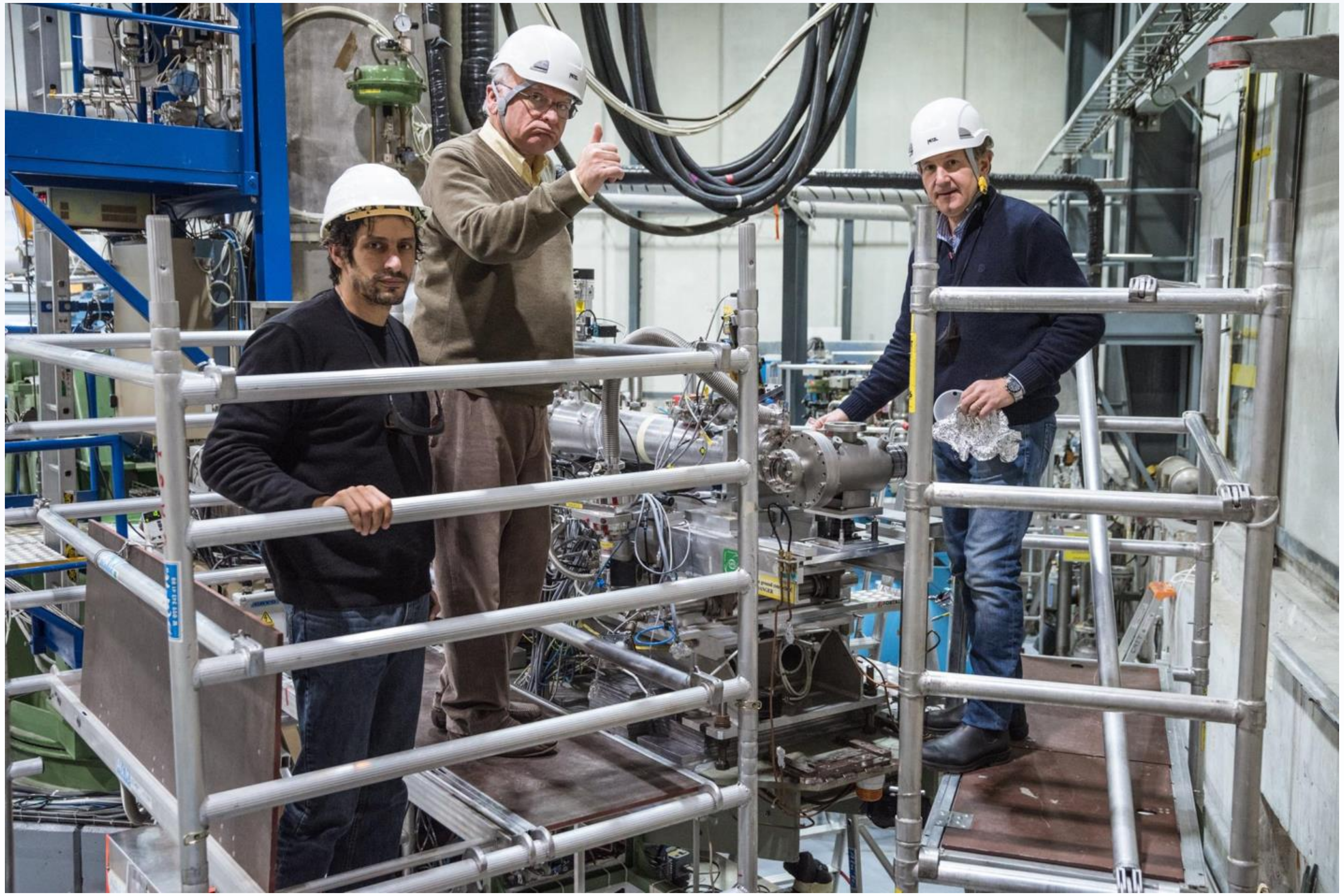

02/2016

Dielectric Haloscopes

(post-inflationary scenario) N_{DW}=1
40 to 180 μeV

Nat. Commun. **13**, 1049 (**2022**)

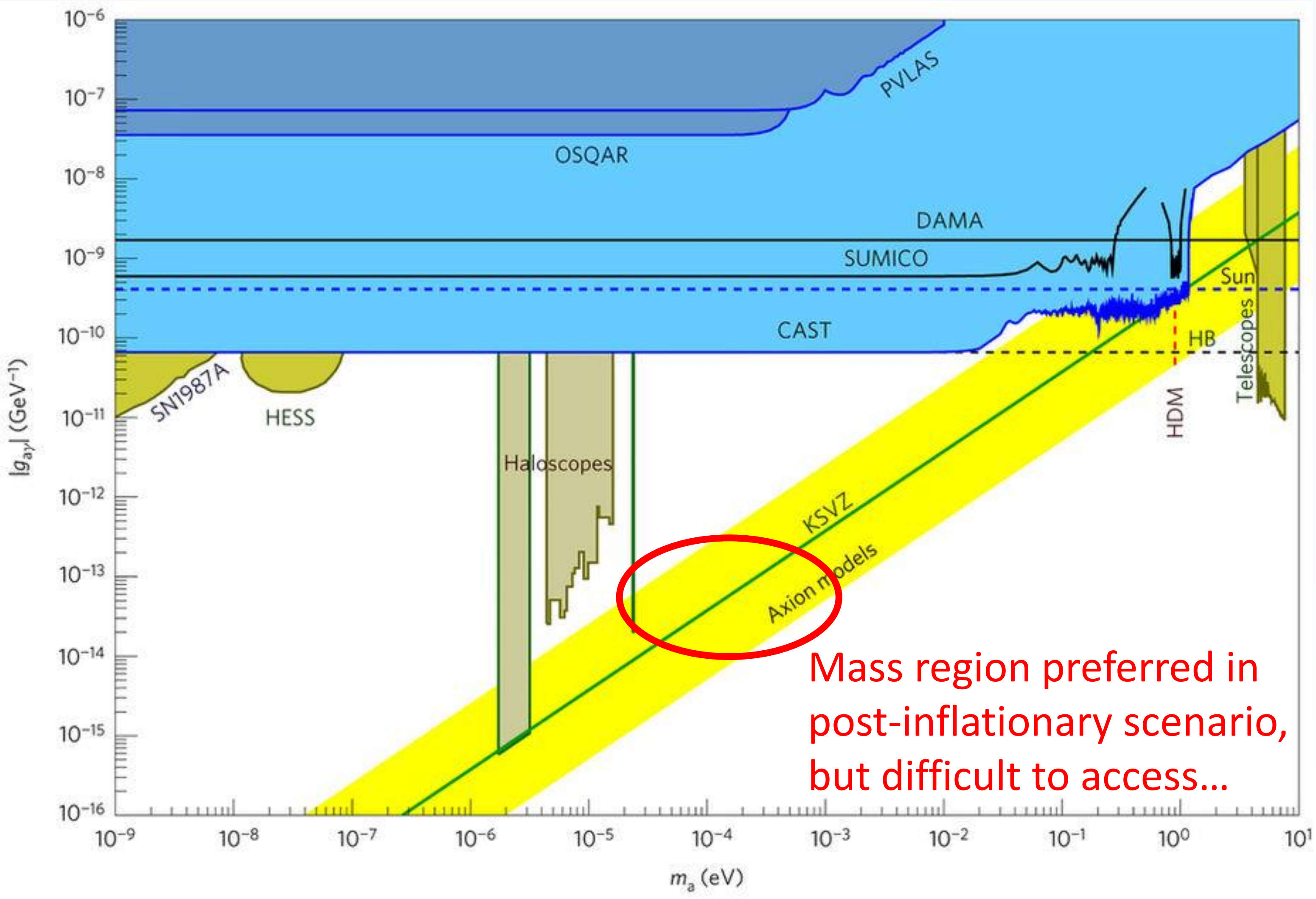

For domain wall number N_{DW}>1
28 μeV to meV

Andreas Ringwald and Ken'ichi Saikawa
Phys. Rev. D 93, 085031
…

Dielectric Haloscopes

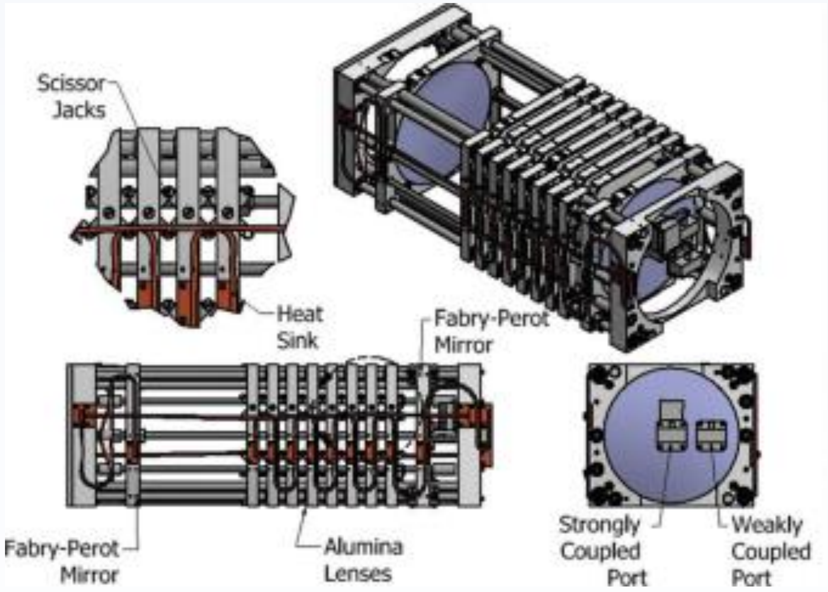

ADMX-Orpheus

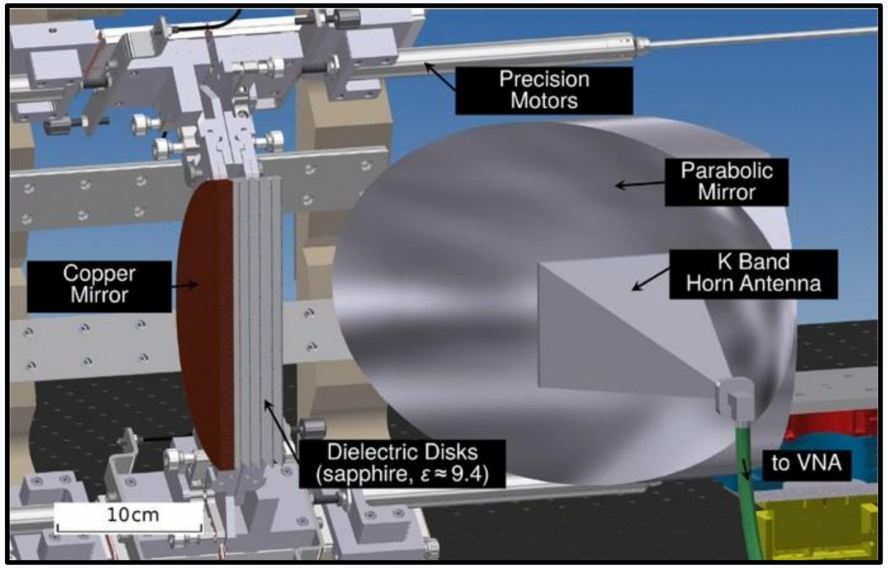

MADMAX

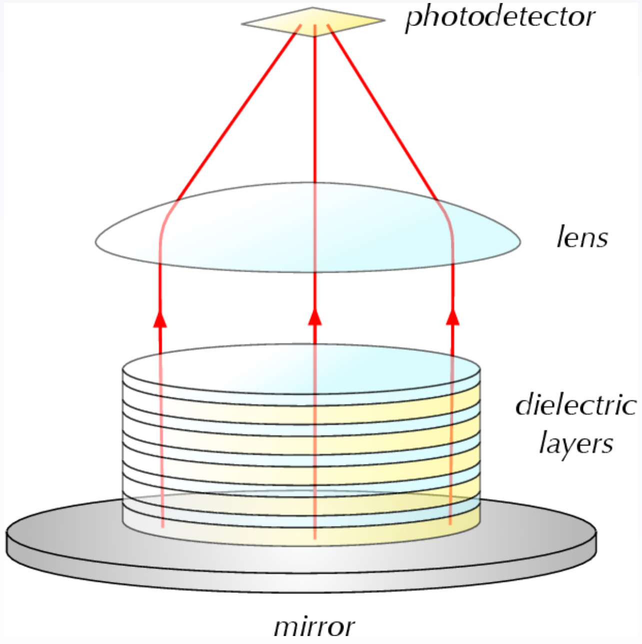

MuDHI

Dielectric Haloscopes - MADMAX

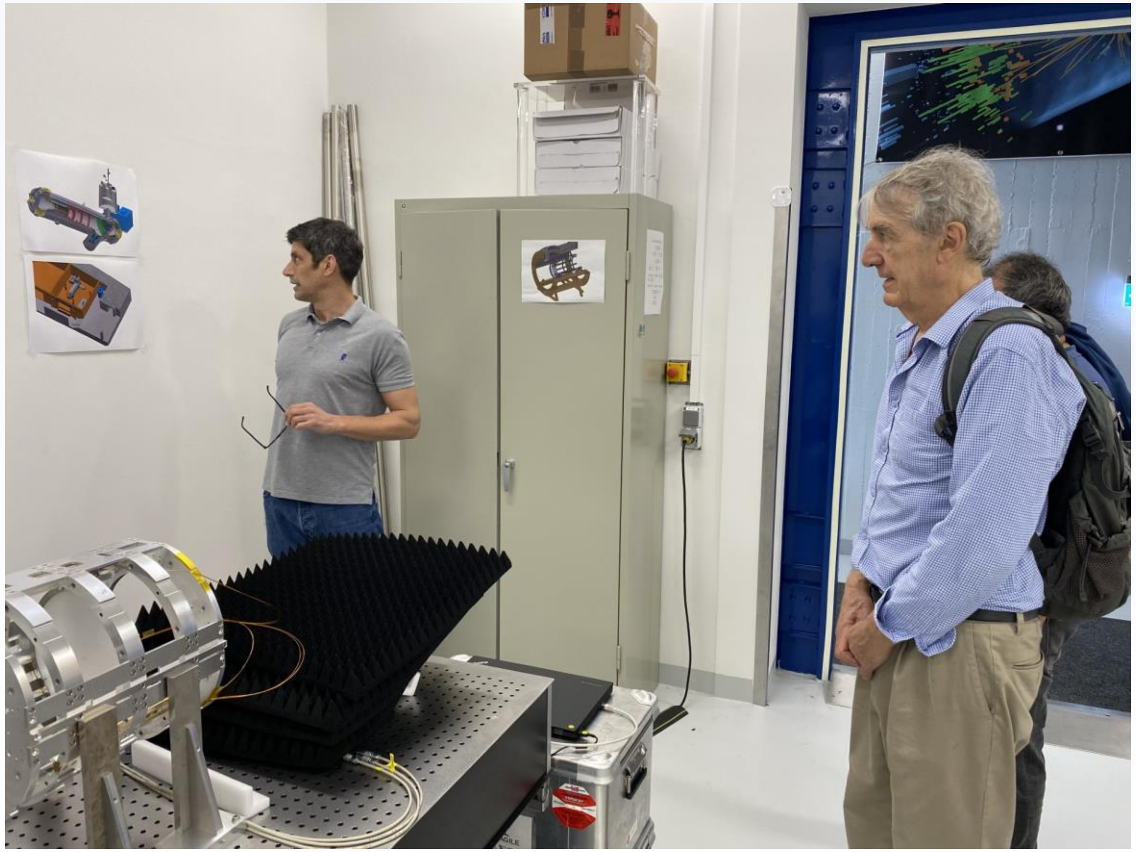

MADMAX Dielectric Haloscope

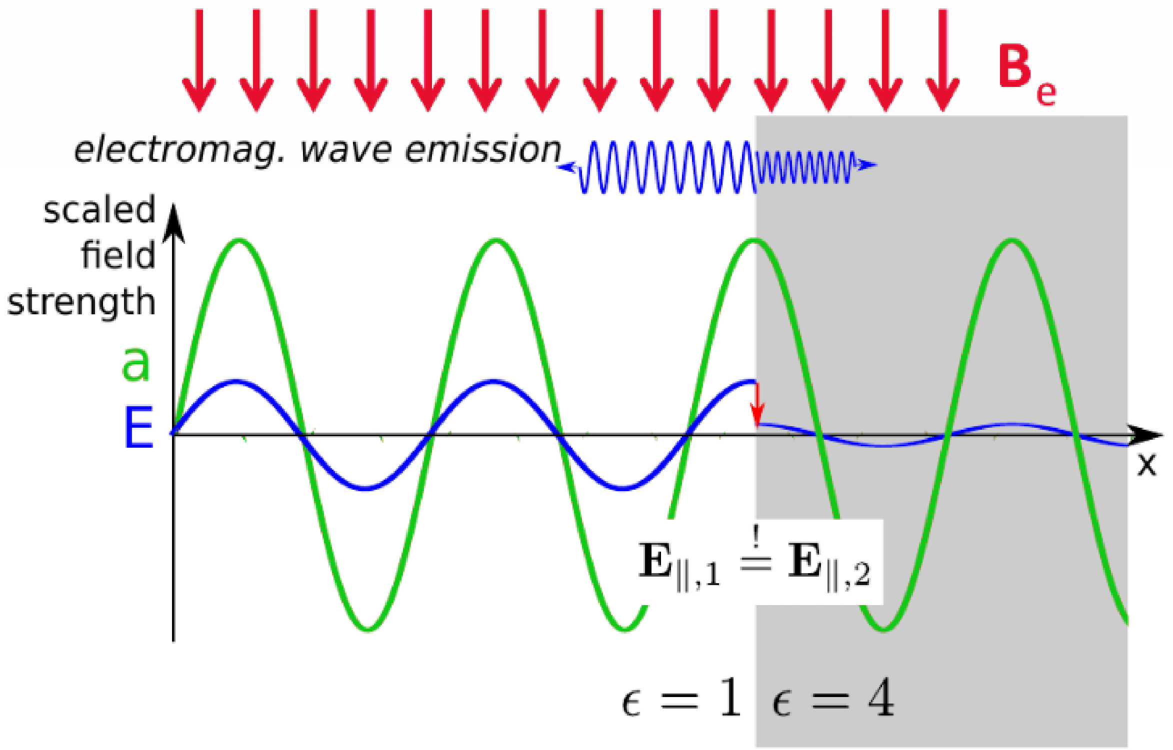

The cosmological axion field **a(t)** inside an external magnetic field $\mathbf{B_e}$ sources a tiny axion induced electric field $\boldsymbol{E_\alpha}$

$\boldsymbol{E_\alpha}$ ~ 10^{-12} V/m for 10 T in vacuum

$\boldsymbol{E_a}$ is different in materials with different ε

$\mathbf{E}_{||}$ must be continuous at the **boundaries**

$$E_\alpha = -\frac{g_{\alpha\gamma}\mathrm{B}_e}{\varepsilon}\alpha \qquad \alpha = \alpha_0 \cos(m_\alpha t)$$

Power emitted from a single surface:

$$P_{sig} = 2.2 \cdot 10^{-27} W \left(\frac{A}{1m^2}\right)\left(\frac{B_e}{10T}\right)^2$$

or 2 photons/hour @ 25 GHz

Detection principle

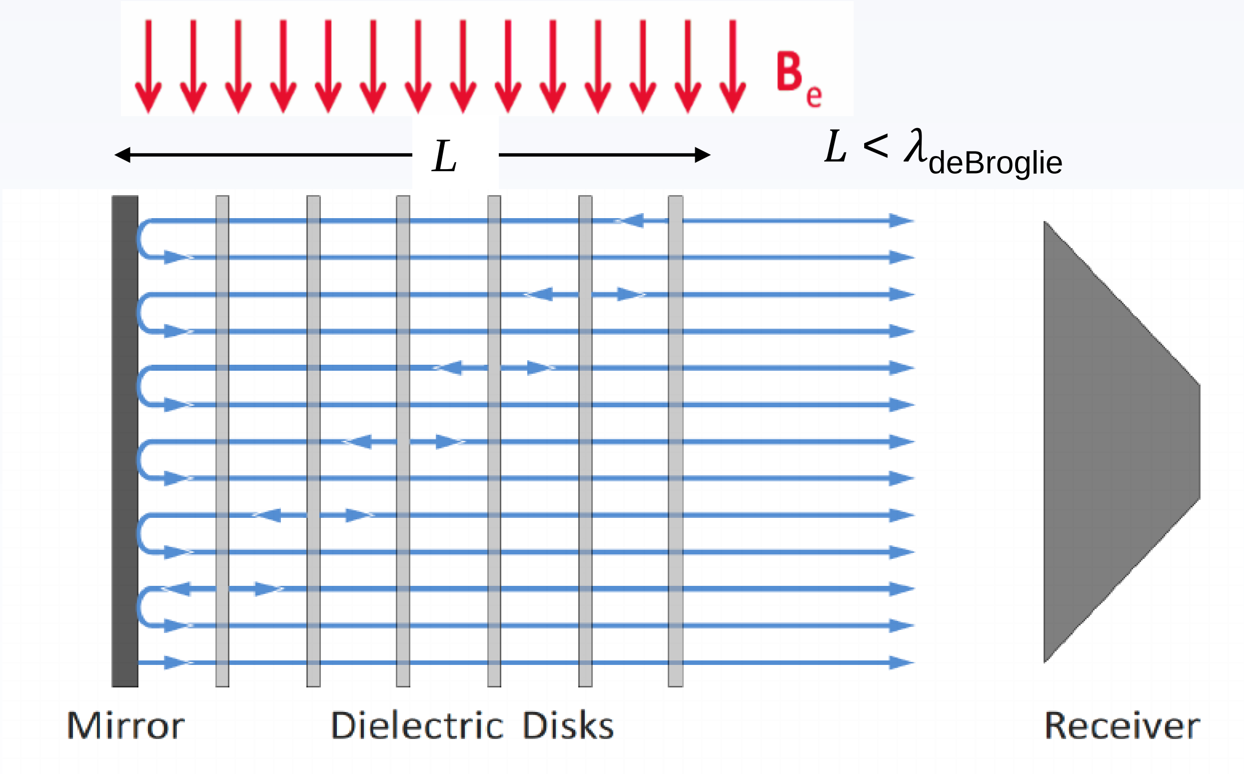

- EM radiation escapes at open end
- Detect Traveling wave instead of standing wave modes

Boosted emitted power :

- coherent emission from multiple interfaces by controlling the discs separations and
- constructive interference

$$P_{sig} = 2.2 \cdot 10^{-27} W \left(\frac{A}{1m^2}\right)\left(\frac{B_e}{10T}\right)^2 \cdot \beta^2$$

power “Boost factor” β^2

$$\beta^2 = \frac{P_{sig}}{P_{mirror}}$$

Detection principle

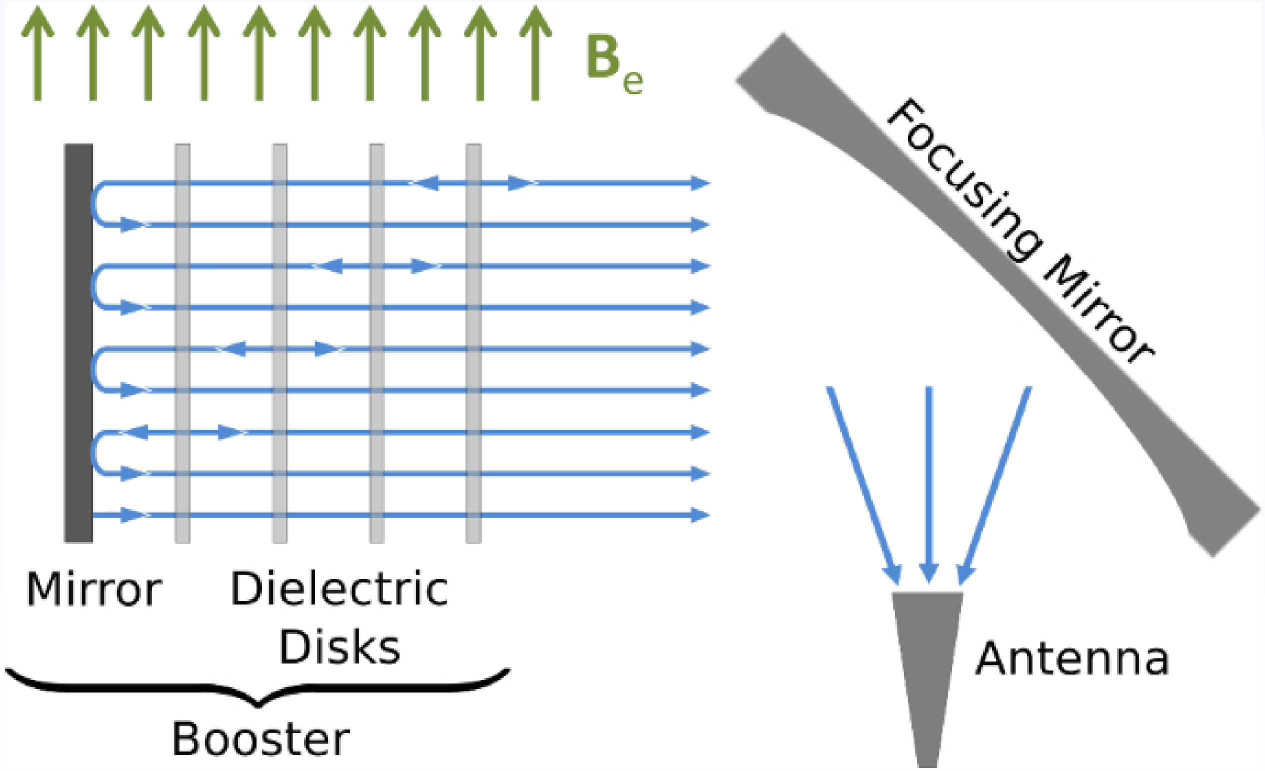

power "Boost factor" β^2

$$\beta^2 = \frac{P_{sig}}{P_{mirror}}$$

Simulations indicate:

$|\beta^2| > 10^4$ achievable with 80 discs
with dielectric constant ε~ 24 ($LaAlO_3$)

β^2 is affected by BC's inaccuracies of the discs:
Disc mis-positioning, tilting, thickness variations

- EM radiation escapes at open end
- Detect Traveling wave instead of standing wave modes (?)

MADMAX full scale experiment

Signal power

$$P_{sig} = 2.2 \cdot 10^{-27} W \left(\frac{A}{1m^2}\right)\left(\frac{B_e}{10T}\right)^2 \cdot \beta^2$$

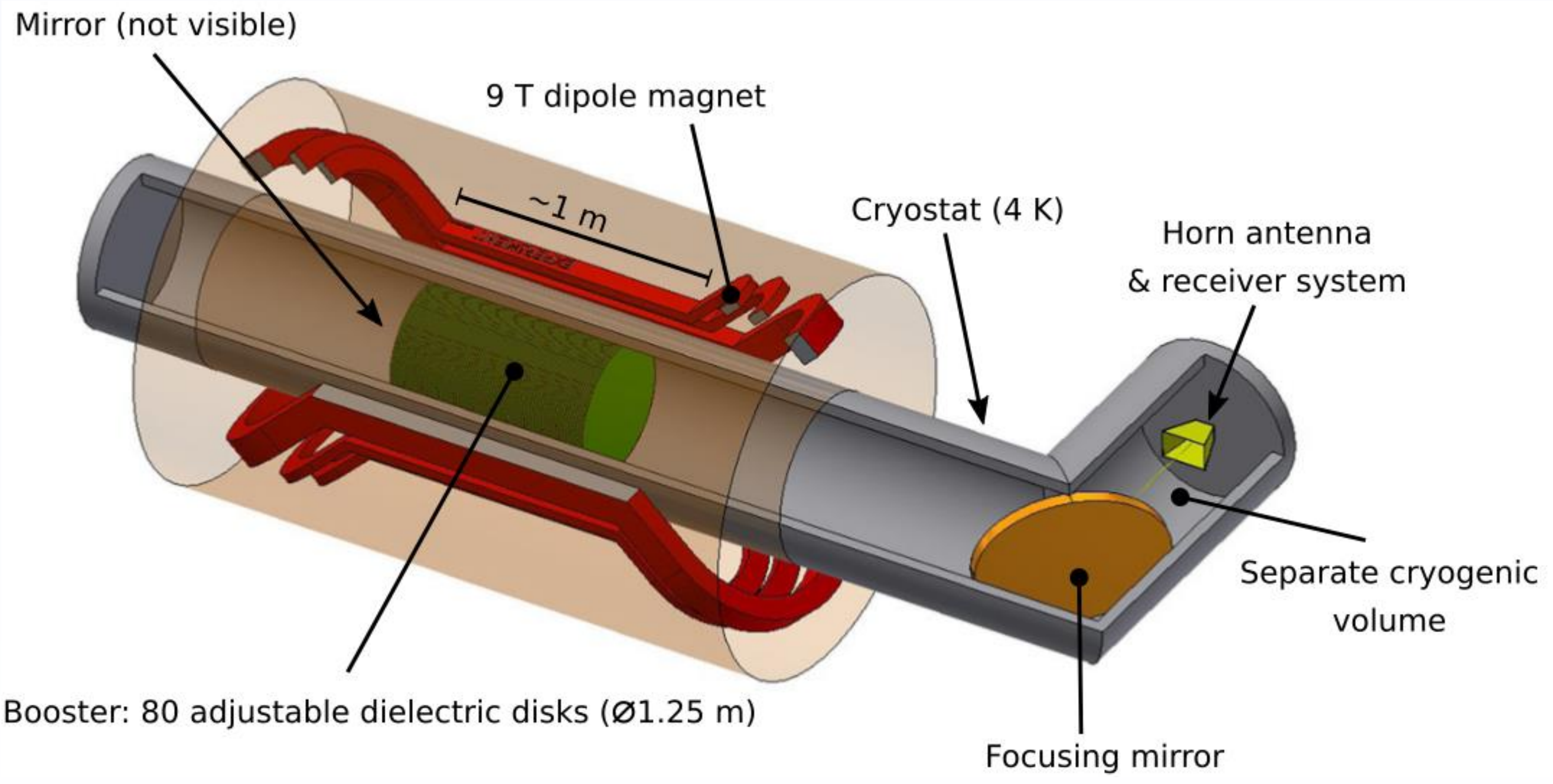

Magnet

Main challenges

- Booster mechanics
- Magnet
- Receiver at cold, B-field environment
- Funding

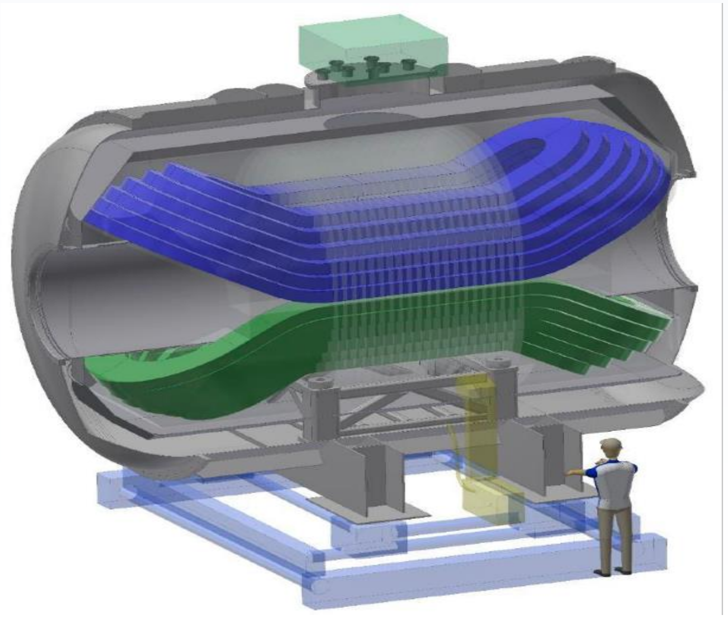

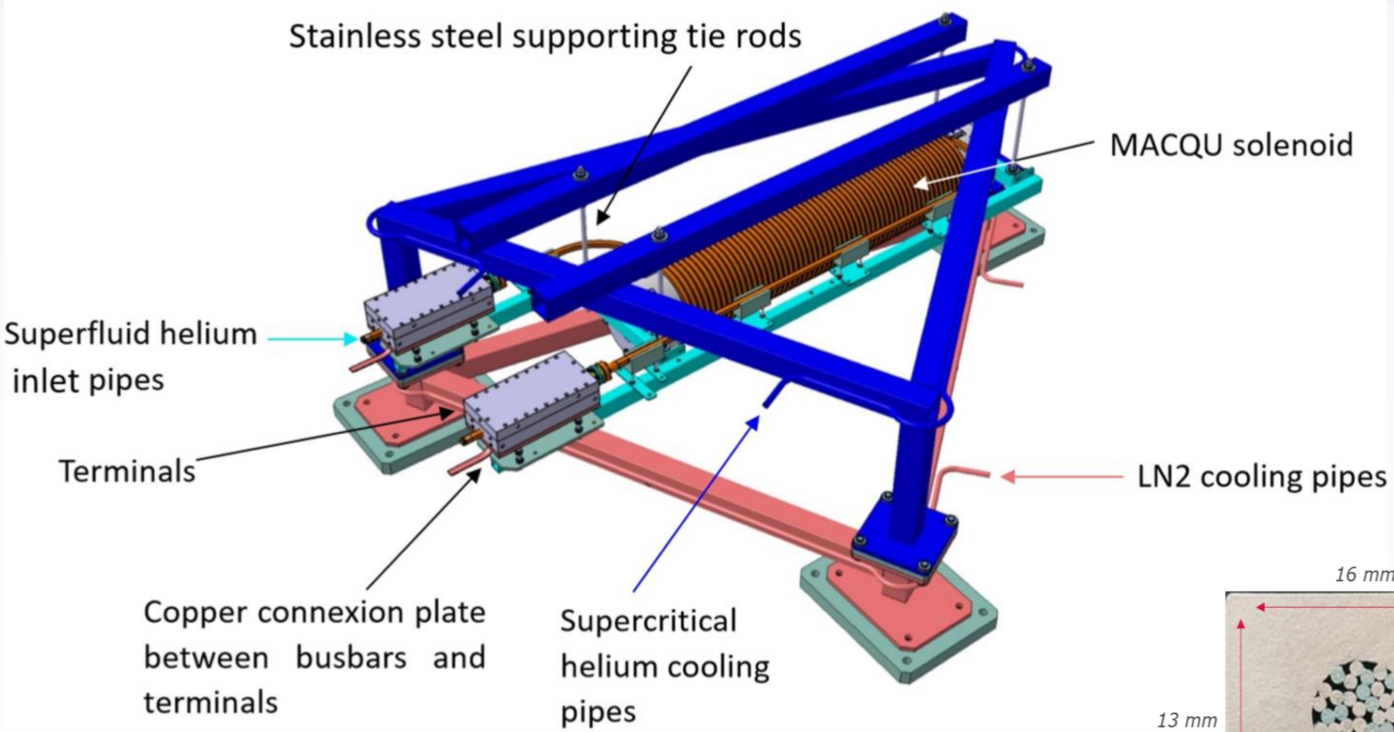

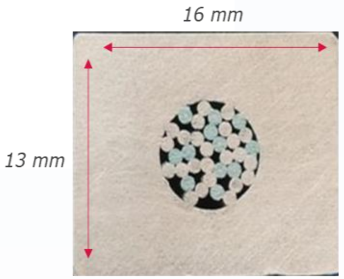

MACQU profile with cable inside

- Quench tests: **MA**dmax **C**oil for **Q**uench **U**nderstanding
- Reliable quench protection
- Feasibility of conductor production

FoM = $B^2 A = 100\ T^2\ m^2$

Timeline

- Commissioning of full-scale MADMAX to start around 2028
- Medium scale prototype:
  - 20 discs with Ø300 mm
  - Frequency range 18 to 25 GHz
  - To be commissioned in 2024 at Hamburg in new RF lab
  - Possible physics measurements in 2022 and 2023
    (currently under discussion: Morpurgo magnet at CERN (1.6 T))

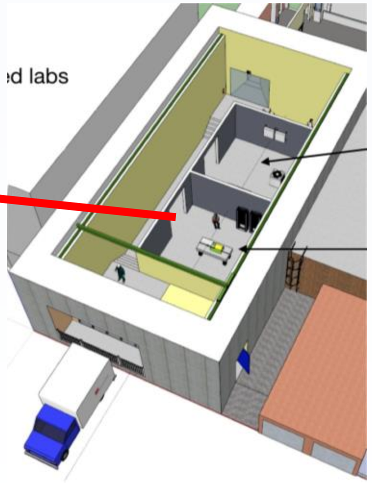

RF lab

Morpurgo magnet

Properties Of The “Boost Factor”

Options for broadband and narrowband scans

- Large single volume
- Approach QCD sensitivity: $\beta^2 > 2*10^3$ possible
- Frequency tuning: Disk spacings control $\beta(f)$

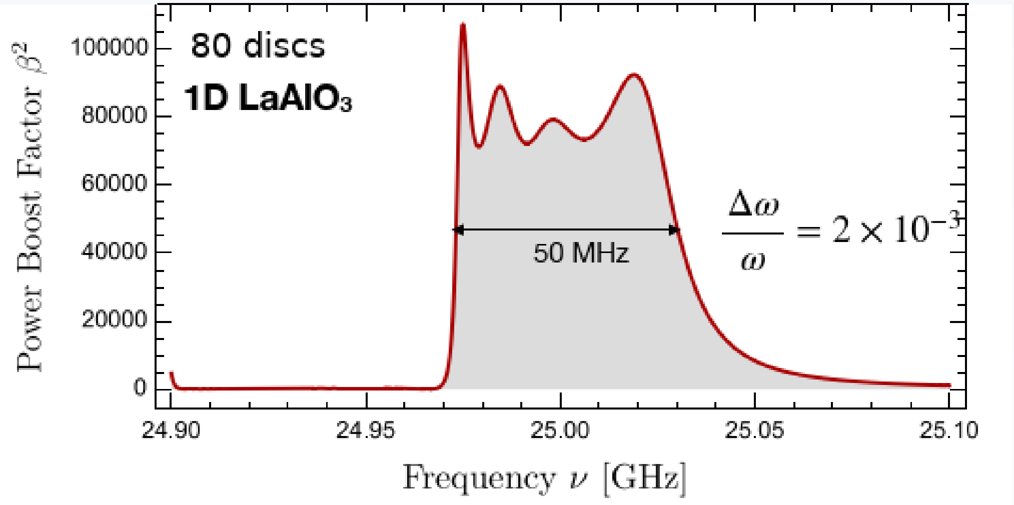

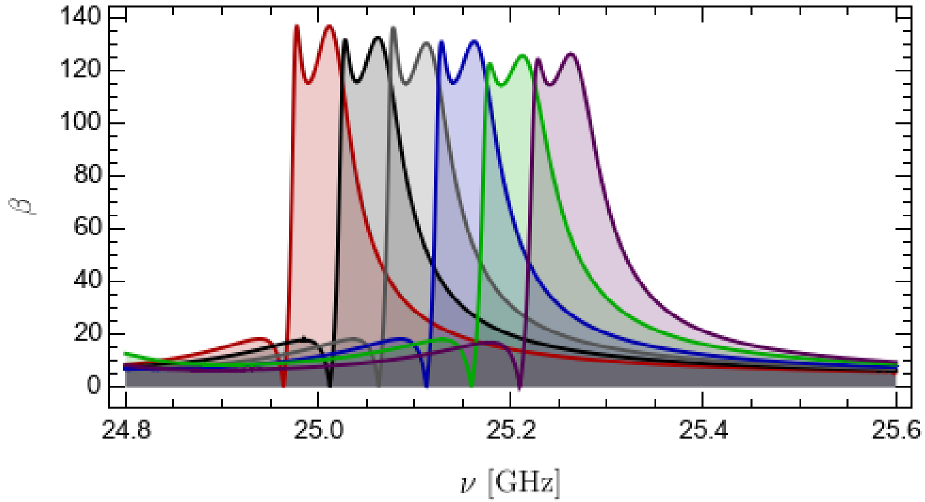

Frequency can be tuned by changing the disc positions

Ideal Booster – simulations

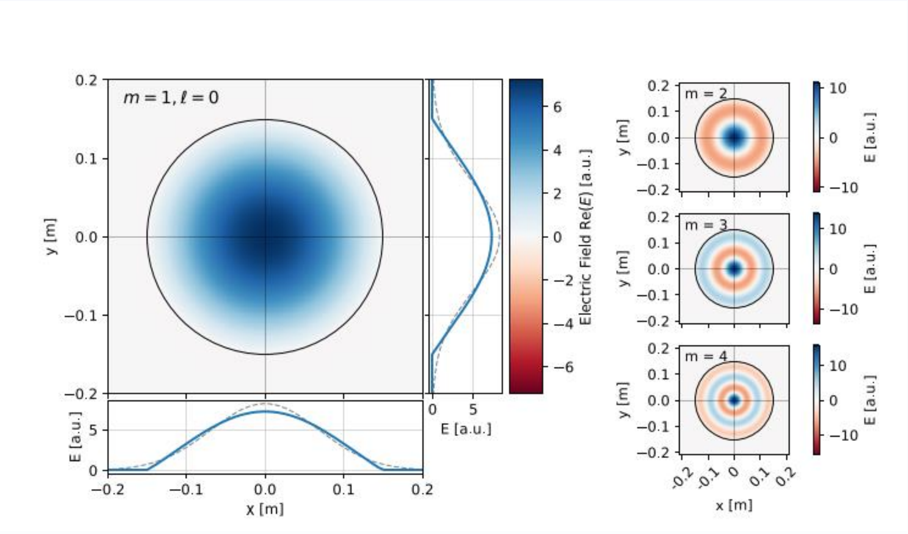

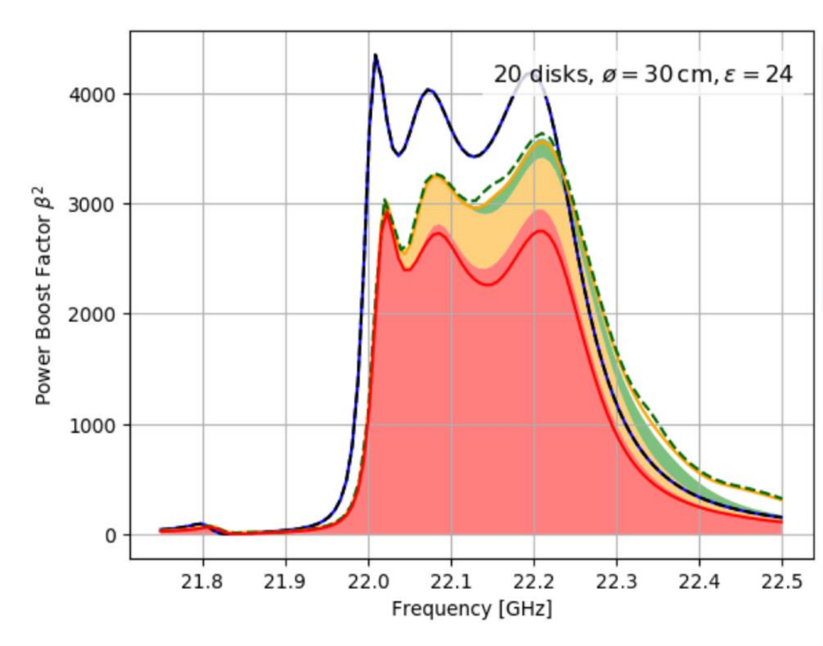

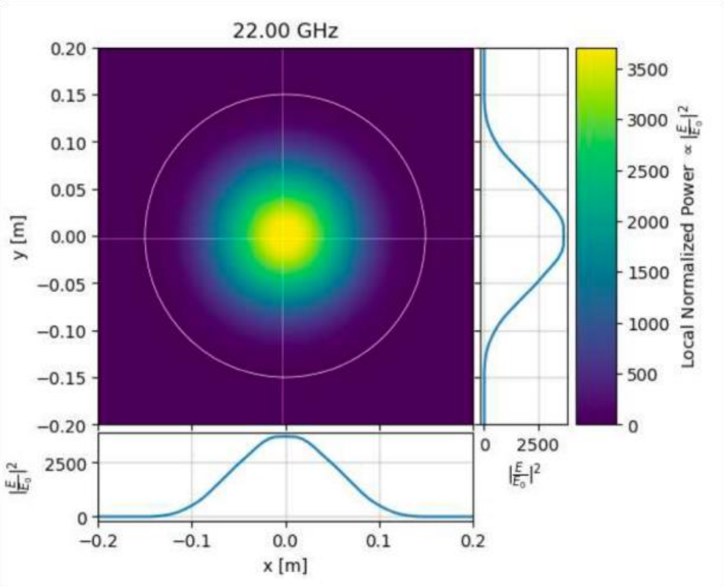

Modes of the circular dielectric haloscope.

Power boost factor β^2 considering dielectric disks of finite size with spacings tuned to cover a bandwidth of ≈ 50 MHz

EXPERIMENTAL CHALLENGES

1. estimating the boost factor in Open Booster

- The boost factor is not a measurable quantity (?)

2. *3D effects can have significant impact on the boost factor*

3. RF receiver chain to detect a signal of 10^{-22} W at 4 K

4. Engineering challenges

- E.g. high field (~9T), large bore (~m^2) magnet

BOOST FACTOR β²: 3D EFFECTS

MADMAX Prototype 20 Disks, ø= 30 cm

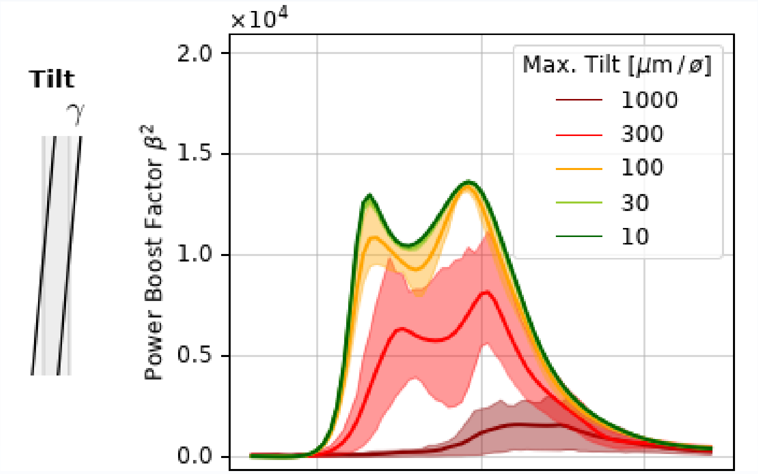

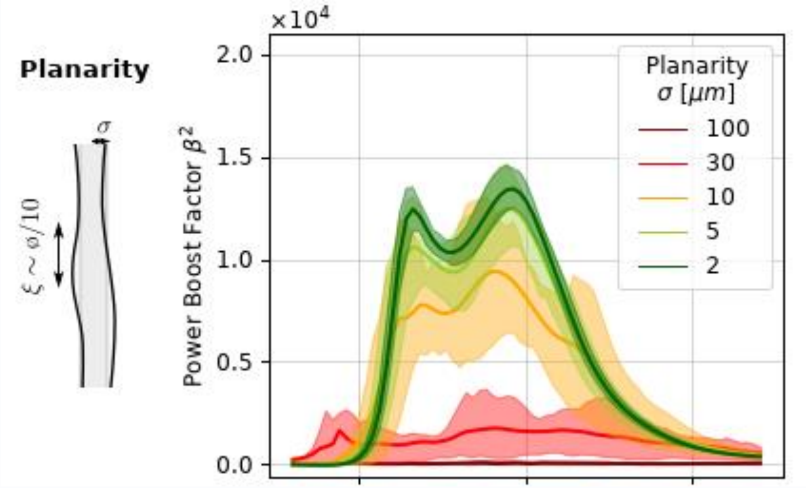

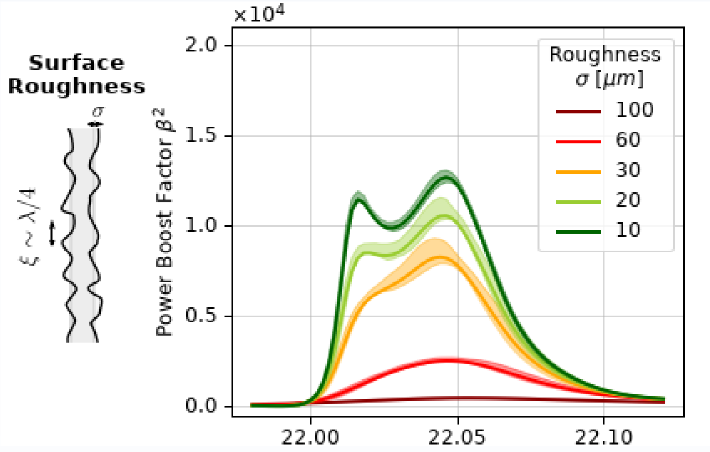

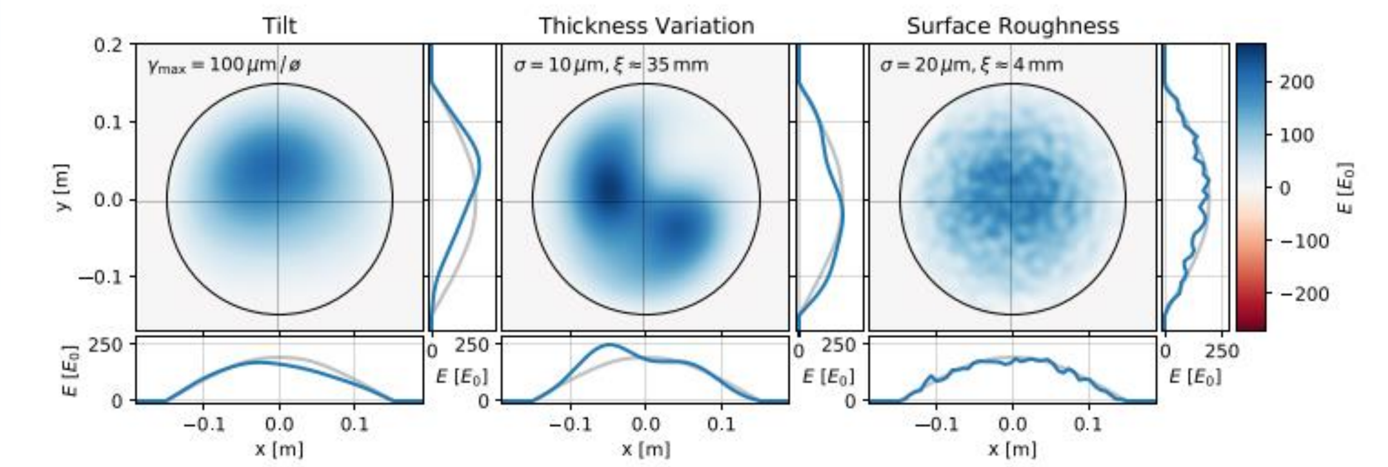

3D effects such as disc tilting, surface roughness and axion velocity have been studied.

Requirements :

(tiling < 0.1 miliradian, surface roughness < 10 μm)

Open and closed Boosters

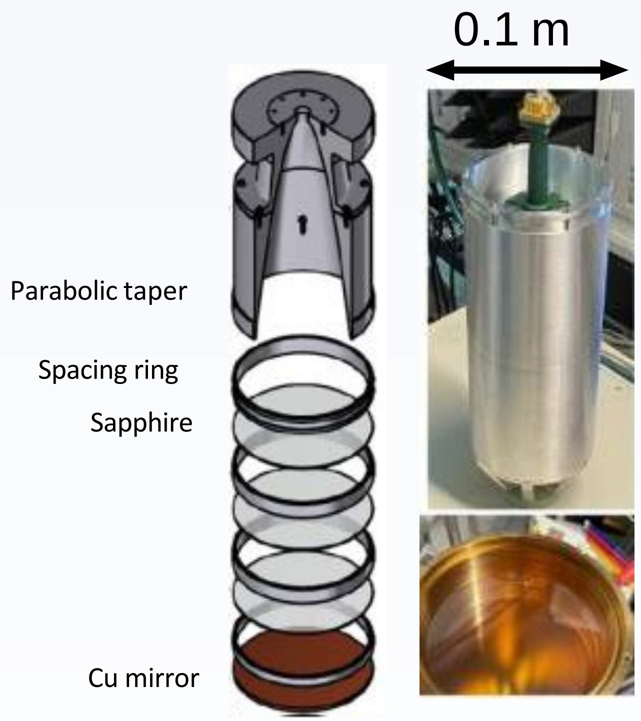

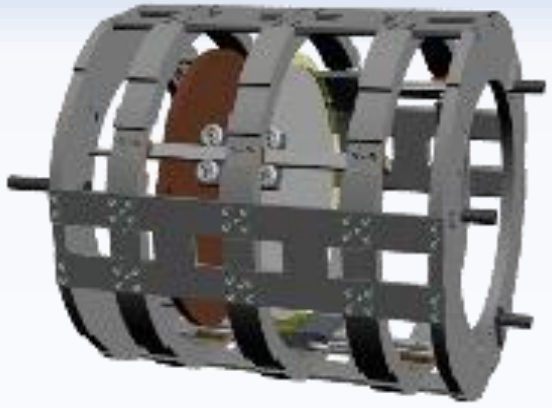

Open Boosters (OB):
⌀ = 200 mm (OB200), 2 Al_2O_3 disks
⌀ = 300 mm (OB300), 3 disks (Al_2O_3 & $LaAlO_3$)

Closed Boosters (CB):
⌀ = 100 mm (CB100), 3 Al_2O_3 disks
⌀ = 200 mm (CB200), 3 Al_2O_3 disks

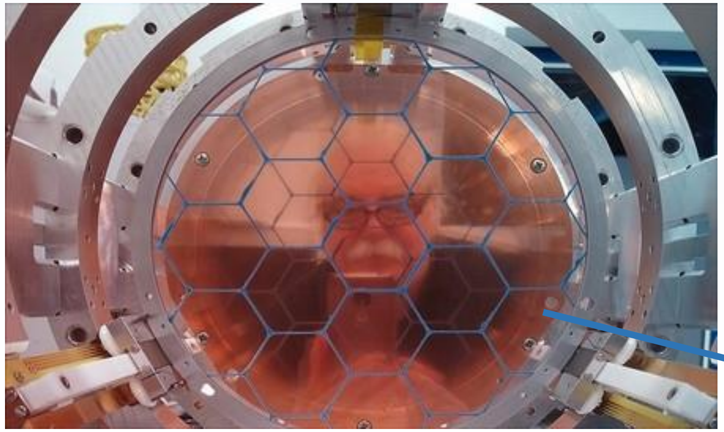

Prototype booster

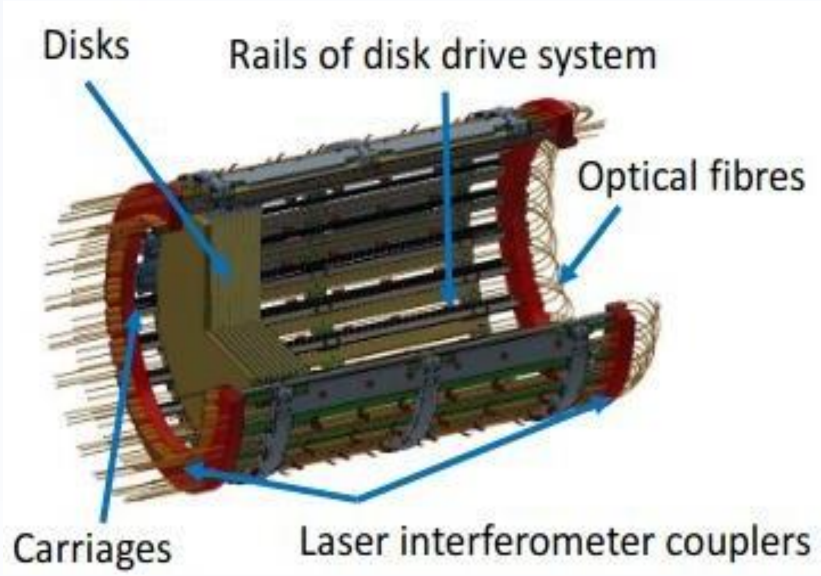

Operating conditions:
− Cryogenic temperatures: 4 K
− High magnetic field: up to ~10 T
− Vacuum or cold He exchange gas

Single Sapphire Ø300 mm discs
or
Tiled discs made of $LaAlO_3$ 3'' wafers

MADMAX Prototype Cryostat

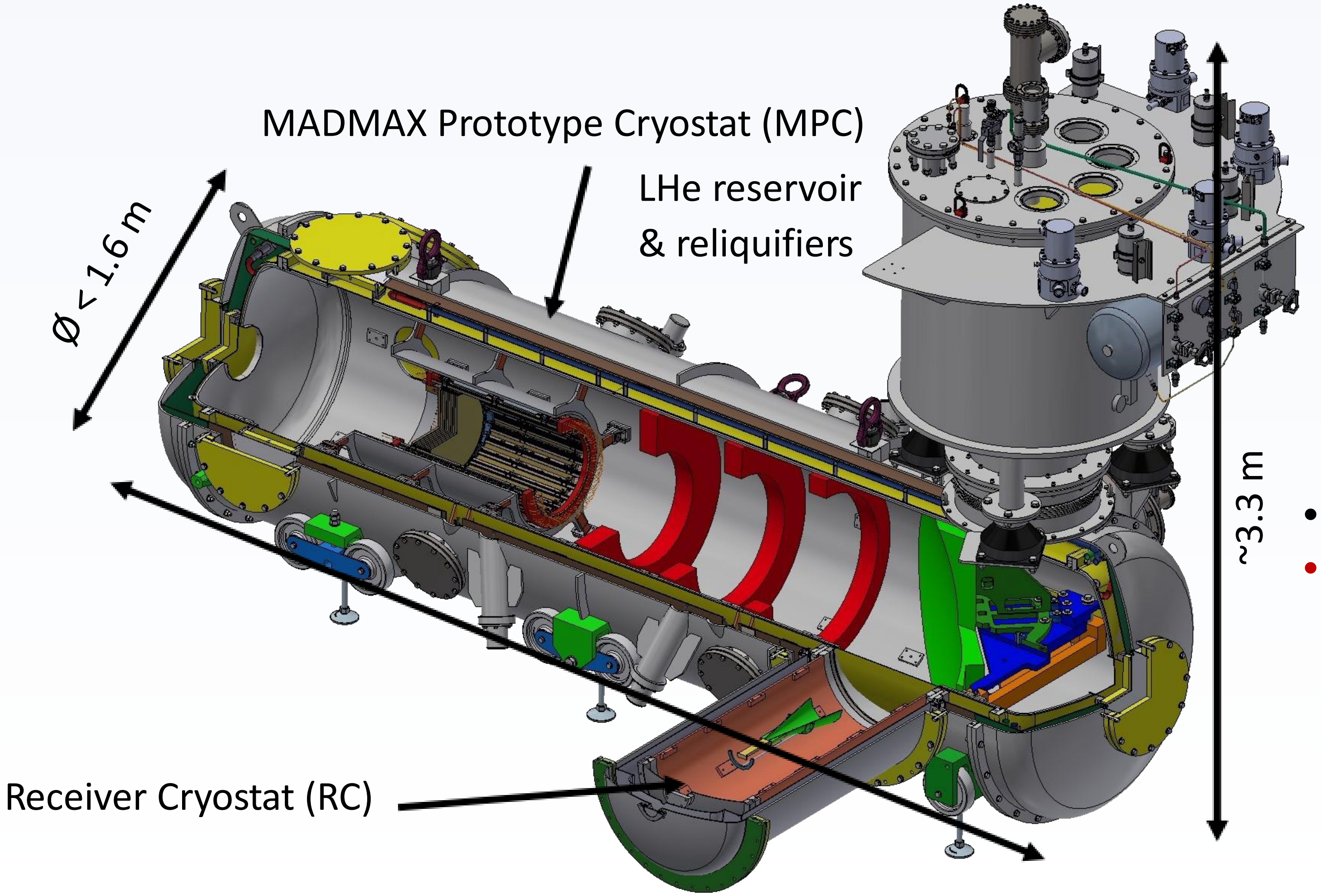

Large bore (Ø = 760 mm) cryostat allows operation of all prototypes
Fits into the 1600 mm warm bore of **MORPURGO** magnet at CERN

- Delivery expected begining of 2024
- Commissioning with OB300 in Hamburg

Use of the MORPURGO magnet @ CERN

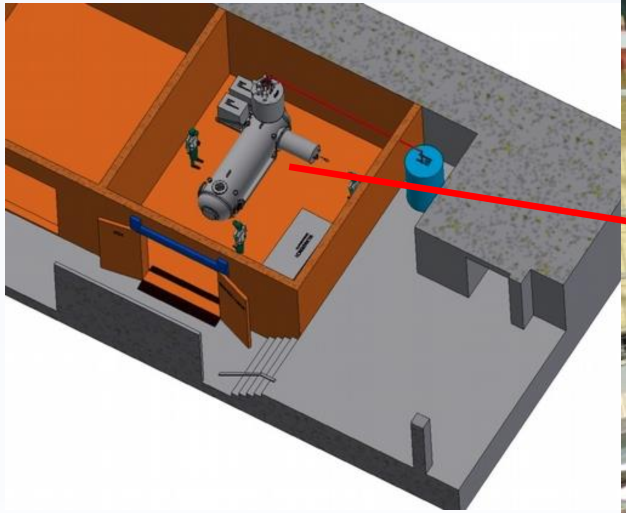

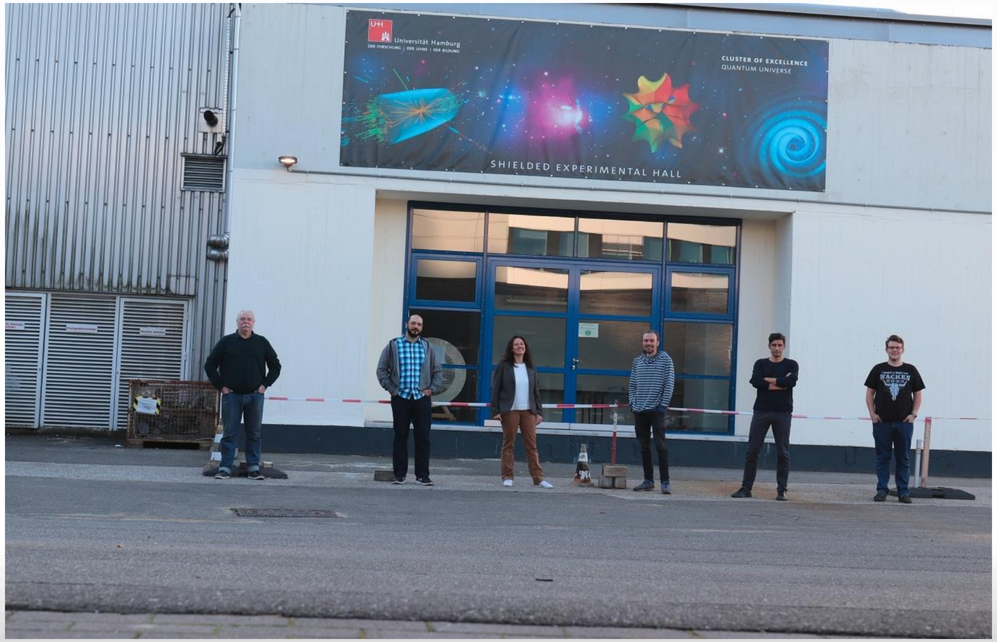

MORPURGO magnet @ CERN

Booster in cryostat operation and commissioning in SHELL @ UHH

First axion physics measurements in MORPURGO magnet @ CERN

SHELL RF measurements

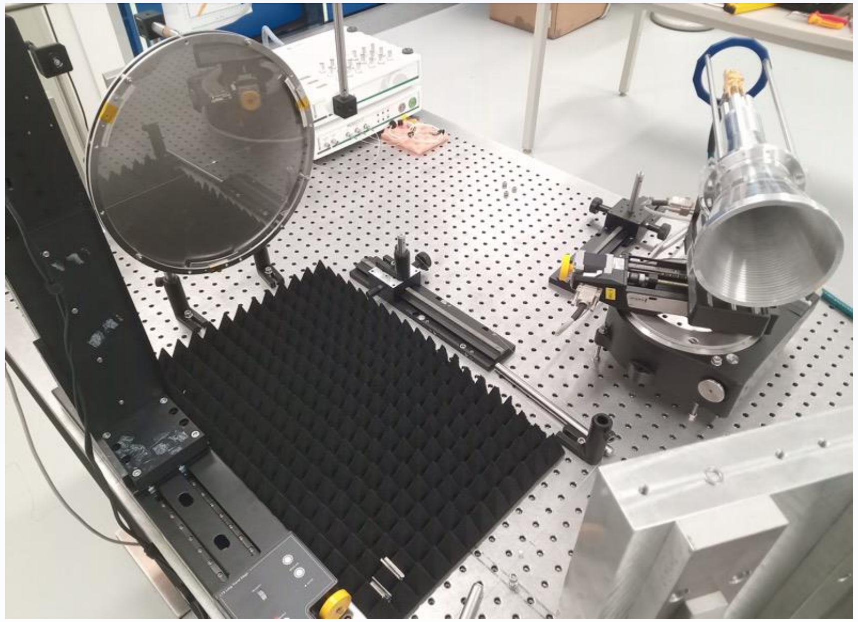

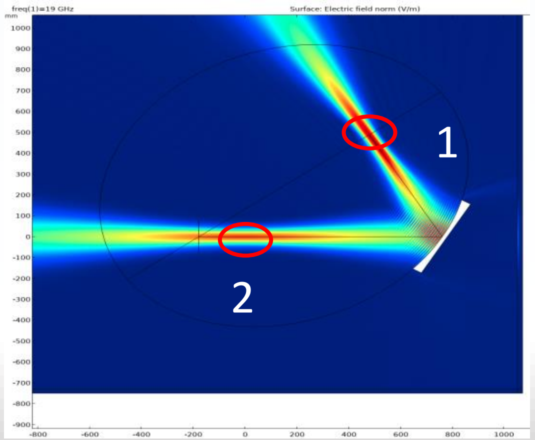

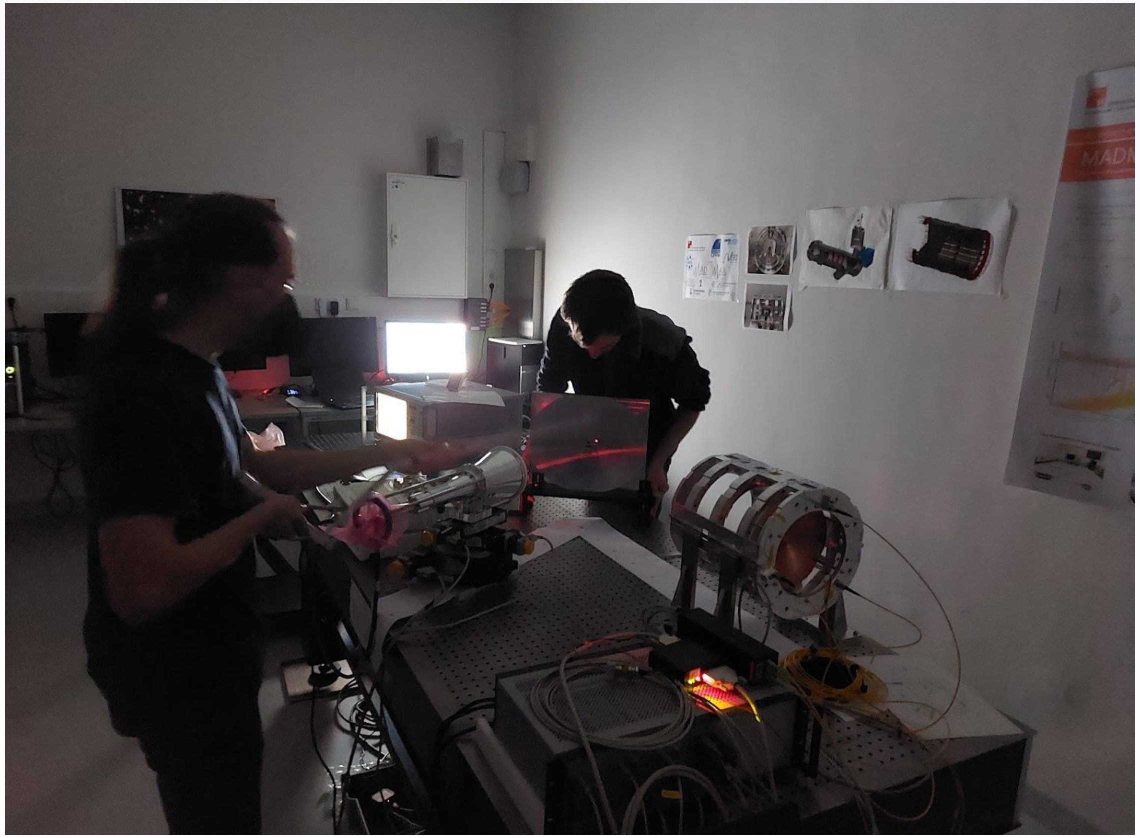

OB 200 (booster) alignment

Signal Power

Change in reflection coefficient → $$\Delta\Gamma = \frac{\alpha_e \omega}{P_{\mathrm{in}}} \boldsymbol{E}_R^2$$ → Electric field

$$\beta^2 = \frac{P_{\mathrm{sig}}}{P_0}$$

$$P_{\mathrm{sig}} = \frac{g_{a\gamma}^2}{16 P_{\mathrm{in}}} \left| \int_{V_a} \mathrm{d}V \, \boldsymbol{E}_R \cdot \dot{a} \boldsymbol{B}_e \right|^2$$

- Measure max. E-field between disk and mirror
- Calculate signal power
- Includes effects currently not simulated:
  - Antenna coupling
  - Transverse field perturbations

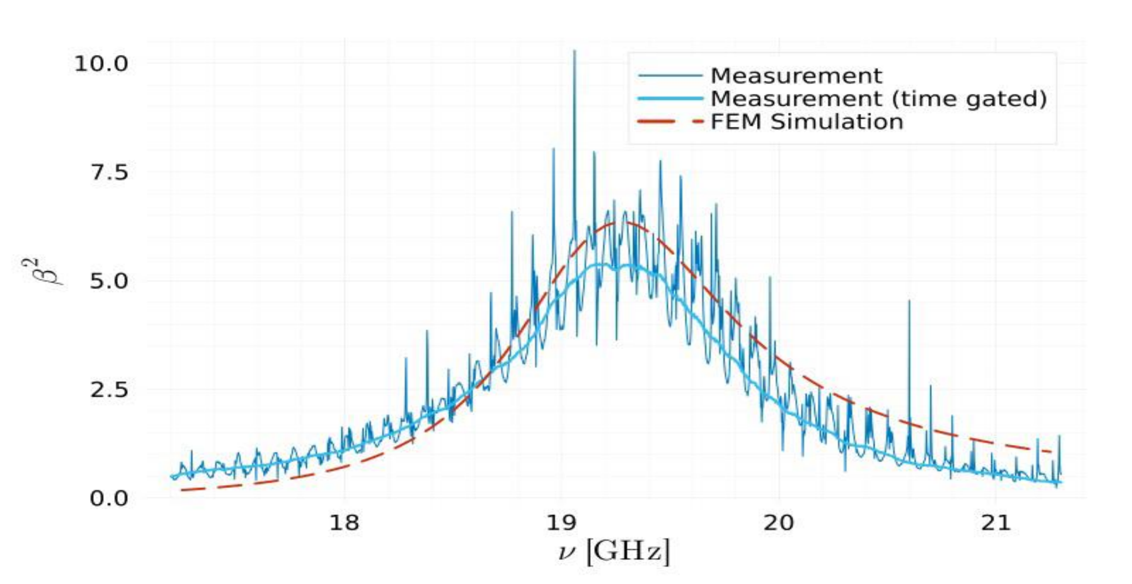

Single disk “low” boost factor

Disk tiling

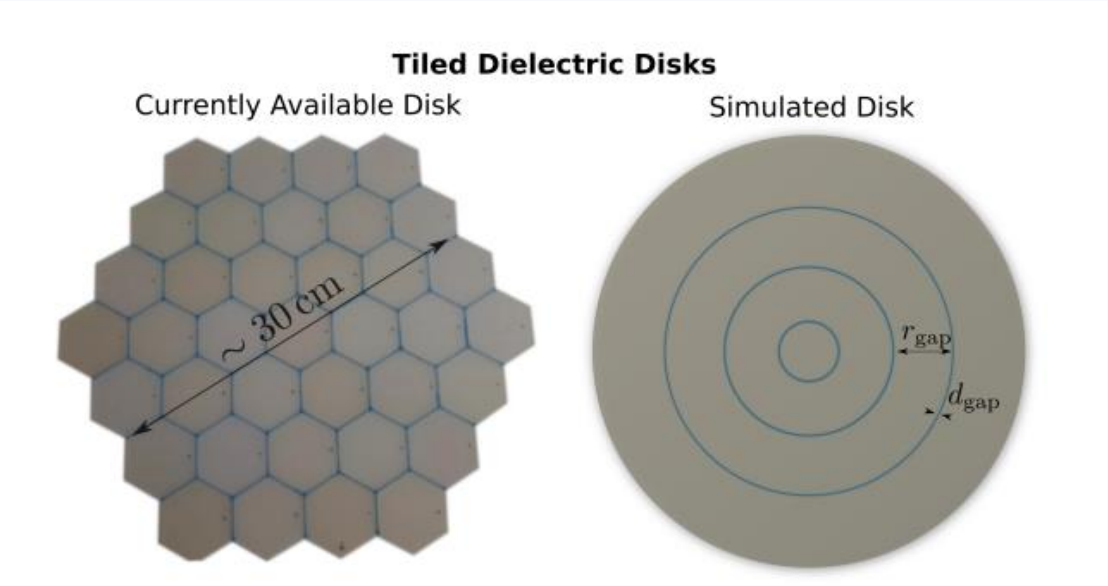

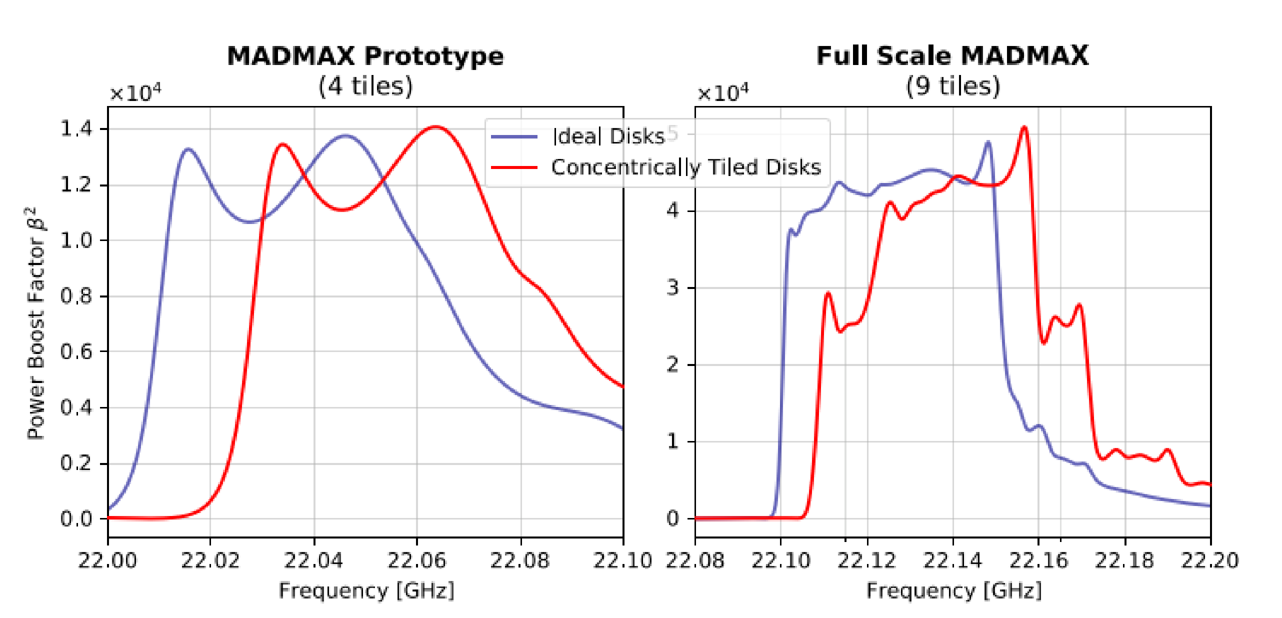

- Tiling of ∅ = 300 mm $LaAlO_3$ disks

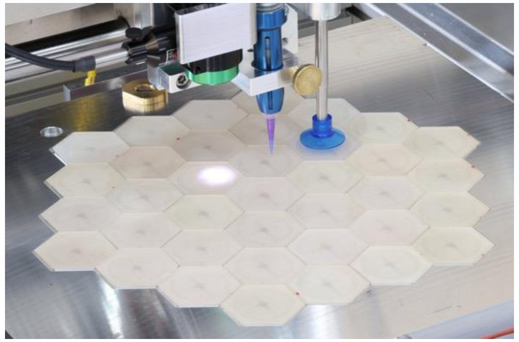

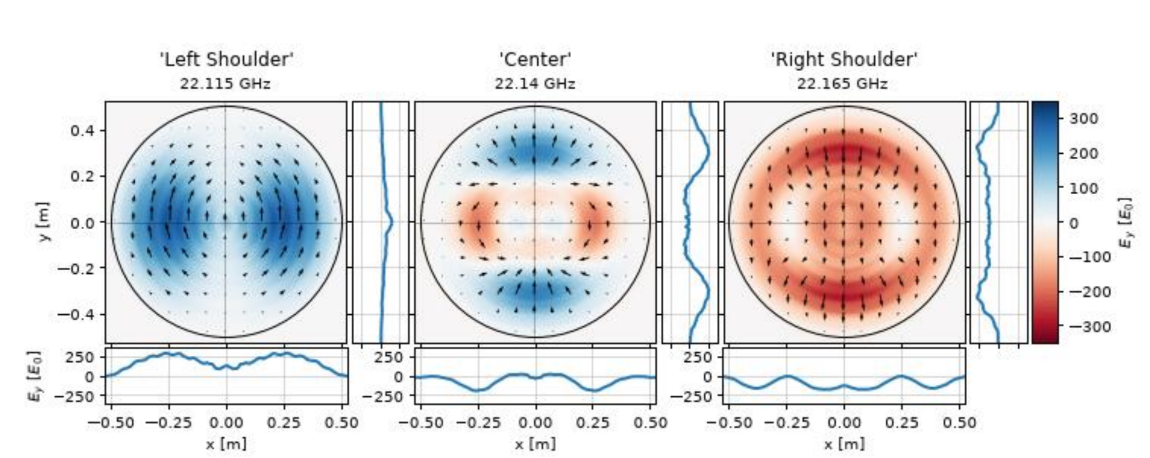

for the full scale MADMAX the beam shape is significantly altered due to polarization effects caused by the tiling

CB measurement at CERN

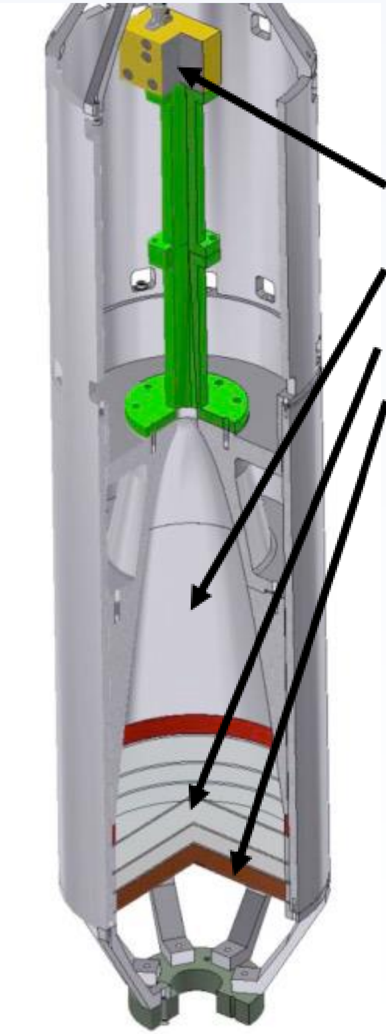

Simple closed system to understand RF behaviour

- Receiver
- Parabolic taper
- 3x Ø100 mm disks (fixed distances)
- Copper mirror

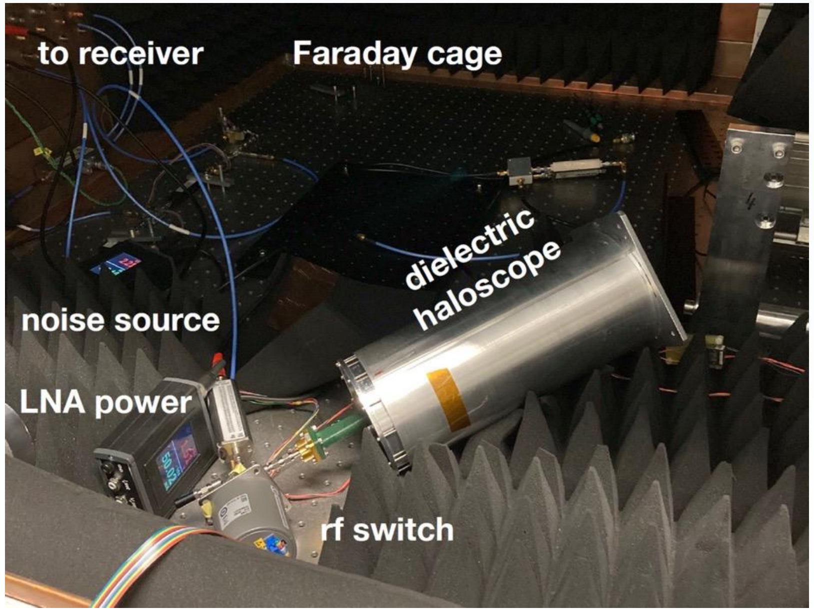

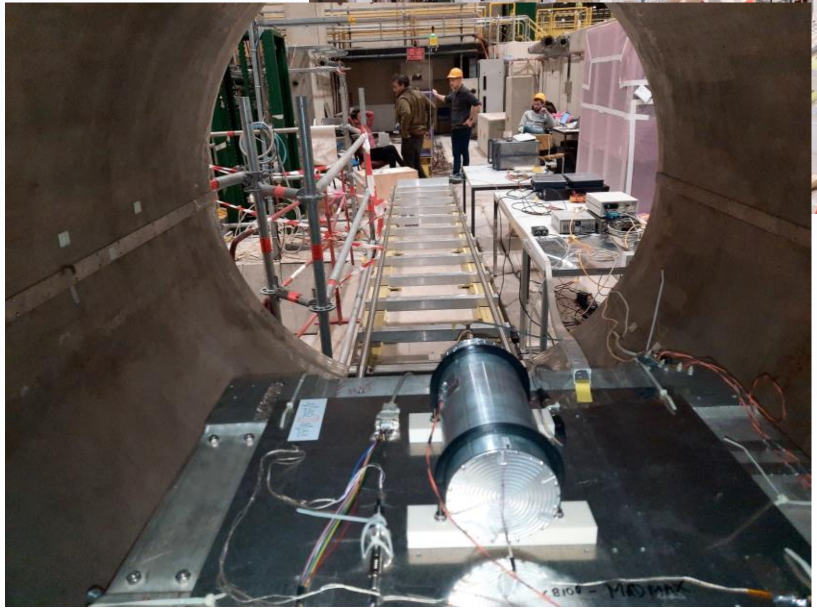

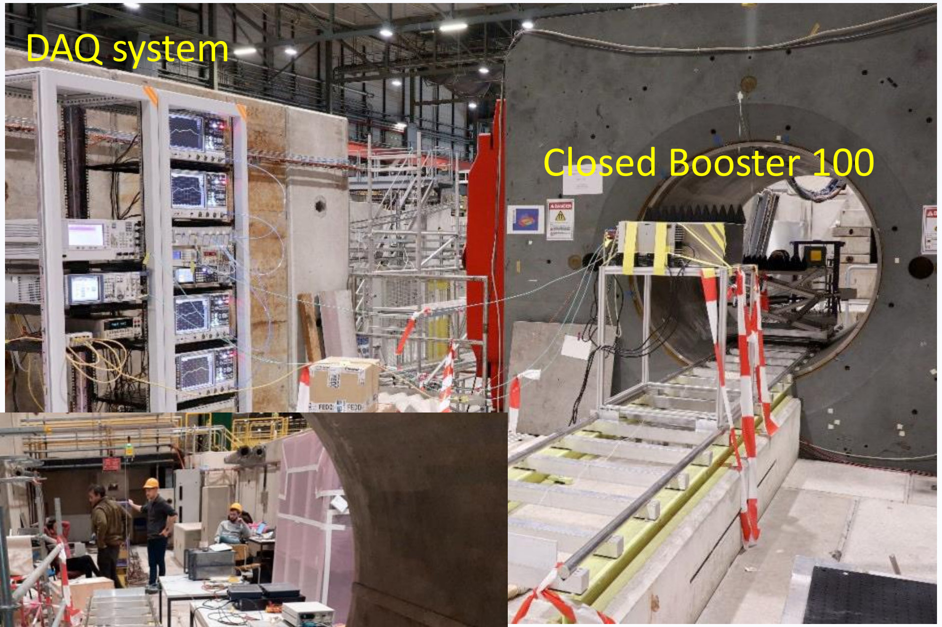

Tested in
MORPURGO
@ CERN
in 2022 and 2023

MADMAX limits

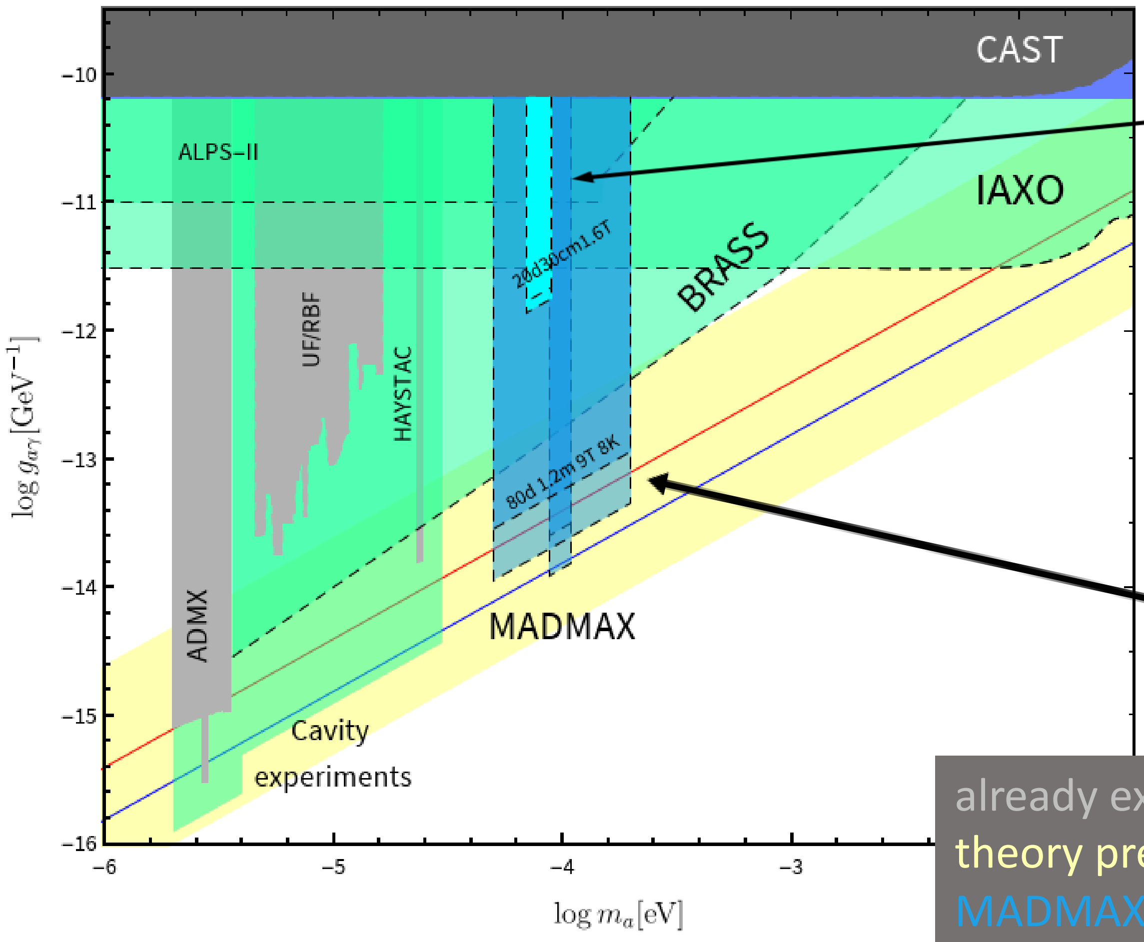

MADMAX Prototype:

N_{disk} = 20

A_{disk} = 0.07 m^2

$B_{\|}$ = 1.6 T

T_{sys} = 8 K

MADMAX:

N_{disk} = 80

A_{disk} = 1.2 m^2

$B_{\|}$ = 9 T

T_{sys} = 8 K

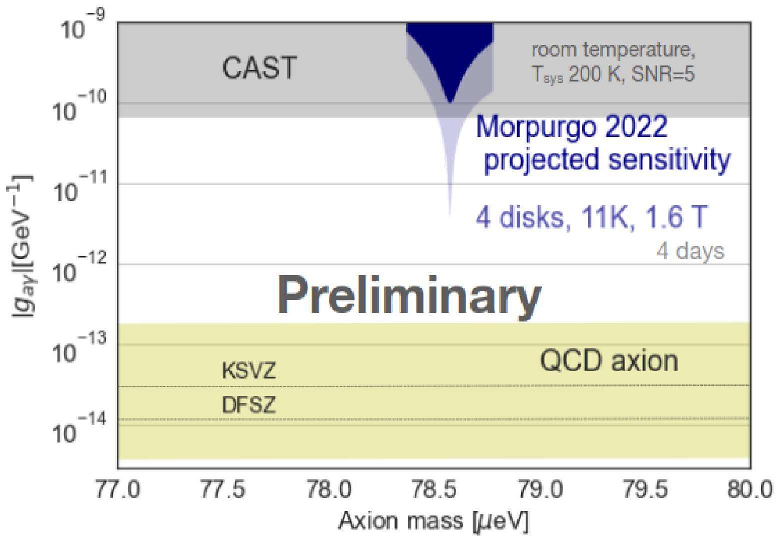

already explored/excluded
theory prediction
MADMAX (Prototype)
other axion experiments

QUAX (QUest for AXions) @ INFN

QUAX a-γ

constructing two haloscopes to search for dark matter axions with the standard Sikivie type technique based on the axion photon coupling.

QUAX a-e

ferrimagnetic haloscope experiment, located at the Laboratori Nazionali di Legnaro, is developing a detector for dark matter axion exploiting the coupling to electrons.

National Institute for Nuclear Physics (INFN)

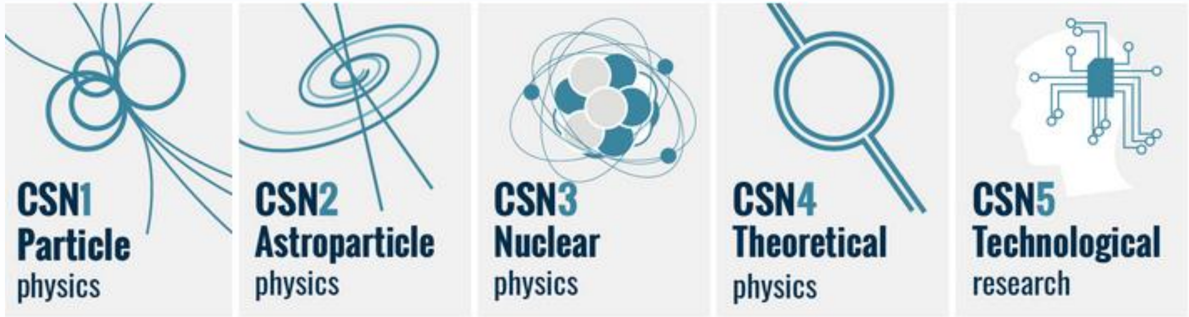

Superconducting Quantum Materials and Systems Center (SQMS) @ Fermilab

EU and US collaborations for the integration of:

1. **high-Q cavities** (SQMS, Fermilab)
2. state-of-the-art **itinerant microwave photon counters** (Quantronics group, Saclay)
3. **TWPA** (N. Roch group, Neel Institute in Grenoble)

cea Quantronics Group
Research Group in Quantum Electronics, CEA-Saclay, France

SQMS
SUPERCONDUCTING QUANTUM MATERIALS & SYSTEMS CENTER

NÉEL institut

QUAX Collaboration

LNL

LNL

LNF

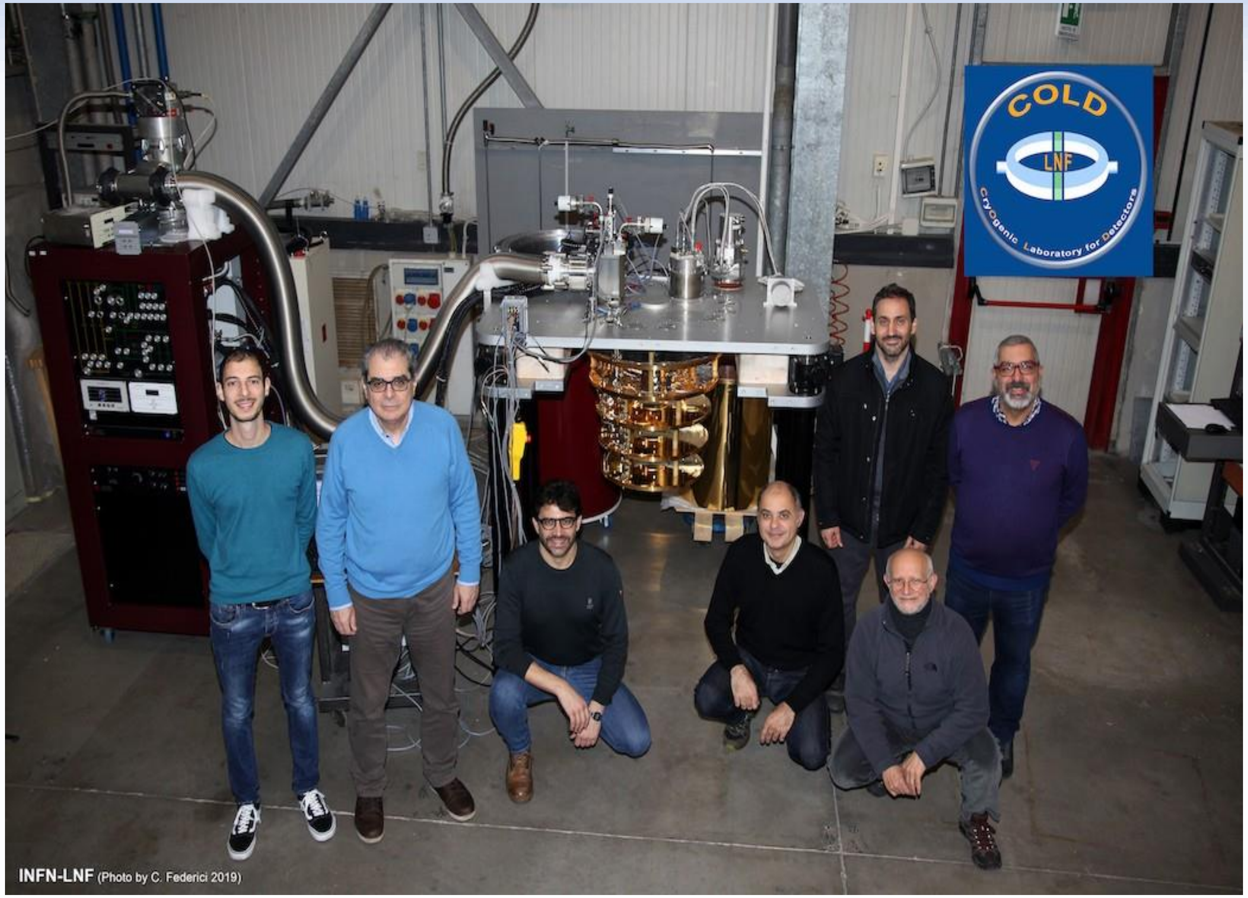

LNF

Funded program to run an axion observatory with two Haloscopes : One in **LNL** & one in **LNF**

Haloscope detection principle

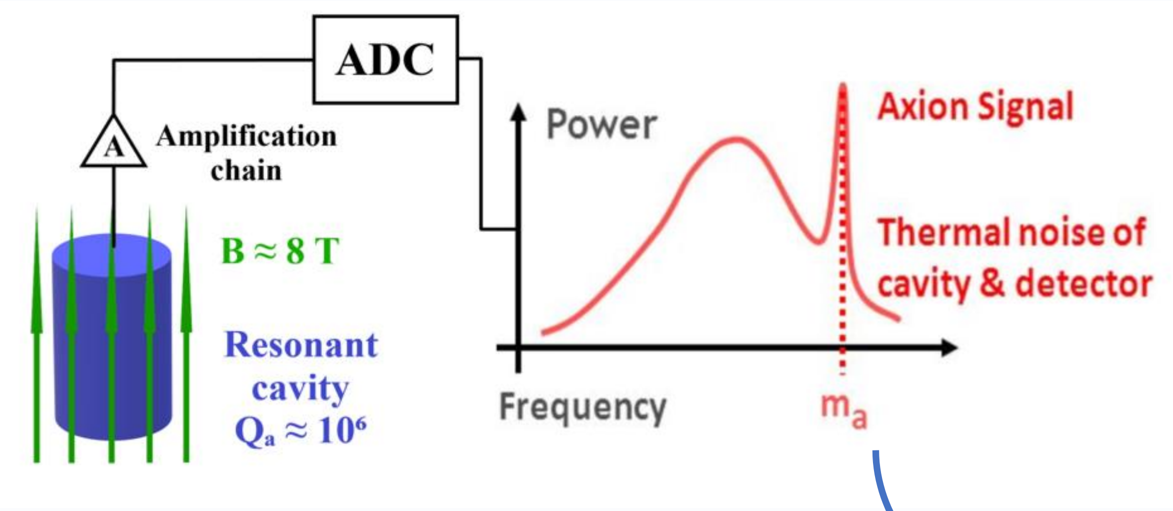

$$P_{\alpha\rightarrow\gamma} = \left(g_{\alpha\gamma\gamma}^2 \frac{\rho_\alpha}{m_\alpha}\right)\left(\frac{\beta}{1+\beta}\boldsymbol{B_0^2 V C Q_L}\right)$$

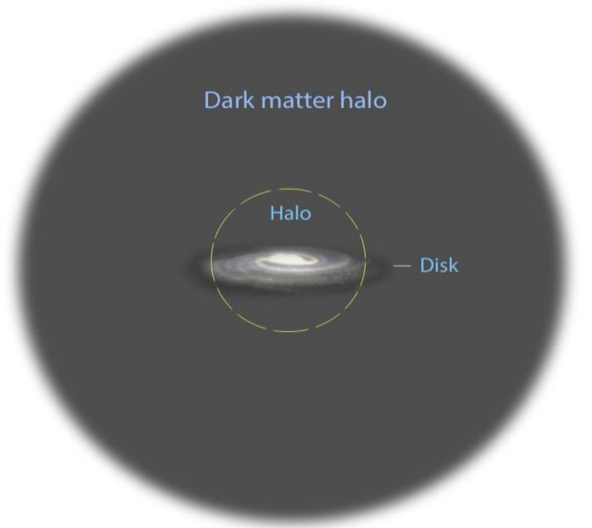

Milky Way model

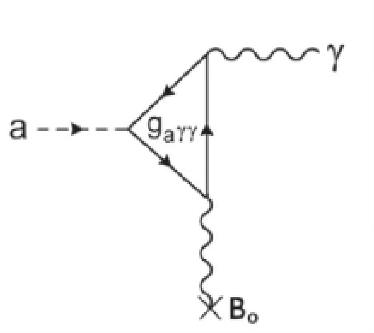

- axions converted to photons inside intense magnetic field
- high-Q microwave cavity collects and integrates signal
- signal amplified by low noise receiver chain, then digitized by ADC
- axion signal revealed as excess power over noise fluctuations

Haloscopes in the parameter space

-Excluded parameter space for axions, zoomed into microwave cavity haloscopes.

-Theoretical predictions for post-inflationary axions.

- How to reach the cosmological relevant region?

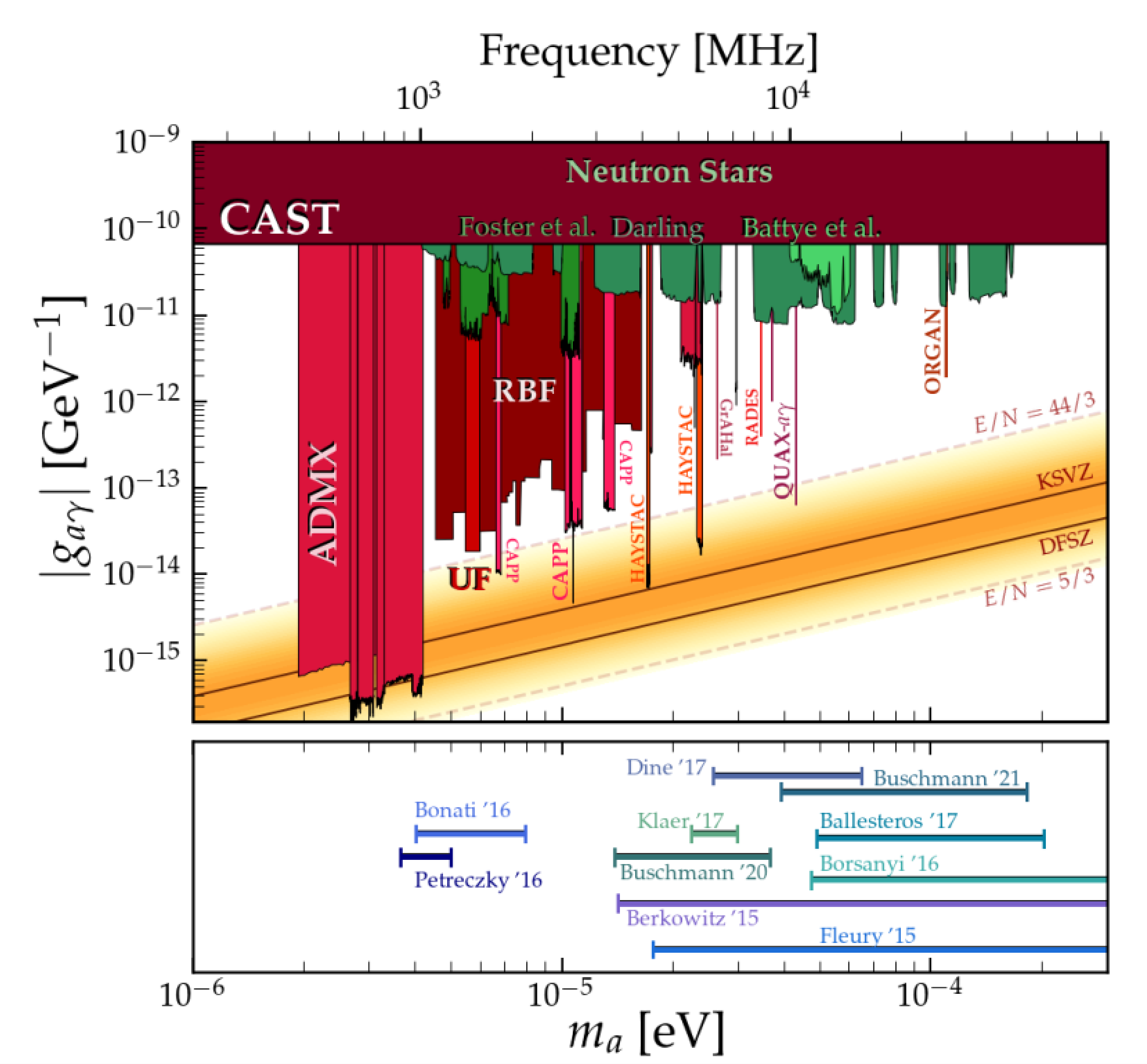

Figure courtesy of Ciaran O'Hare
https://doi.org/10.5281/zenodo.3932430

QUAX scientific program

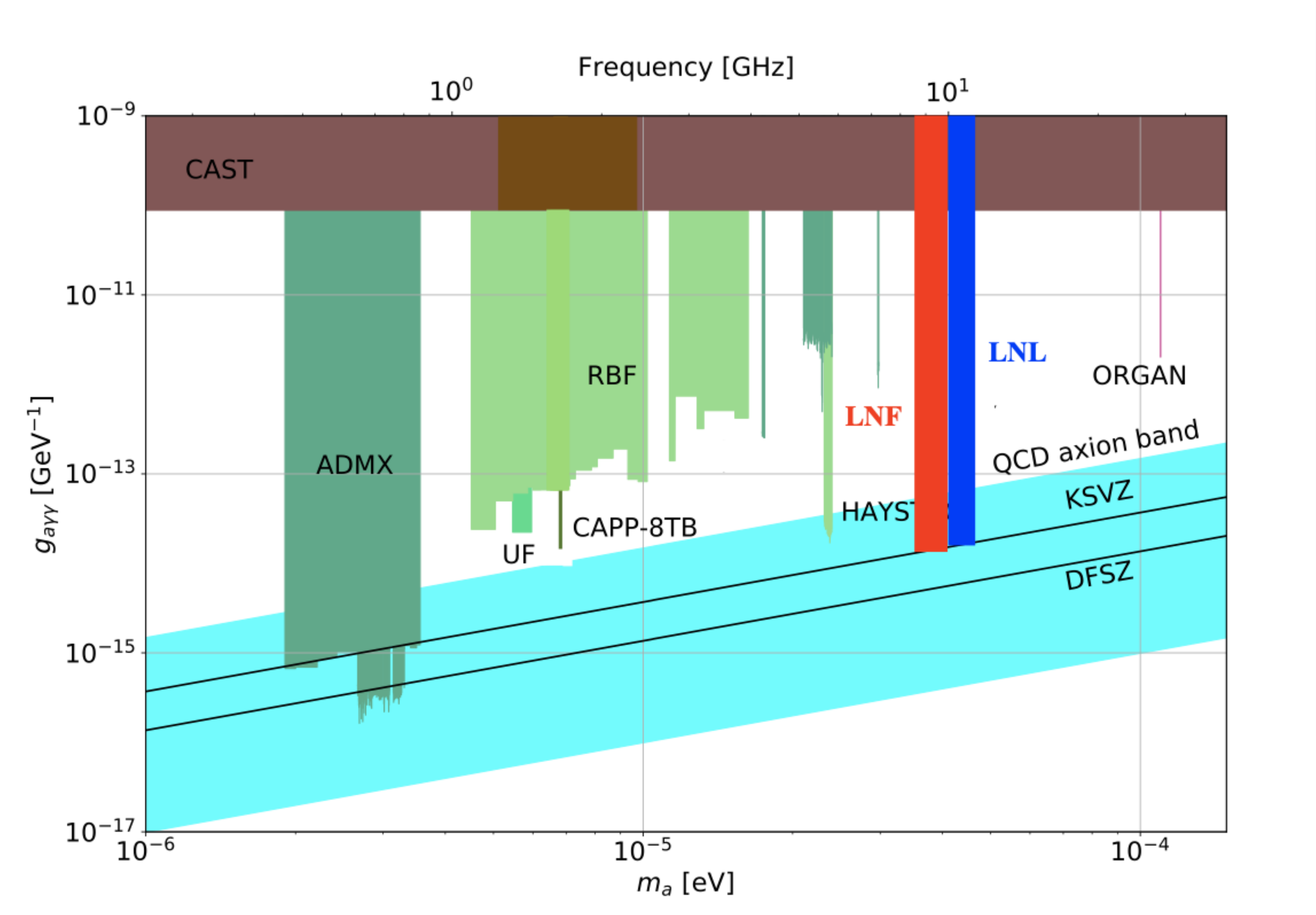

	LNF	**LNL**
Magnetic field	9 T	14 T
Magnet length	40 cm	50 cm
Magnet inner diameter	9 cm	12 cm
Frequency range	8.5 - 10 GHz	9.5 - 11 GHz
Cavity type	Hybrid SC	Dielectric
Scanning type	Inserted rod	Mobile cylinder
Number of cavities	7	1
Cavity length	0.3 m	0.4 m
Cavity diameter	25.5 mm	58 mm
Cavity mode	TM010	pseudoTM030
Single volume	$1.5 \cdot 10^{-4}$ m^3	$1.5 \cdot 10^{-4}$ m^3
Total volume	7⊗0.15 liters	0.15 liters
Q_0	300 000	1 000 000
Single scan bandwidth	630 kHz	30 kHz
Axion power	$7 \otimes 1.2 \cdot 10^{-23}$ W	$0.99 \cdot 10^{-22}$ W
Preamplifier	TWJPA/INRIM	DJJAA/Grenoble
Operating temperature	30 mK	30 mK

Outline

- **High Q** dielectric resonators / novel tuning mechanisms and geometries
- **TWPA** – based amplification chain characterization and measurements
- **Single Microwave Photon Detectors** (**SMPD**) for "itinerant " photons

Dielectric resonators

Tunable cavity with dielectric shells
"**dielectric boosted**" resonator

TM_{030} higher order mode
for axion detection

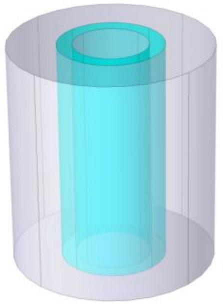

2 shells → $C_{030} = 0.03$
1 shell → $\mathbf{C_{030} = 0.49}$

$Q_0 \sim 9 \cdot 10^6$ @ **10.3** GHz – 4.2 K

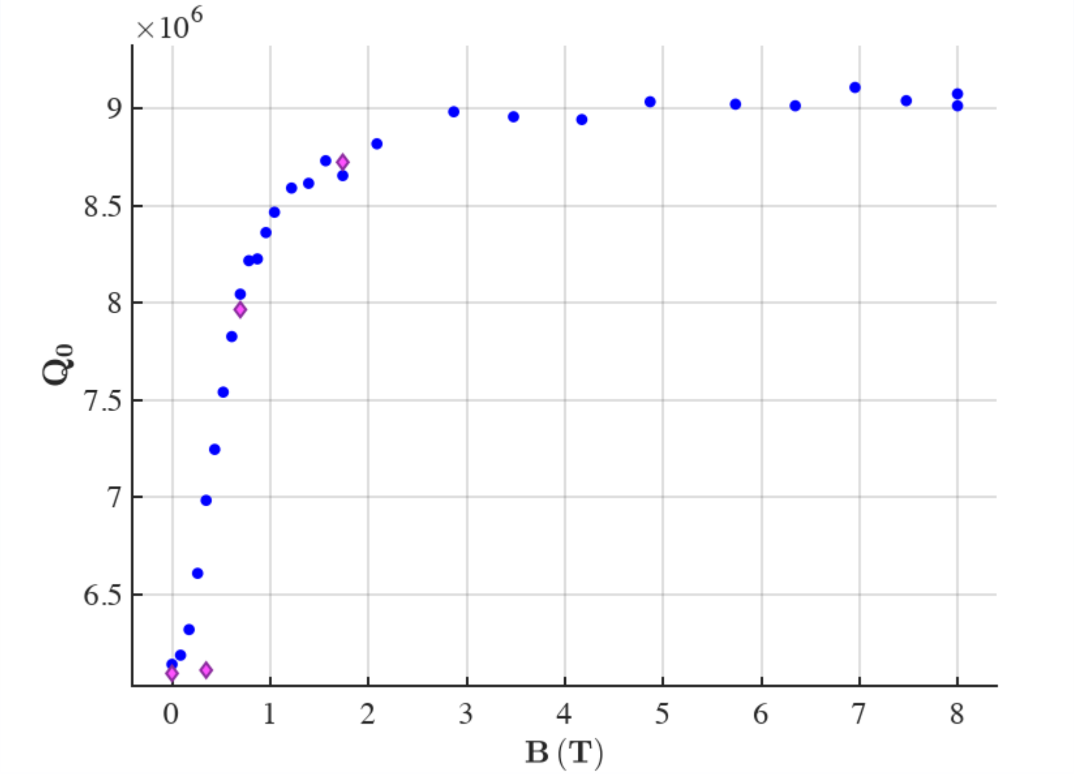

paramagnetic impurities in sapphire :
@ high B-fields they are completely swept away

Phys. Rev. Appl. 17, 054013 (**2022**)
Nucl. Instrum. Methods A **985**, 164641 (**2021**)

Wet DU Cryostat

- He^3-He^4 “wet” dilution refrigerator (refurbished) ! recovery system + compressor at LNL
- Cooling power of 1 mW at 120 mK

8 T field magnet

base temperature of 50 mK after ~ 9 hours

Magnet and DU

Nb-Ti SC magnet
surrounds the cavity and
provides the 8T magnetic field

Compensation coil shields
the cryogenic electronics
and TWPA
from ~ 0.3 T residual field

^3He–^4He wet dilution refrigerator: refurbished unit previously installed in the gravitational wave bar antenna Auriga test facility

Tuning mechanisms

V = 0.158 liters
$Q_0 \approx$ 50.000
freq. ~ 10 GHz
T = 4 K

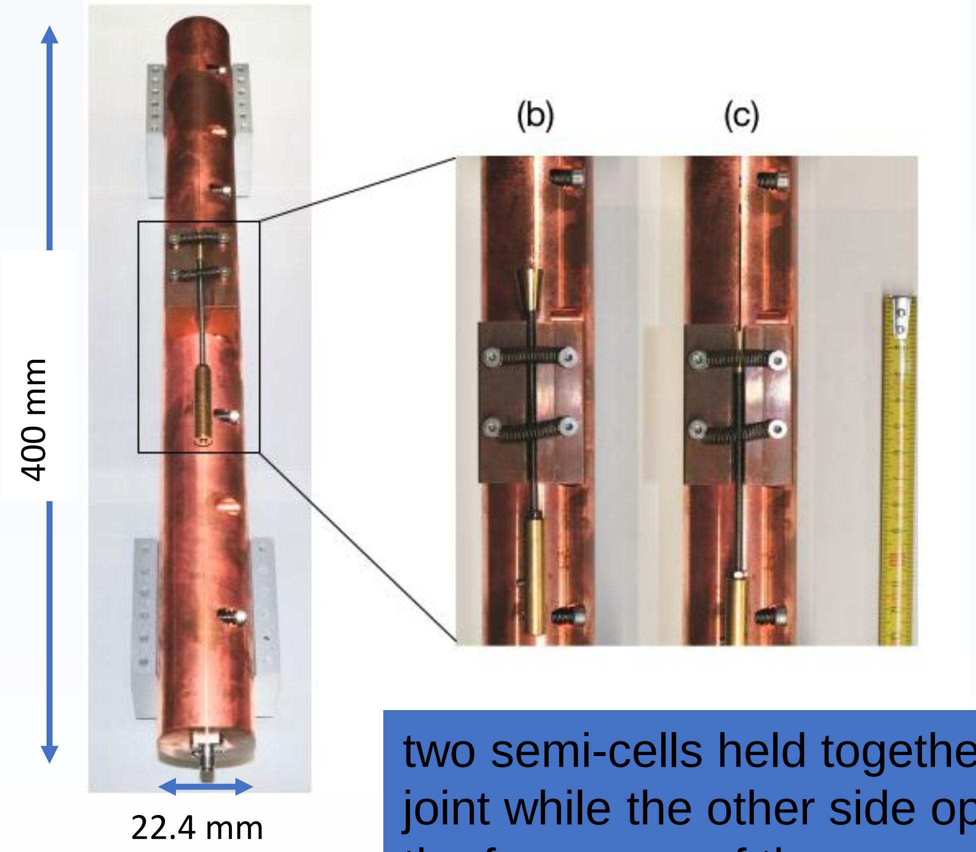

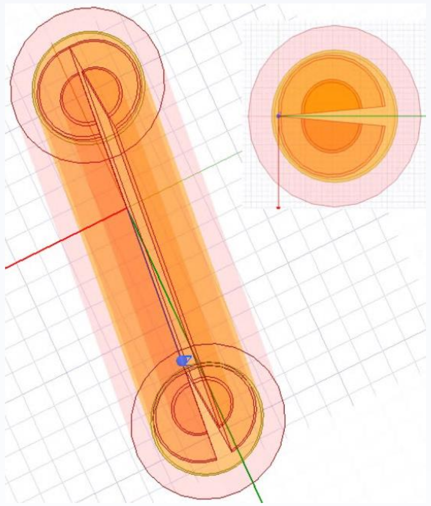

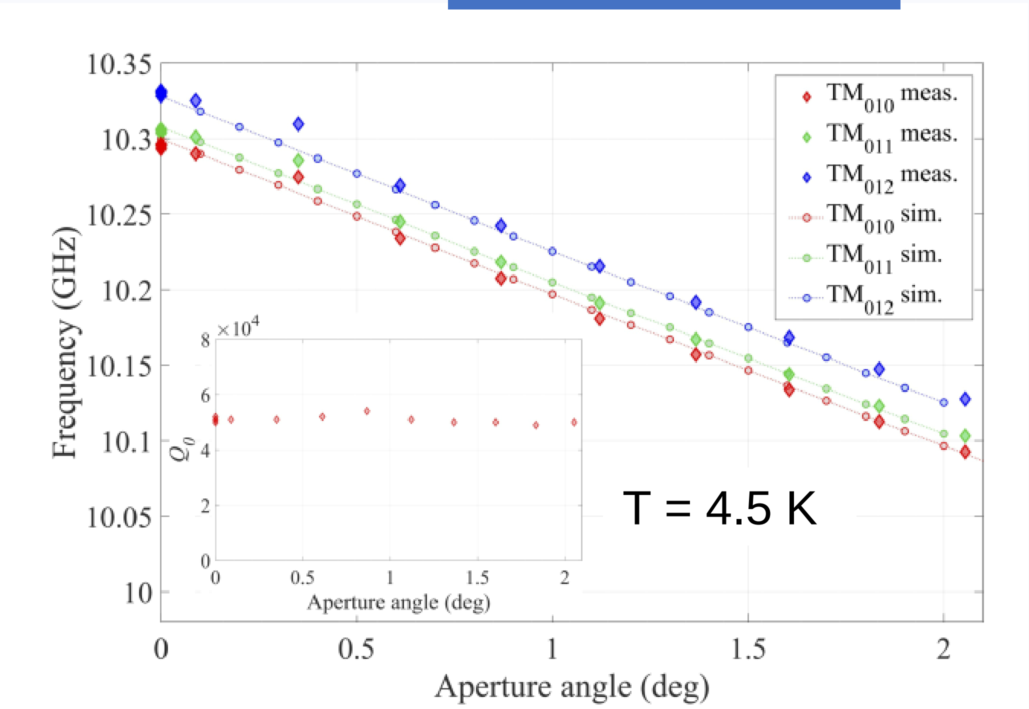

two semi-cells held together at a fixed joint while the other side opens to tune the frequency of the resonant mode

maximum aperture of ~ 2 degrees, is equivalent to a 2% increase in effective volume

Tuning a range of at least 200 MHz for the **fundamental mode TM_{010}**

Rev Sci Instrum 94, 045111 (2023)

TWPA characterization

In axion DM research we need:

- **quantum-limited noise performance**
- **GHz amplification bandwidth**

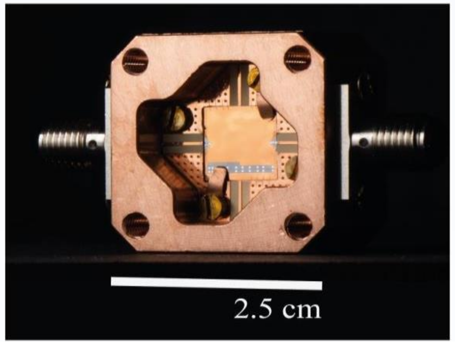

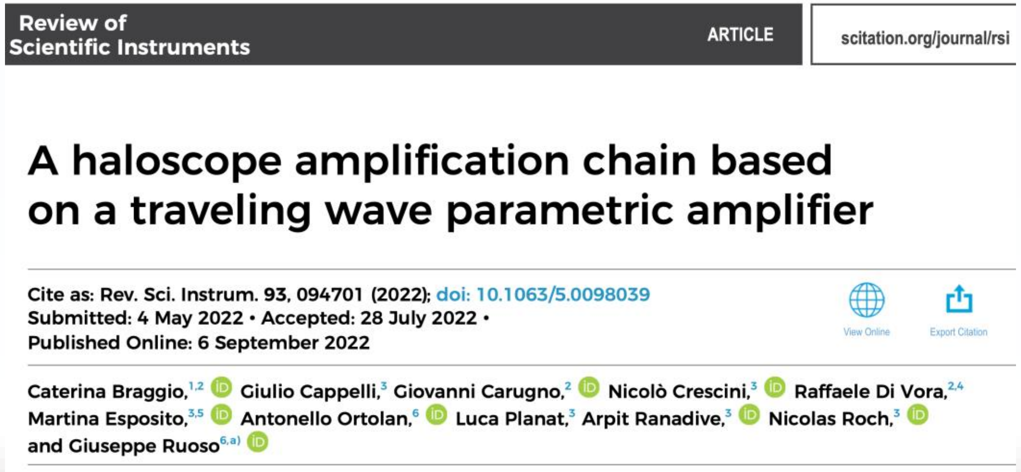

Review of Scientific Instruments — ARTICLE — scitation.org/journal/rsi

A haloscope amplification chain based on a traveling wave parametric amplifier

Cite as: Rev. Sci. Instrum. 93, 094701 (2022); doi: 10.1063/5.0098039
Submitted: 4 May 2022 • Accepted: 28 July 2022 •
Published Online: 6 September 2022

View Online   Export Citation

Caterina Braggio,[1,2] Giulio Cappelli,[3] Giovanni Carugno,[2] Nicolò Crescini,[3] Raffaele Di Vora,[2,4] Martina Esposito,[3,5] Antonello Ortolan,[6] Luca Planat,[3] Arpit Ranadive,[3] Nicolas Roch,[3] and Giuseppe Ruoso[6,a)]

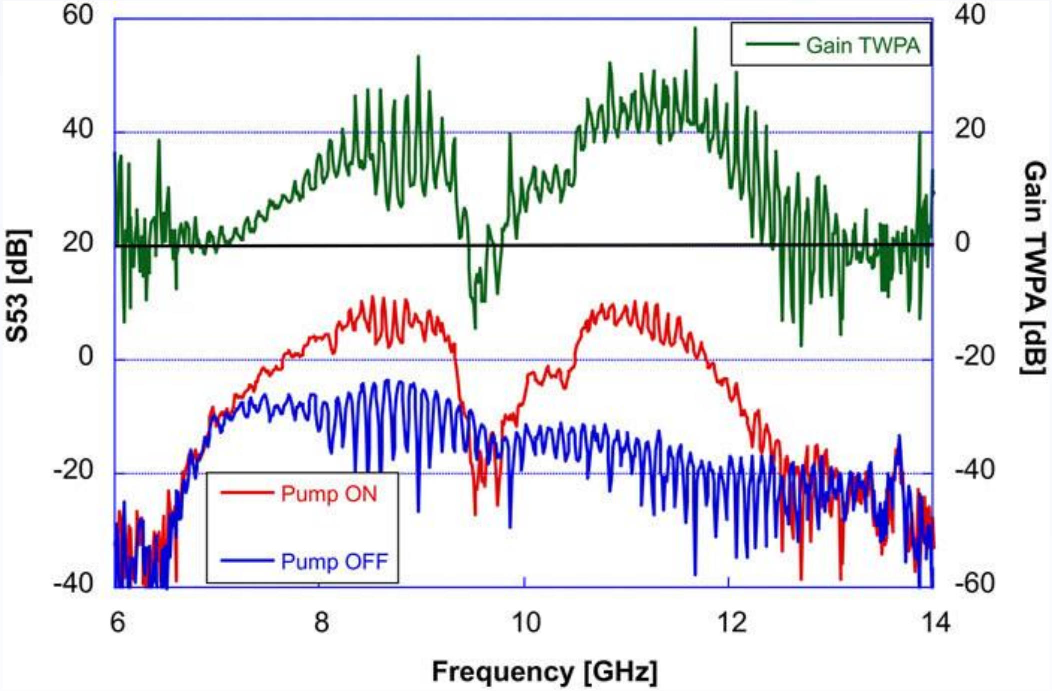

T_{sys} = 2.1 ± 0.1 K @ 10.353 GHz

Novel, reliable calibration scheme to measure T_{sys} exactly at the cavity output and without the need for switches nor heated load.

Schematics of the experimental apparatus

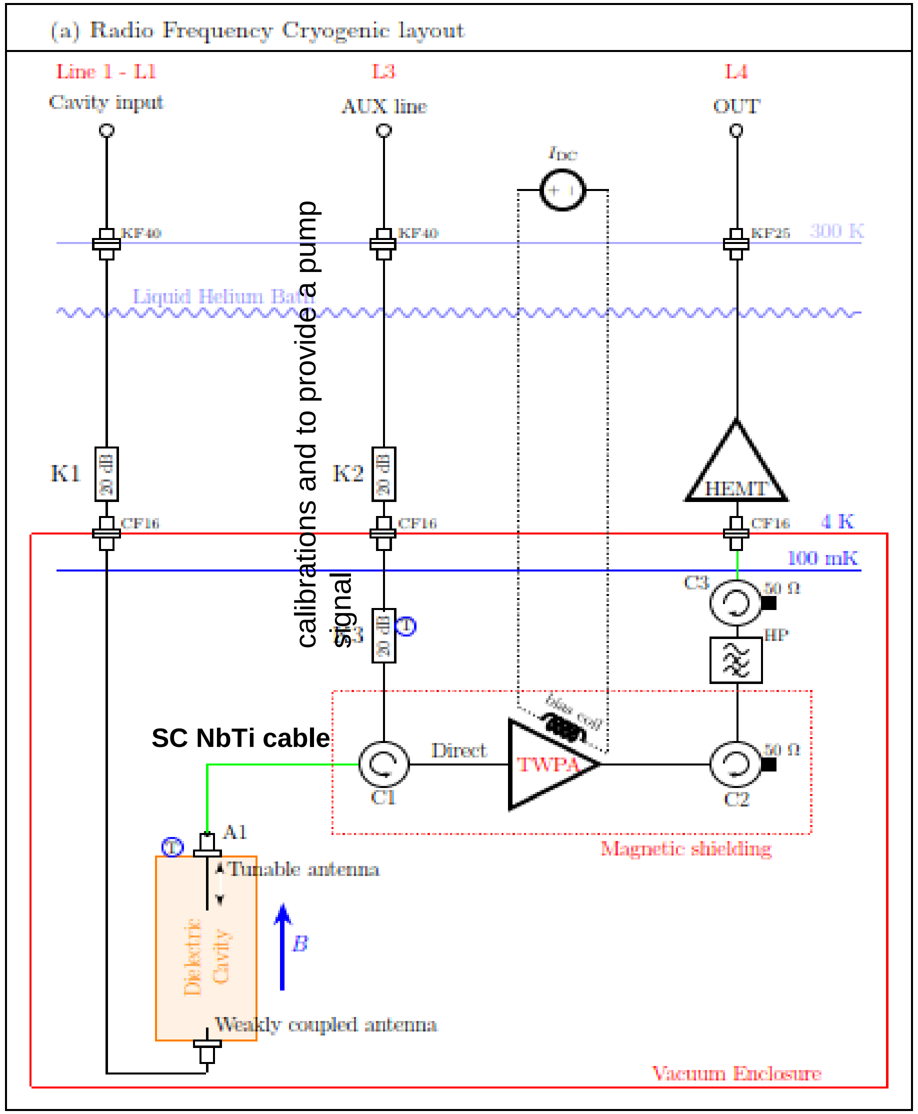

TM030 mode
Effective volume 3.4×10^{-2} lt
Freq. = 10.353 GHz
Tuned by 3 2-mm sapphire rods

- pre-amplifier TWPA
- HEMT amplifier
- C1, C2 and C3 are circulators,
- HP is an 8 GHz high pass filter
- K1, K2, and K3 are attenuators

high-Q microwave resonant cavity:
internal quality factor of ~ 9×10^{6}

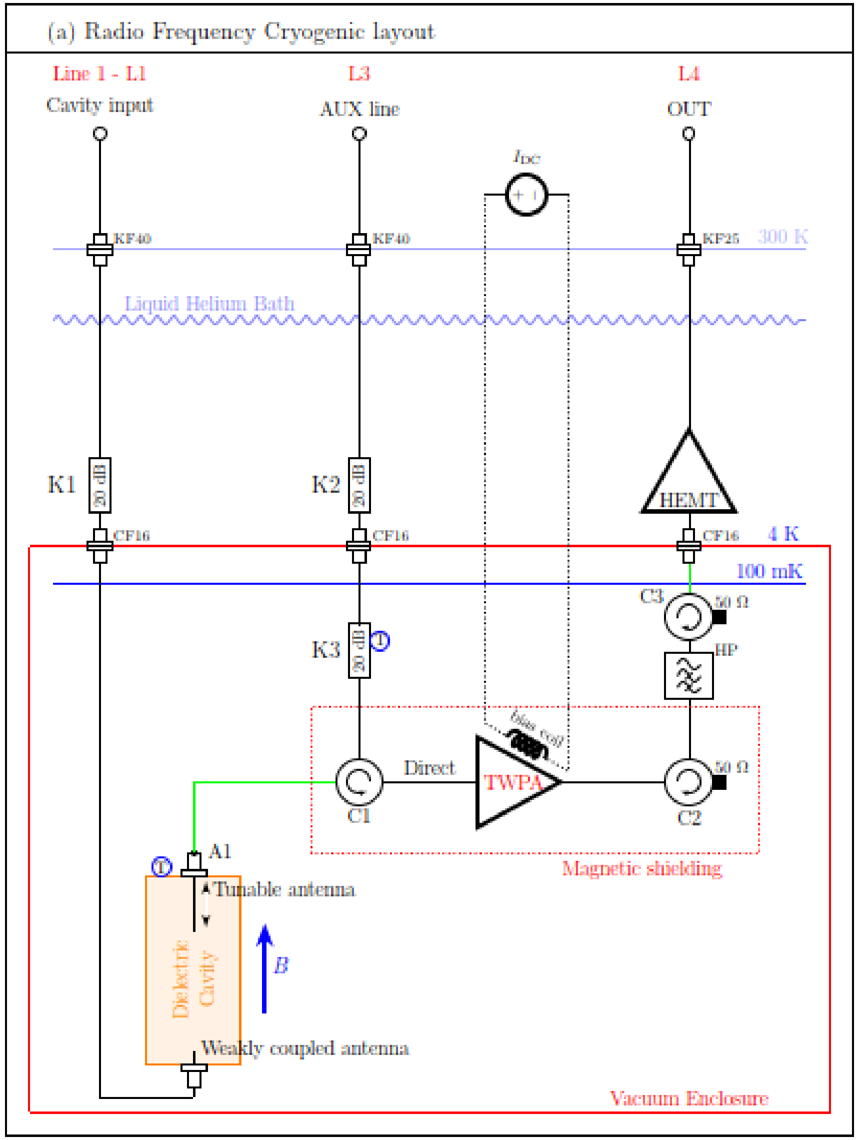

Tuning by 3 2-mm sapphire rods

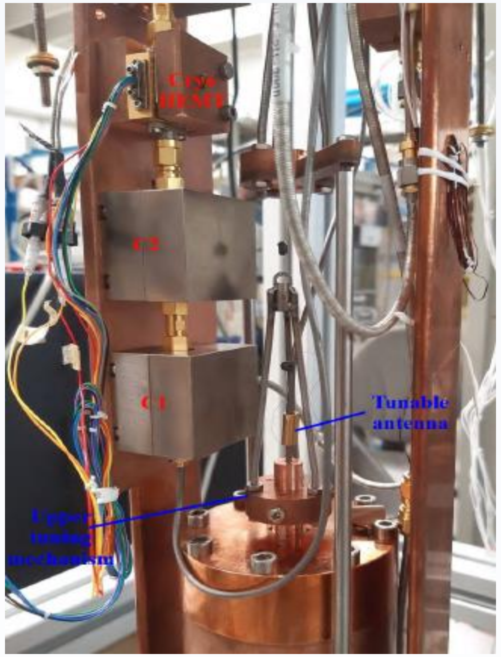

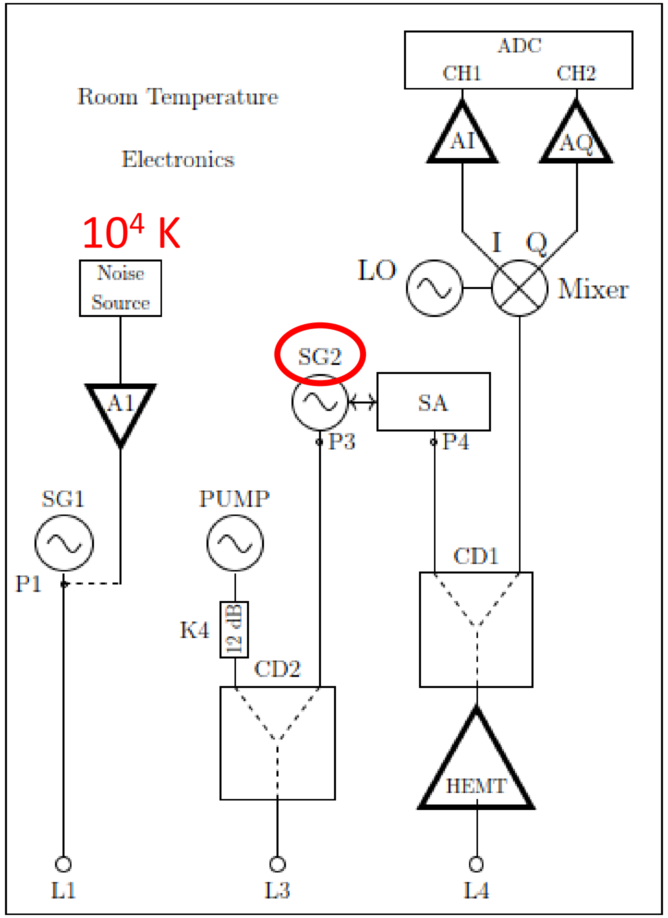

high-Q microwave resonant cavity:
internal quality factor of more than 9×10^6

-cavity reflection spectrum S43
(input from line L3 - output from line L4)

-information on the loaded quality
Q_L, resonance frequency f_c and coupling β of the tunable antenna

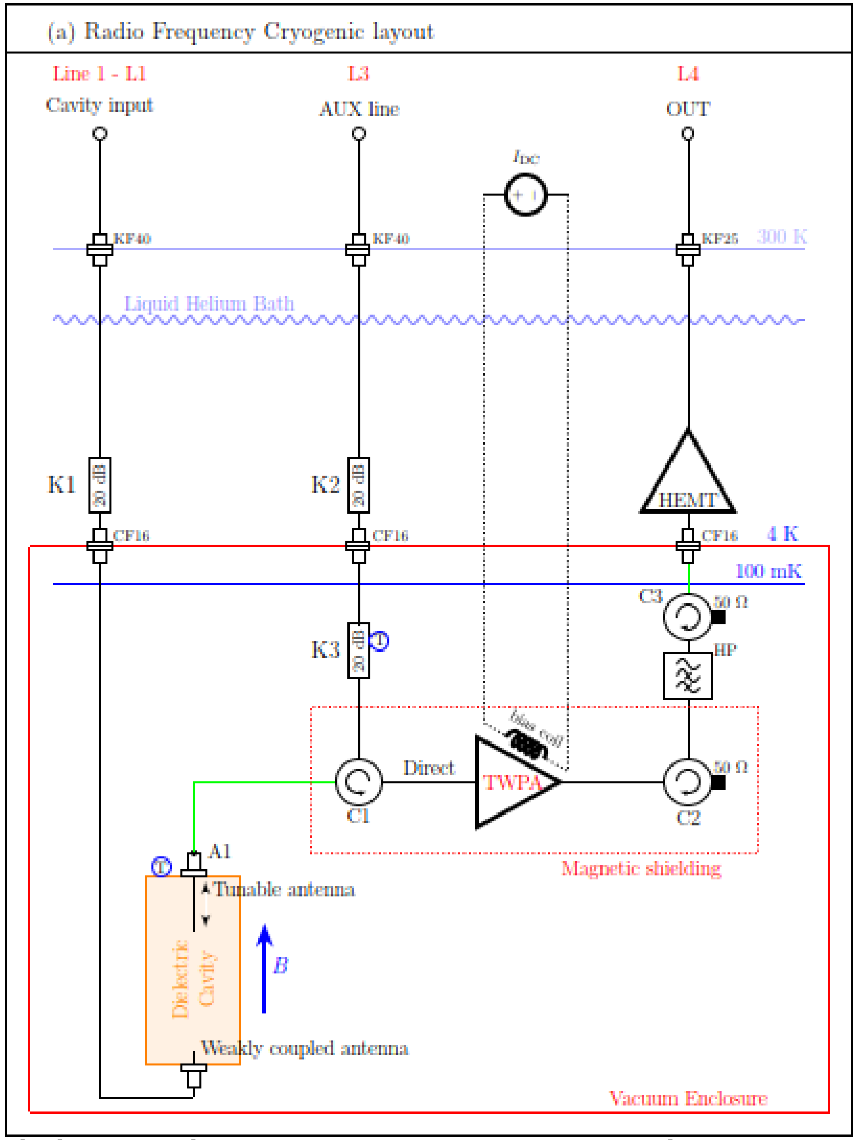

high-Q microwave resonant cavity: internal quality factor of more than $9{\times}10^6$

TWPA with circulators inside the shielding box

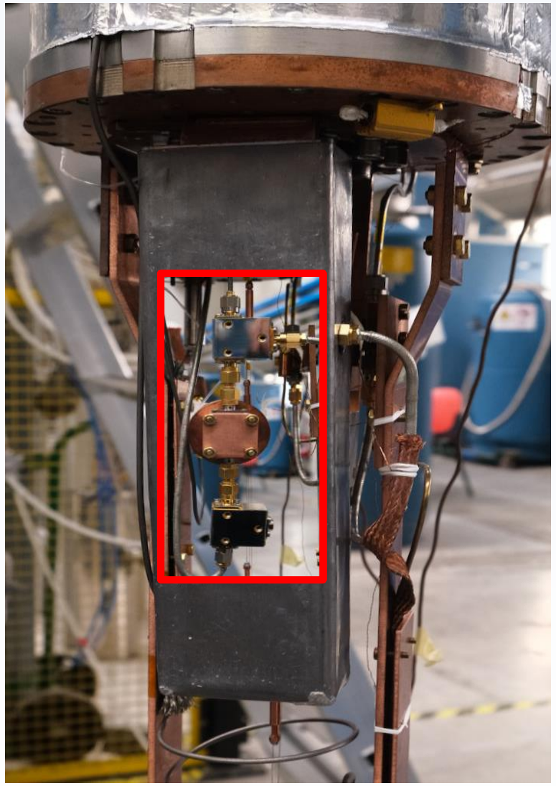

- Mixing chamber @ 50 mK
- Cavity @ 110 mK

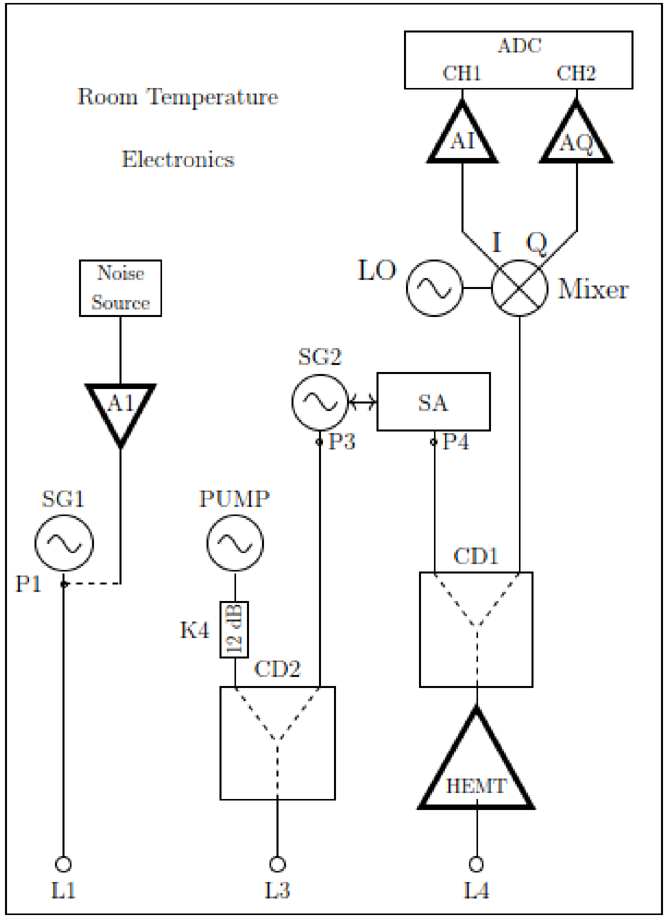

QUAX$_{a\gamma}$ TWPA-based amplification measurement

Phys. Rev. D (R. Di Vora et al)

$$N_{\text{sys}} = \frac{k_B}{h\nu_s} T_{\text{sys}} = 4.2 \pm 0.3.$$

T_{sys} = 2. 06 ± 0.13 K @ 10.353 GHz

Term	Value (K)	N photons
$N(\nu_s, T_s)$	0.27	0.5
$N(\nu_i, T_i)$	0.27	0.7
$N_{\text{HEMT}}/\Lambda_1\Lambda_2 G_{\text{TWPA}}$	0.39	0.8
N_{sys}	2.06	4.2
$N_{\text{TWPA}}/\Lambda_1$		2.2

Data taking for 17 hours

- 8 T magnetic field
- ν_c =10.353 GHz
- Q ~ 2.5•10^5

This is the first time a wide bandwidth quantum limited amplifier has been used in a haloscope working at high frequency

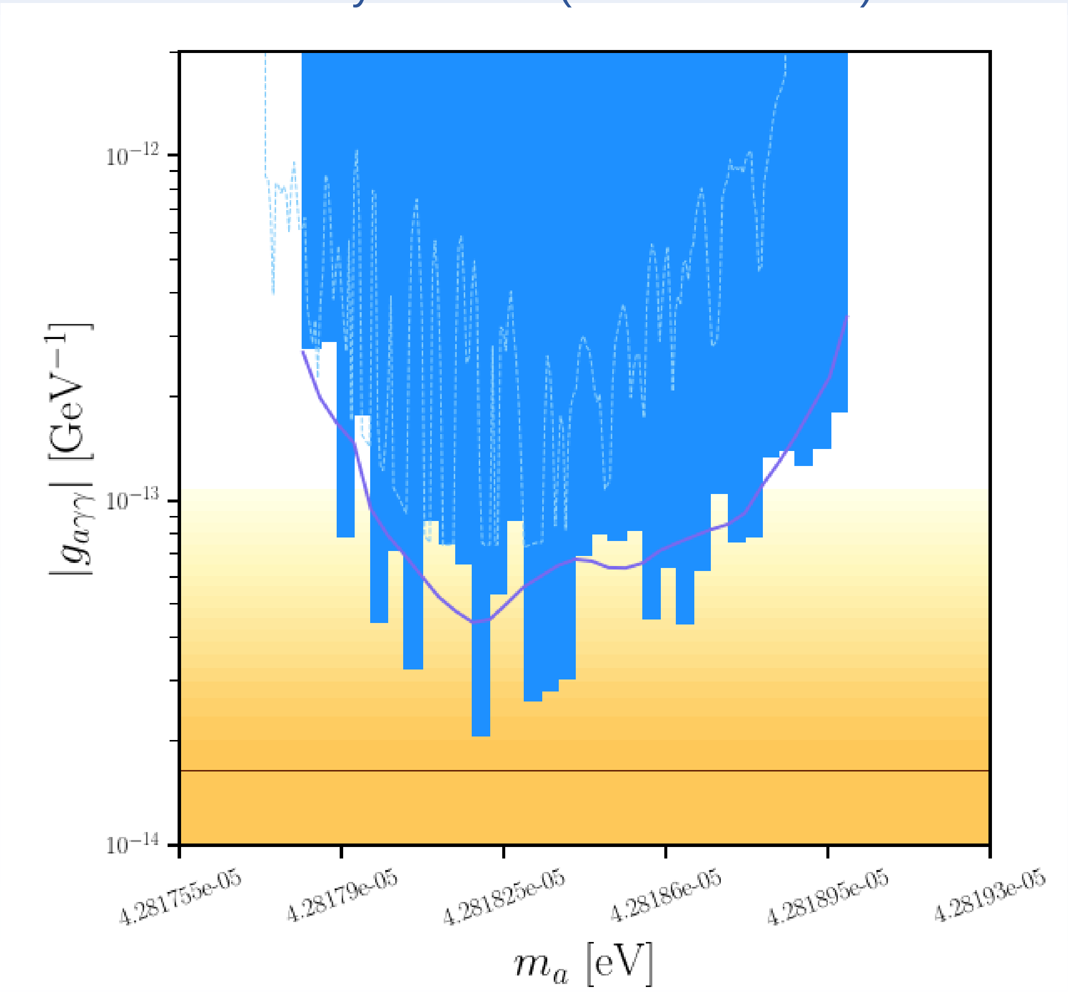

We set a limit for the axion-photon coupling a factor about 4 from the benchmark axion-QCD band

Analysis of single-photon and linear amplifier detectors for microwave cavity dark matter axion searches

at higher frequencies, and thus higher axion masses, single-photon detectors become competitive and ultimately favored, when compared to quantum-limited linear amplifiers, as the detector technology in microwave cavity experimental searches for galactic halo dark matter axions.

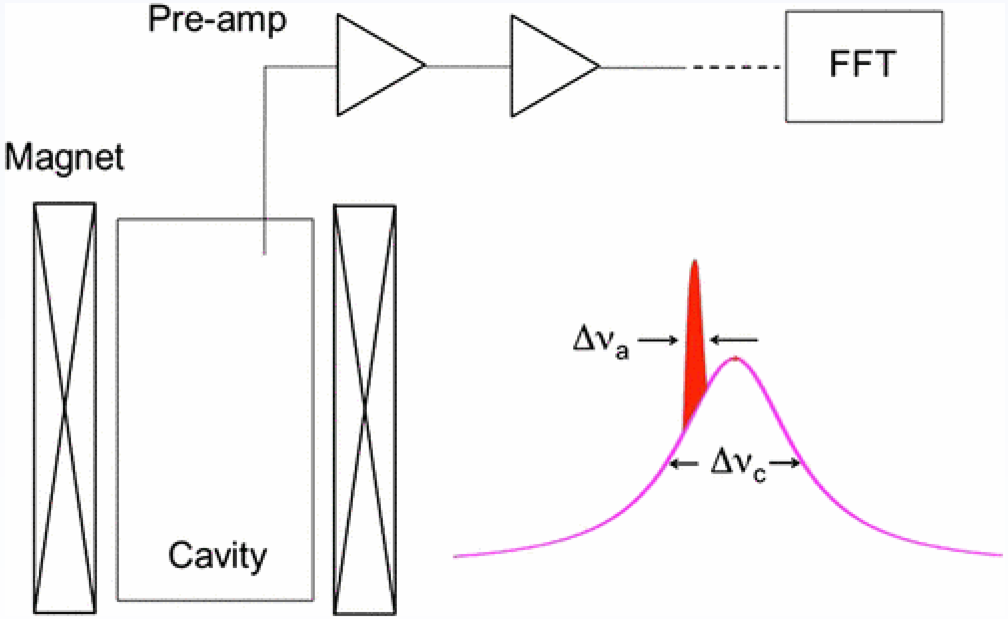

$$\frac{P_\ell}{P_{\rm sp}} = \left[\sqrt{\bar{n}} + \frac{1}{\sqrt{\bar{n}}}\right]\sqrt{\frac{Q_c}{2\pi\eta Q_a}}.$$

At achievable temperature T=10 mK,
$\bar{n} \approx 3\times 10^{-11}$ then
P_ℓ/P_{sp}~17,000

S. K. Lamoreaux, K. A. van Bibber, K. W. Lehnert, and G. Carosi
Phys. Rev. D 88, 035020 – Published 23 August 2013

Single Microwave Photon Detector

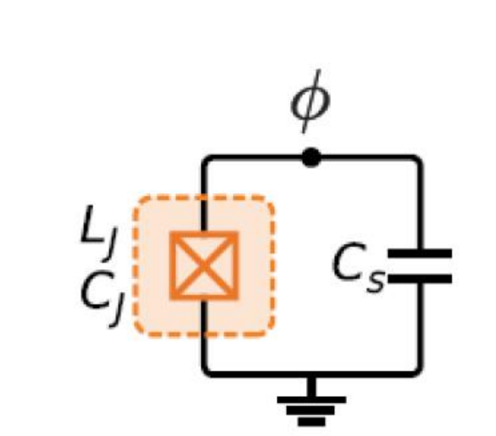

Transmon qubit circuit. The orange box represents a Josephson junction with inductance L_J and capacitance C_J

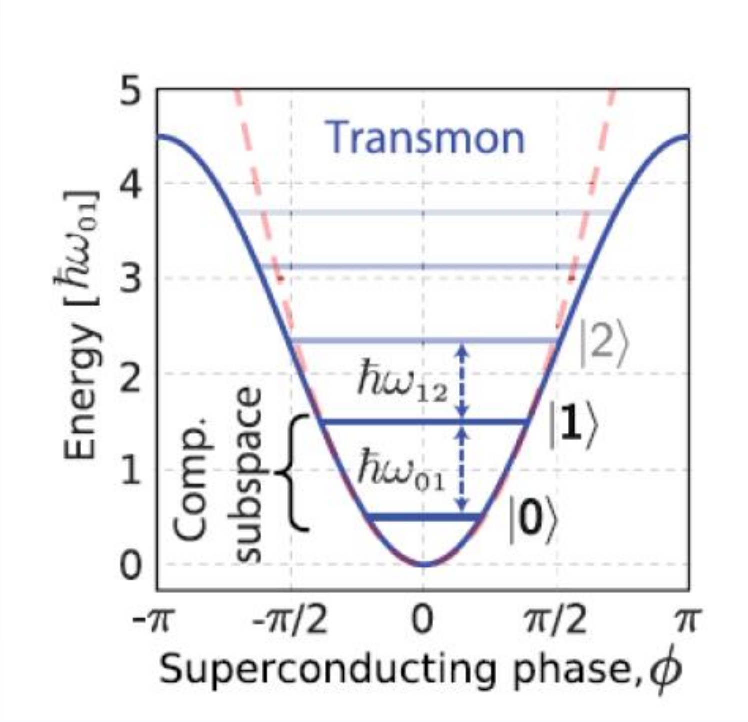

The transmon anharmonic potential yields non-equidistant energy levels. This allows to isolate the two lowest energy levels $|0\rangle$ and $|1\rangle$ that constitute the two-dimensional qubit subspace

A **Single Photon Microwave Counter (SMPD)** architecture is significantly different whether it is meant for **cavity photons** or **itinerant** (traveling) photons.
We are interested in the itinerant version due to the *intense magnetic fields* involved in axion search.

cavity photons ≠ itinerant photons

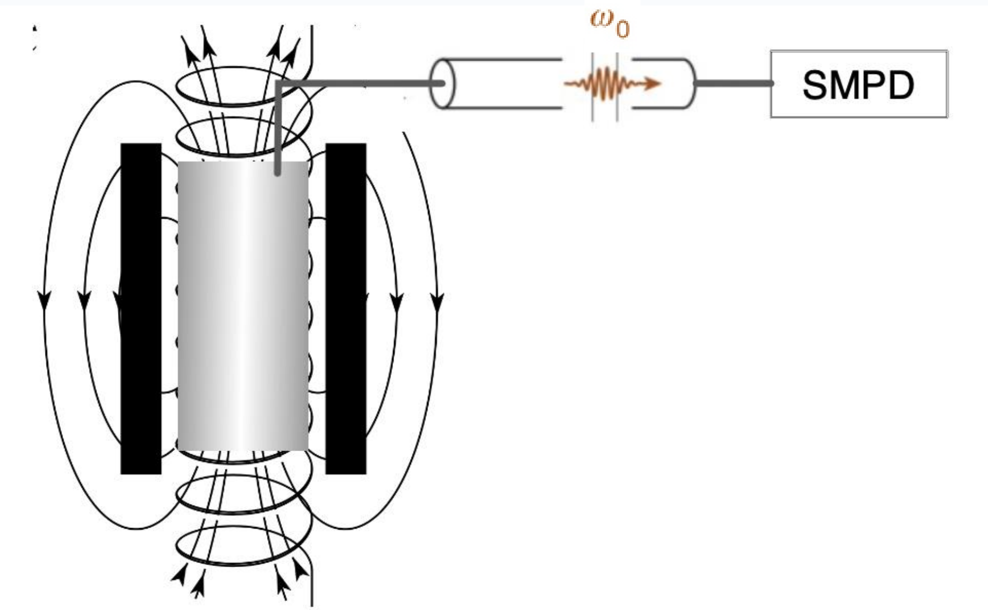

-detection of individual microwave photons is a challenging task because of their low energy ~ 10^{-5} eV

-a solution: use “artificial atoms” introduced in circuit QED, their transition frequencies lie in the ~GHz range

-or: rely on a single current-biased Josephson junction

Transmon-based SMPD

In the Quantronics group (CEA, Saclay) a transmon-based counter has been developed and used to make **spin fluorescence measurements**, paving the way to single spin flip detection with SMPDs.

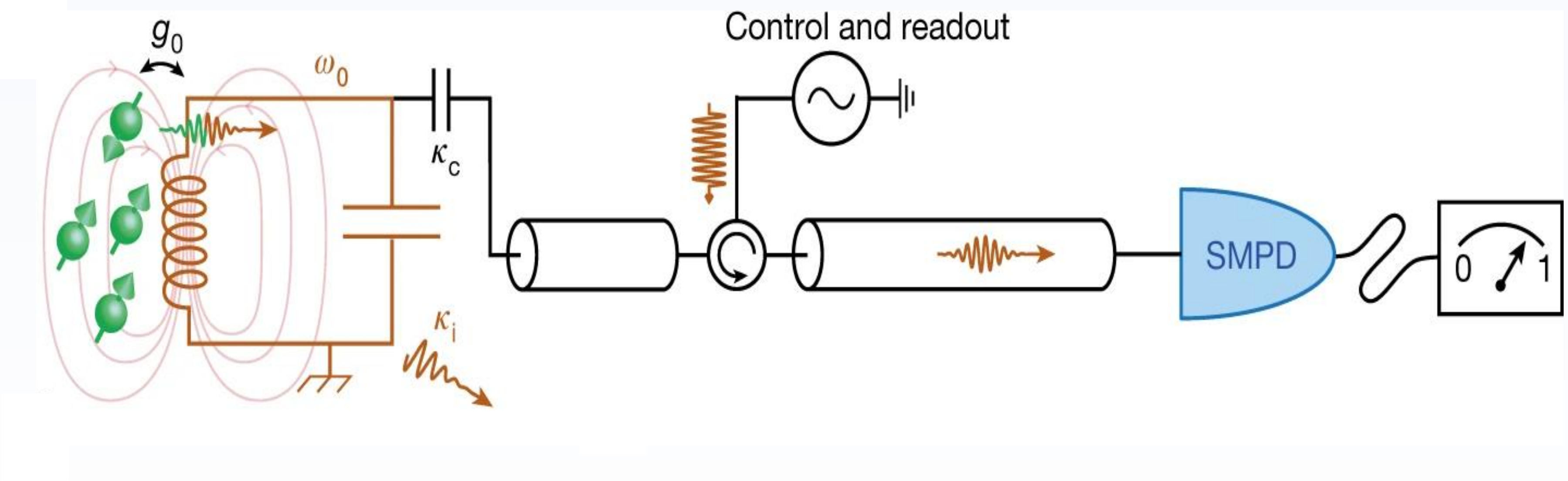

R. Lescanne et al, Phys. Rev. X 10, 021038 (2020)
E. Albertinale , Nature 600, 434 (2021)

Quantronics Group
Research Group in Quantum Electronics, CEA-Saclay, France

Detecting dark matter through quantum science

cavity photons ≠ itinerant photons

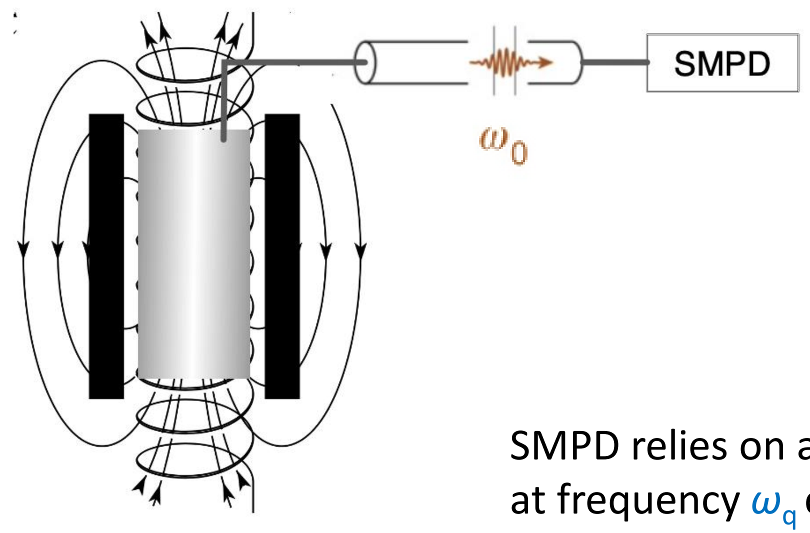

SMPD relies on a transmon qubit at frequency ω_q coupled to three ports:
buffer, pump and waste

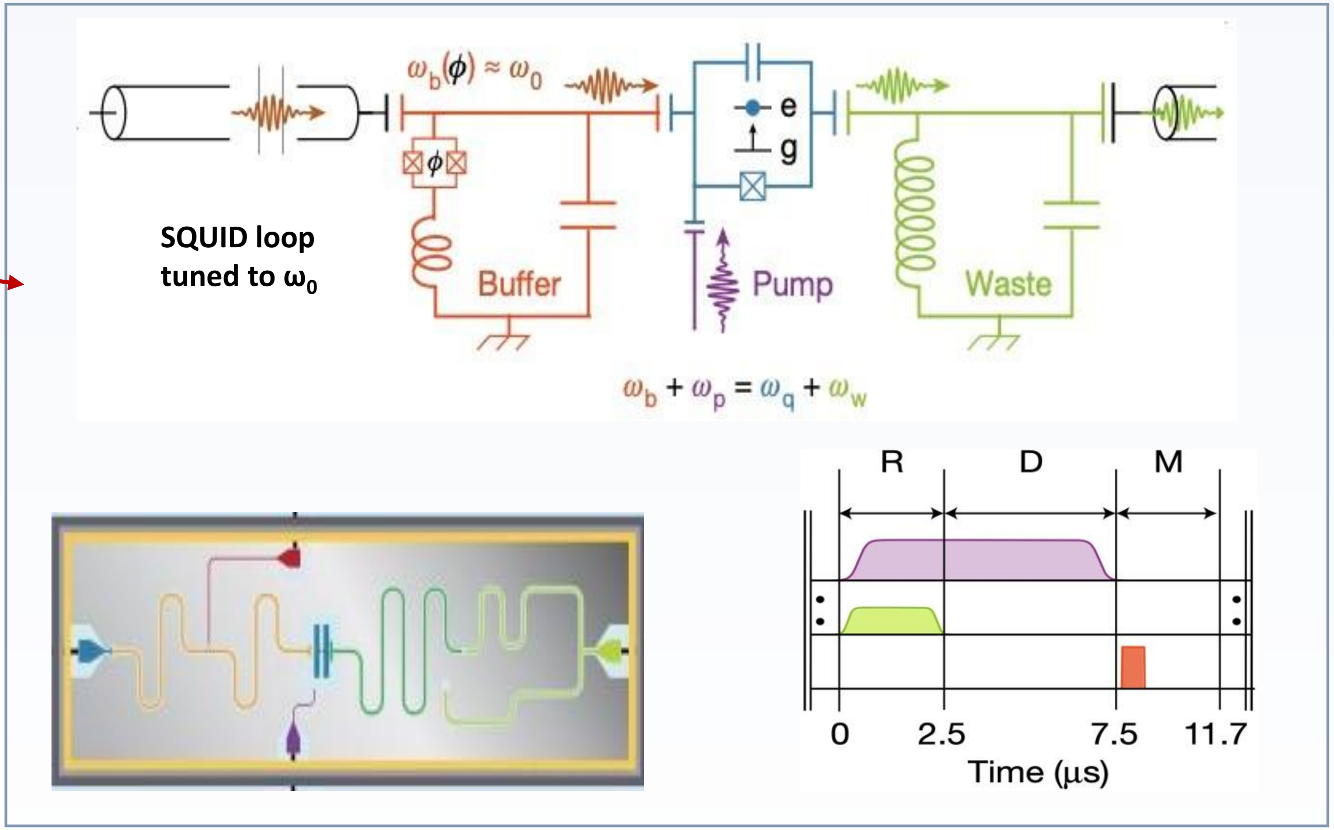

a three-step process repeated continuously

-- qubit reset (R) performed by turning on the pump pulse
+ weak resonant coherent pulse to the waste port

-- detection (D) step with the pump pulse on

-- measurement (M) step probes the dispersive shift of the buffer resonator to infer the qubit state

E. Albertinale , Nature 600, 434 (2021)

Detecting dark matter through quantum science

irreversible transfer of an incoming photon to an excitation of a transmon qubit

the resonator and qubit do not directly interact but instead dissipate energy to a common cold bath

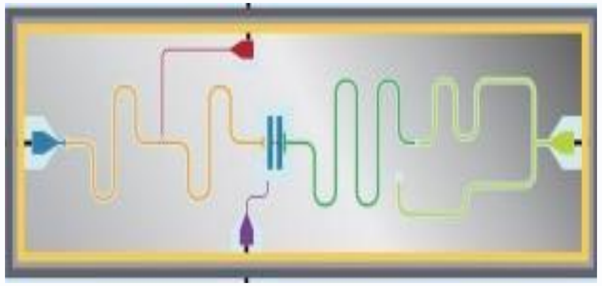

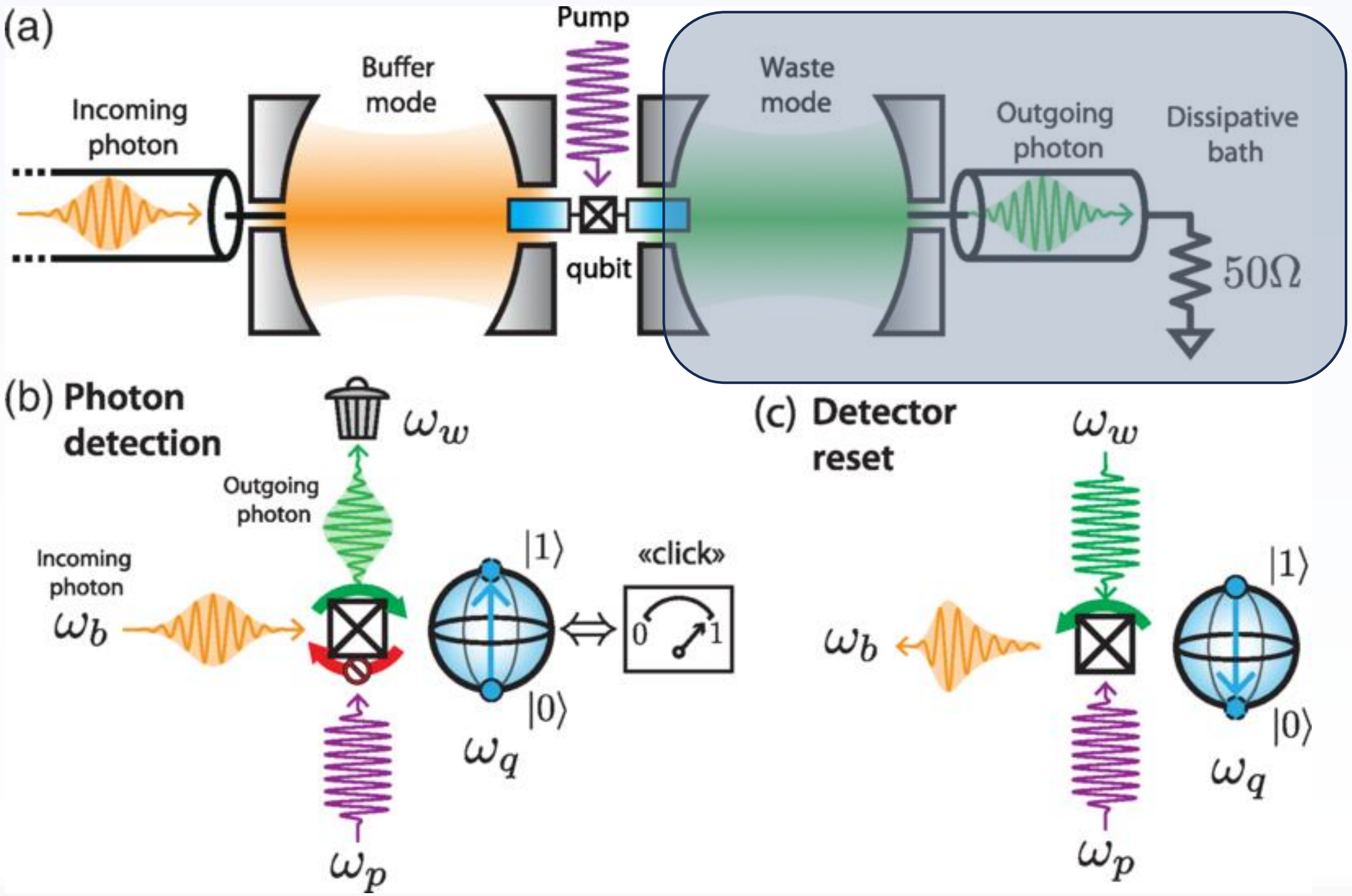

$$\omega_b + \omega_p = \omega_w + \omega_q$$

R. Lescanne et al, Phys. Rev. X 10, 021038 (2020)
E. Albertinale , Nature 600, 434 (2021)

Detecting dark matter through quantum science

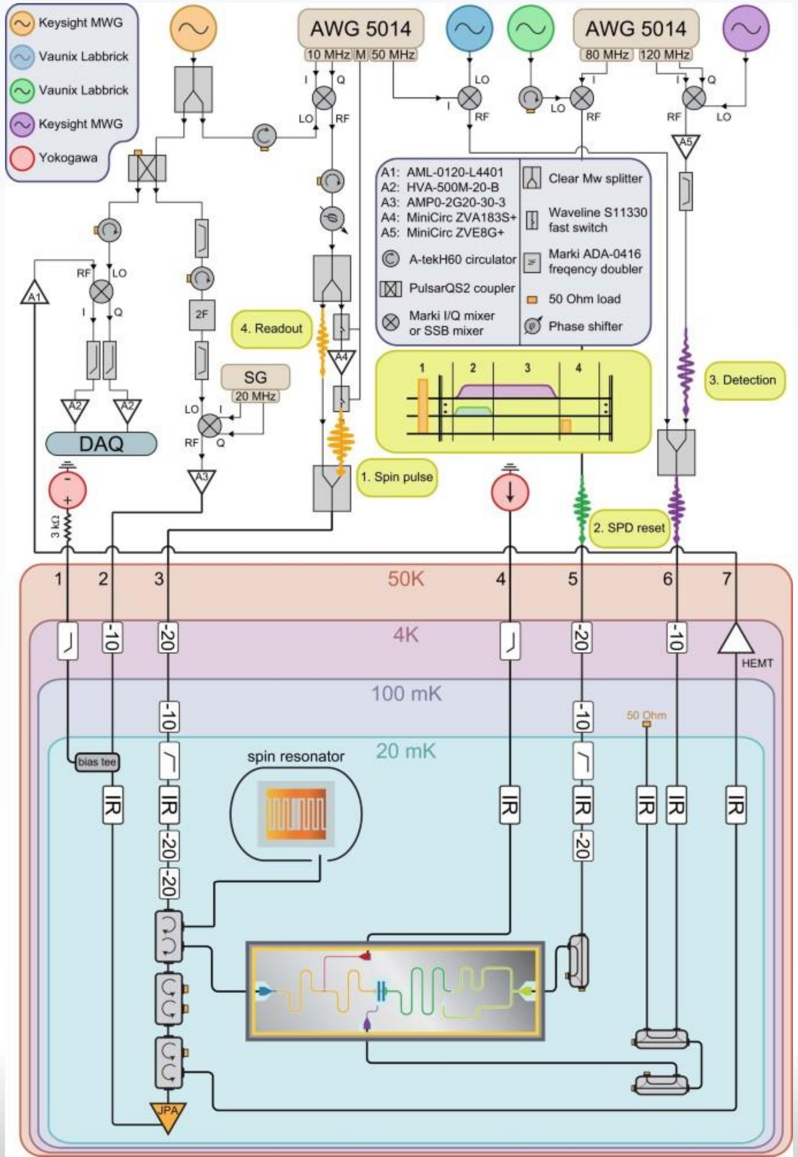

Quantronics Group
Research Group in Quantum Electronics, CEA-Saclay, France

E. Albertinale , Nature 600, 434 (2021)

SMPD in axion dark matter search

single microwave photon detectors (SMPDs) developed in the context of quantum information science have the potential to **greatly improve the search speed at haloscopes**

A pilot experiment performed with researchers from **INFN** (Padova, LNL) and the **Quantronics group** (CEA Saclay)

- tunable, high quality factor cavity
- TM_{010} mode $\nu_c \rightarrow 7.3\ \mathrm{GHz}$ is readout by a SMPD

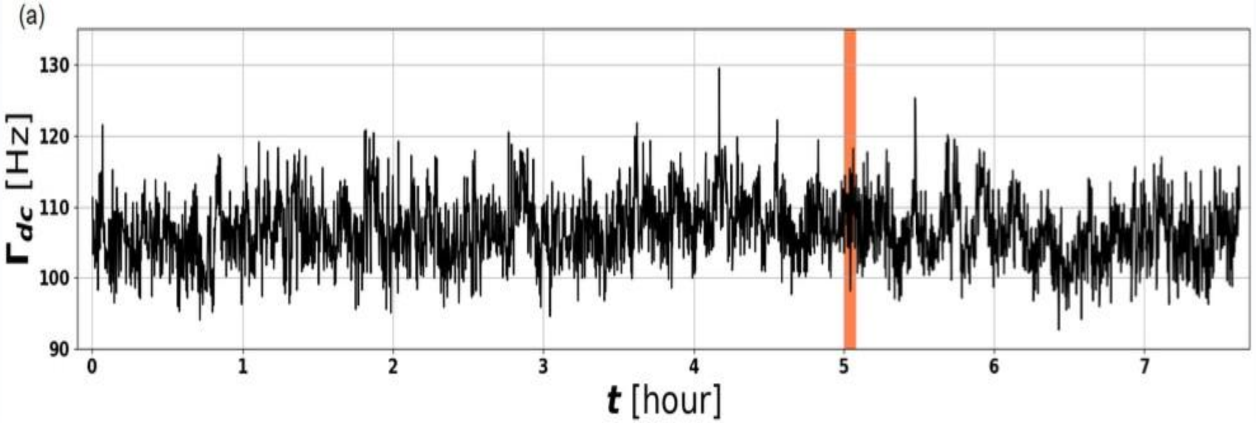

Detector bandwidth	~	1 MHz
Tunabilty range	~	200 MHz
Dark count rate	~	100-120 Hz
Efficiency	~	0.4

Unwanted photons: false-positive events

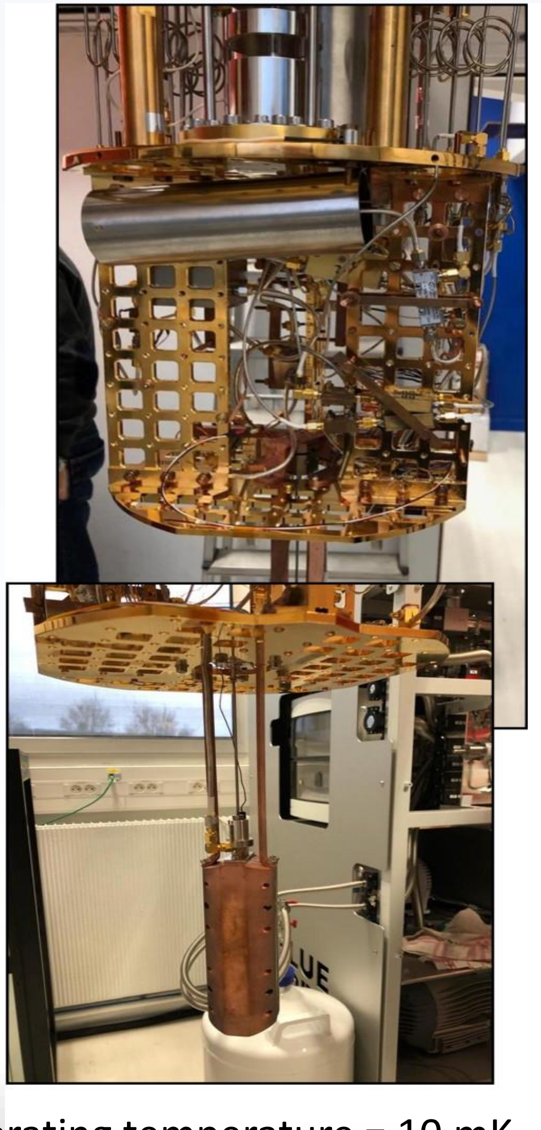

Operating temperature = 10 mK

Detecting dark matter through quantum science

PHOTON DETECTOR PERFORMANCES

The efficiency η of the detector is defined as the probability of detecting the qubit in its excited state assuming a single incoming photon

the dark count rate α defined as the number of false positive detection per unit of time

power sensitivity S of the detector as the noise equivalent power (NEP) for an integration time of 1 s

$$\mathcal{S} = \frac{\hbar\omega\sqrt{\alpha}}{\eta}.$$

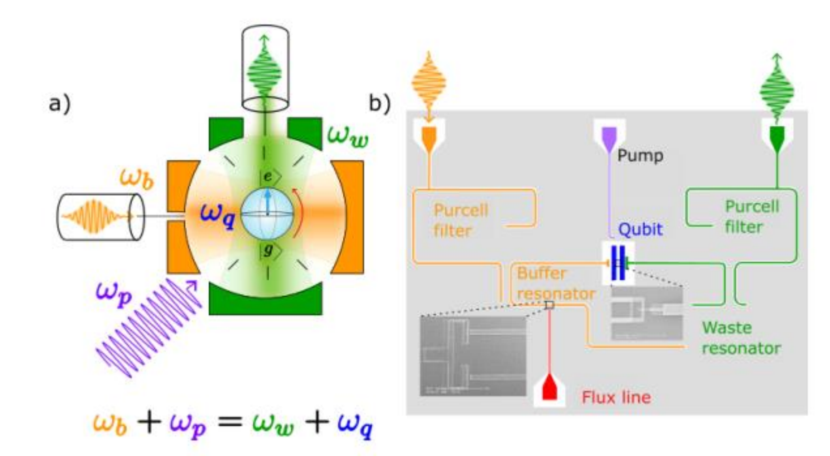

Bolometer : $\mathcal{S} = 7 \cdot 10^{-19}\ \mathrm{W}/\sqrt{\mathrm{Hz}}$ at 7.9 GHz,

SMPD : $\mathcal{S} = 10^{-22}\ \mathrm{W}/\sqrt{\mathrm{Hz}},$ 7.005 GHz to 6.824 GHz

https://arxiv.org/pdf/2307.03614.pdf

New DU refrigerator + SRF searches

New dilution unit → 7 mK base Temperature

Paris test-run was successful so the SMPD device will be transferred to Italy for haloscope developments in INFN-LNL:

- QUAX$_{\alpha\gamma\gamma}$
- QUAX$_{\alpha e}$

- Superconductive cavity
  (copper cavity sputtered with **NbTi**)

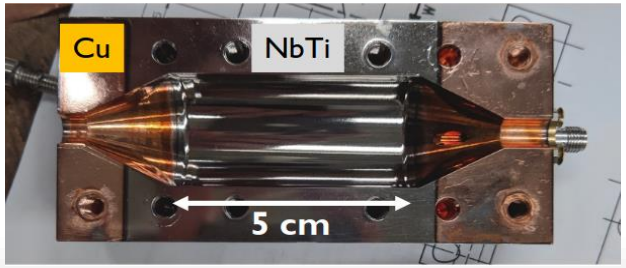

Model CF-CS110-

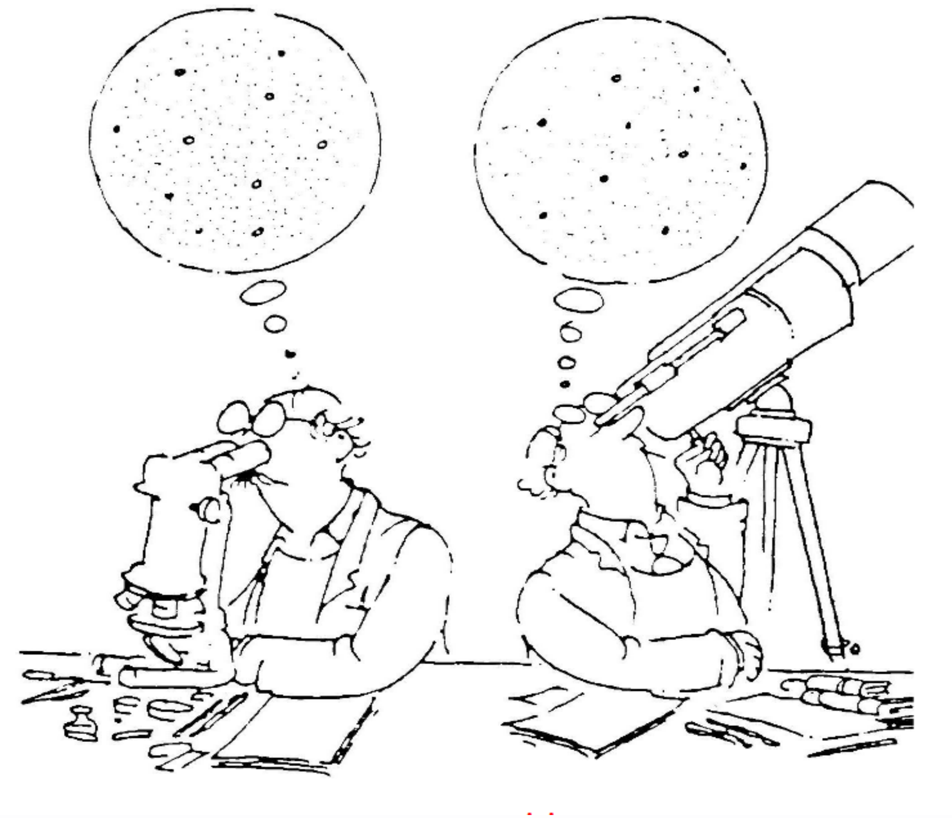

Thank you